THE EFFECT OF SURFACE STRUCTURE ON CATALYTIC REACTIONS: A SUM FREQUENCY GENERATION SURFACE VIBRATIONAL SPECTROSCOPY STUDY

by

Keith Ryan McCrea

B.S. (Western Washington University) 1997

A dissertation submitted in partial fulfillment of

the requirements for the degree of

Doctor of Philosophy

In

Chemistry

in the

Graduate Division

of the

University of California, Berkeley

Committee in charge:

Professor Gabor A. Somorjai, Chair

Professor Norman E. Phillips

Professor Yuen R. Shen

Fall 2001

The dissertation by Keith Ryan McCrea is approved:

Chair Date

Date

Date

University of California, Berkeley

Fall 2001

The EFFECT OF SURFACE STRUCTURE ON CATALYTIC REACTIONS: A SUM FREQUENCY GENERATION SURFACE VIBRATIONAL SPECTROSCOPY STUDY

Keith Ryan McCrea

Abstract

EFFECT OF SURFACE STRUCTURE ON CATALYTIC REACTIONS: A SUM FREQUENCY GENERATION SURFACE SPECIFIC VIBRATIONAL SPECTROSCOPY STUDY

by

Keith Ryan M^{c}Crea

Doctor of Philosophy in Chemistry

University of California, Berkeley

Professor Gabor A. Somorjai, Chair

Using Sum Frequency Generation (SFG) and gas chromatography (GC), molecular level investigations of catalytic reactions were performed on platinum single crystal surfaces. The SFG spectra and GC data was correlated to elucidate the nature of active species present on the surface under high-pressure catalytic reactions.

The effect of structure sensitivity and insensitivity of several catalytic reactions were investigated. Ethylene hydrogenation, a structure insensitive reaction, was performed over both Pt(111) and Pt(100). The reaction rate was the same on both surfaces (11 molecules/site/sec 300 K), although the relative concentrations of surface species were observed to be different. Both ethylidyne and di-σ bonded ethylene, strongly adsorbed species, were present on the surface under reaction conditions. These species were not responsible for catalytic turnover. Weekly adsorbed species

such as π-bonded ethylene and ethyl intermediates are responsible for surface turnover as revealed by SFG.

Cyclohexene hydrogenation and dehydrogenation were also performed on Pt(100) and Pt(111). Cyclohexene dehydrogenation is structure sensitive and it was found that the rate of dehydrogenation was higher on the (100) surface of platinum. From SFG results, it was concluded that dehydrogenation can proceed through both 1,3- and 1,4-cyclohexadiene intermediates, although, the rate proceeds faster through the 1,3- intermediate. The rate dehydrogenation on Pt(100) was higher because there was a higher concentration of 1,3-cyclohexadiene on the Pt(100) surface as compared to the (111) surface.

By exposing Pt(111), Pt(100), and Pt(557) single crystal surfaces to high pressures of CO, it was found that Pt-carbonyls could be produced leading to the dissociation of CO. In addition, it was found that CO dissociation was structure sensitive when the crystals were exposed to 40 Torr of CO. The Pt(100) surface was the most active and showed dissociation at 500 K, while the Pt(111) surface was the least active with a dissociation temperature of 673 K. Pt(557) exhibited a dissociation temperature at 548 K, between the two other surfaces. Surface roughness was found to affect the temperature of dissociation and Pt-carbonyls were responsible for roughening of the surface. Pt(100) was the most active because the surface reconstructs and roughens at a lower temperature than the other two surfaces. In addition, CO oxidation experiments were performed on all three surfaces and the ignition temperature followed

the same trend observed for CO dissociation. This indicates that CO dissociation is important for the onset of ignition.

An in depth study of CO oxidation on Pt(557) was performed on both clean and carbon-covered prepared surfaces. Under excess O_2 and excess CO conditions, a clean prepared platinum surface will remain carbon free below and above ignition. It was found that a carbon oxide species was formed on carbon covered platinum surfaces. The carbon oxide species was also found to form on clean prepared platinum below ignition when it was exposed to equal partial pressures of CO and O_2. The turnover rates on the carbon covered platinum surfaces below ignition were higher than on clean surfaces. This indicates the surface carbon oxide species is better at oxidizing CO than platinum. Below ignition, the reaction followed Langmuir-Hinshelwood surface reaction kinetics while above ignition there are multiple reaction channels. Because of the very high turnover rates the combustion of CO becomes mass transport controlled. However, our findings that two different CO/O_2 ratios yield different rates of reaction above ignition indicate that a surface reaction controlled process is also present. The ignition temperature on the carbon-covered surface was lower than on the clean prepared platinum surface at equal pressures of CO and O_2. This is additional evidence that CO dissociation is an important step during the onset of ignition.

ACKNOWLEDGMENTS

I would like to thank Professor Gabor Somorjai for all of the advice and support that he has offered me throughout my career here at Berkeley. His enthusiasm for science is truly amazing and makes learning enjoyable. Because of his direction, I have grown both as a scientist and as an individual. He has truly been a great mentor and working in this research group has been the greatest opportunity of my life.

Berkeley is an amazing place to learn and perform research. I do not think that it is possible to have an institution with a greater number of renowned scientists and colleagues. It is a wonderful place to learn and live new experiences that are not possible anywhere else.

I would like to acknowledge the support and direction I received from Professor Mark Bussell at Western Washington University. He is the first person who gave me the opportunity to learn how to be a research scientist. Without his guidance, I would not have had the desire to extend my education beyond my Bachelor of Science degree.

I must thank all of my friends and colleagues I have had the pleasure to meet and work with at Berkeley. I must especially thank Xingcai Su for teaching me SFG and vacuum techniques. I express my gratitude to Steve Baldelli for sharing with me his wisdom and expertise of SFG and non-linear optics. I thank Saskia Hoffer and Yong Chen for their friendship, we came to the group the same year and we had to go through the hurdles of graduate school together. I thank all of the past and present Somorjai Group members that have offered me advice with regards to lasers and

vacuum equipment, particularly Keith Rider, Craig Tewell, Peilin Chen, Enrico Magni, Aric Opdahl, Jessica Parker, Erin Eppler, Seong Kim, Zhan Chen, Kyle Kung, Joel Roberts, Staffan Westerberg, Ji Zhu and Kevin Hwang. I would also like to thank Inger Coble and Denise Logsdon for all of their help with administrative issues.

I would especially like to thank Jenni for all of her support and enthusiasm she has given me these last few years. She has truly made Berkeley a much more enjoyable place for me. I look forward to our many years together yet to come.

None of this would have been possible with the constant love and support that my parents have given me throughout my life. They have always supported me through all of my endeavors I have attempted an achieved, and they have always been there for me. I thank my sister for always believing in me and for her encouragement. She always kept my best interests in mind. She is truly a great sister.

This work was supported by the Director, Office of Energy Research, Office of Basic Energy Sciences, Materials Science Division of the U.S. Department of Energy.

TABLE OF CONTENTS

LIST OF FIGURES

Chapter 1: Introduction:

Motivation to Study Catalysis *in situ* under High-Pressures

Since the advent of modern surface science, ultrahigh vacuum (UHV) techniques have been used to probe the identity of molecules adsorbed on the surfaces of single crystals. Information about structure and bonding was obtained with low-energy electron diffraction (LEED), Auger electron spectroscopy (AES), X-ray photoelectron spectroscopy (XPS), high-resolution electron energy loss spectroscopy (HREELS), and other techniques.[1,2,3,4,5] These techniques utilize electrons to probe and characterize surfaces; however, they are limited to low pressures because of the large mean free path required for the electrons to reach either the sample or detector.

Obviously, these techniques are not practical for *in-situ* characterization of surfaces during high-pressure catalytic reactions. To understand the surface composition during reactions with these electron-utilizing techniques, a single crystal was characterized in UHV prior to application of catalytic reaction conditions. A catalytic reaction was then monitored by gas chromatographic analysis of the gas phase composition during the reaction to provide data for the determination of kinetics. Once the reaction was completed, the sample was again exposed to a low pressure to allow the use of these electron techniques to characterize the surface after the reaction.[6,7,8,9] These investigations were very insightful in showing that many reactions can cause

surface restructuring. In addition, certain reaction pathways were proposed to explain catalytic reactions from this indirect characterization method.

Additional characterizations allowed the identification of reaction intermediates on catalysts by performing reactions in UHV and using techniques such as high-resolution electron energy loss spectroscopy (HREELS). The catalyst was exposed to a few Langmuirs of reactants, usually at low temperatures. The sample was then heated, and surface species were observed to change; reaction intermediates were then proposed. Temperature program desorption experiments also gave insight to products produced from adsorbates under UHV conditions. However, it is difficult to extrapolate these results to actual high-pressure reactions because the surface compositions under UHV and reaction conditions are most likely substantially different from each other. The concentration of adsorbates on the surface under high-pressures can be very different than a saturated surface under UHV conditions.

Because of the limitations described above, it became clear that molecular-level investigations of surfaces under actual high-pressure catalytic reaction conditions are necessary to obtain a better understanding of catalytic reactions. Photons, in contrast to electrons, are not limited to UHV conditions and can readily probe surfaces under high pressure. As long as photons can reach the surface unperturbed by the high-pressure gasses under catalytic reaction conditions, photon techniques can be utilized to study surfaces. Vibrational spectroscopies such as infrared (FTIR) and Raman are useful because they give the molecular identity of adsorbates on the surface. The difficulty in using techniques such as IR spectroscopy is that both the bulk material of the catalyst and gas-phase reactants can interfere with surface measurements, necessitating the

subtraction of both gas-phase and bulk spectra from IR data to obtain surface information. IR spectroscopy is a great technique for use under low-pressures, but once pressures become too high, the gas phase molecules can completely absorb an infrared beam inhibiting the use of any normalization method. In addition, IR spectroscopies are governed by linear optics which means output photons are at the same frequency as the input photons, requiring detection in the IR region. Unfortunately, if a catalytic reaction needs to be heated to high temperatures, the IR photons produced by black-body radiation can interfere with the acquired IR spectrum. These problems associated with IR spectroscopy prohibit it from being a useful technique to study catalysis under high-pressures and high-temperatures.

Thus, a technique utilizing photons with surface specificity under high-pressures and high-temperatures was required. Recently, sum frequency generation (SFG) has been developed to study surfaces and interfaces.[10,11,12,13,14] SFG is a second order nonlinear optical process in which a tunable IR beam and a fixed visible beam are overlapped on a surface to generate third beam at the sum of the two input beams, which is also in the visible region. SFG has the advantage in that its selection rules necessitate that a vibrational mode must have a change in dipole and a change in polarizability in order for the process to occur. Only at surfaces and interfaces are these selection rules met. Thus, SFG is surface specific, allowing the use of this technique under high-pressures of gasses. Another advantage of SFG is that it is sensitive to sub-monolayer coverages of adsorbates. In addition, because the photons that are detected are in the visible spectrum, IR photons generated by black-body radiation to not interfere in the detection of an SFG spectrum allowing the use of SFG at high-

temperatures as well as high-pressures. A comparison of the pressure accessibility for the techniques just discussed is shown in Figure 1.1.

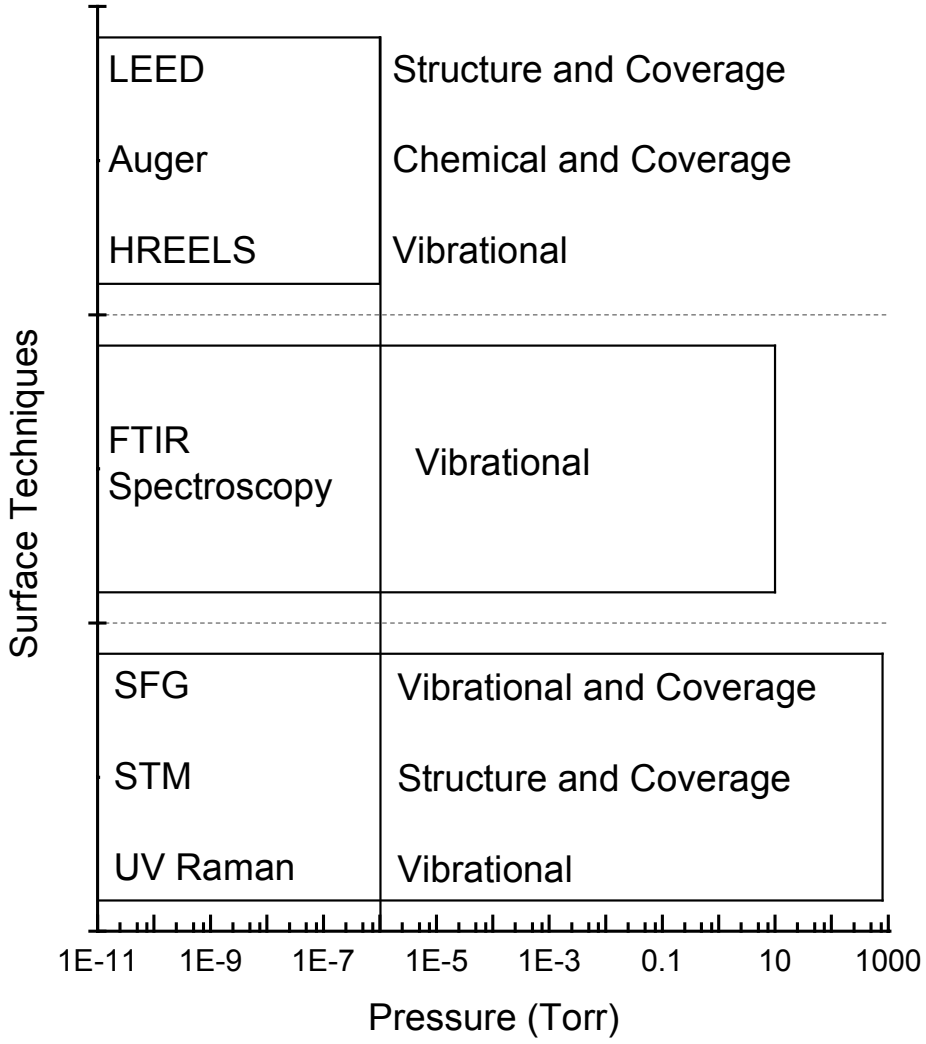

Figure 1.1 Comparison of some common surface science techniques. Type of information gained and pressure the techniques can be used.

The Concept of Structure Sensitivity of Catalytic Activity and Selectivity

An important area in modern catalysis research is devoted to the understanding of what determines the selectivity of a catalyst. One of the Department of Energy's goals in waste minimization is to "Identify reactions and catalysts for synthesizing chemical products at greater than 90% yields without forming toxic by-products."[15] Current industrial practices release thousands of metric tons of waste from catalytic by-products. The 50 top commodity chemicals produced by catalysis release 20.9 billion pounds of CO_2 a year either by direct release or through the incineration of unwanted bi-products.[16] With catalysts that perform at a higher selectivity, these emissions could be greatly decreased. As of 1992, chemical industry produced roughly 120 thousand tons of waste material through catalytic processes.[17] This waste included sludge from oil refining and also contaminated clays used to purify desired products by removing by products. Much of this waste is deposited in landfills. In order to increase selectivity of catalysts, we must have an understanding at the molecular level of catalytic processes so better catalysts can be engineered with the ingredients that control selectivity.

The only way to gain an understanding of what controls selectivity is to investigate the processes of catalytic reactions at the molecular level. Techniques are required that can probe catalysts under conditions similar to those used in industry processes (high-pressure and high-temperature). SFG is a powerful technique to study single crystal surfaces under high-pressure catalytic conditions because it is surface

specific and has such a high sensitivity. One of the ingredients that have been identified to be important in selectivity is surface structure. Different single crystal surfaces have been shown to exhibit different selectivity characteristics.

In the late 1960's, Boudart classified catalytic reactions as being either structure sensitive or structure insensitive. The experimental data that was the basis of the classification correlated the turnover rates for a given reaction with catalyst particle size; if the reaction rate stayed constant the reaction was insensitive to the catalyst structure[18]. This was the case for most hydrogenation processes including that of ethylene[19]. If the reaction rate varied with changes of particle size the reaction was structure sensitive. This was the case for ammonia synthesis and the dehydrogenation of cyclohexene and cyclohexane as well as for hydrogenolysis of alkanes.[20,21] When ammonia synthesis was studied on iron single crystal surfaces, the reaction of nitrogen and hydrogen to form ammonia, showed extreme structure sensitivity.[22] The (111) and (211) surfaces were orders of magnitude more active than the close packed (110) crystal face of body centered cubic iron.

An example of how structure effects selectivity can be found in the conversion of n-hexane and n-heptane to various products (reforming). This reaction can follow at least four reaction channels to form aromatic molecules, cyclic molecules, branched isomers, and undergo C-C bond breaking leading to hydrogenolysis.[23] Depending on the crystal structure (the surface structure) the reaction selectivity can be altered. On the (111) crystal face the aromatic molecules are produced at higher concentrations. On the (100) crystal face the isomerization reaction is predominant. In the presence of

kinked surface sites in the steps, C-C bond breaking has been observed leading to the undesirable hydrogenolysis reaction.[24]

The foundation of structure sensitivity has been well laid out but the understanding of why structure effects a reaction is still in question. The goal of this research is to understand how structure effects a catalytic reaction at a molecular level using SFG to probe catalytic reactions under high-pressure conditions. Simultaneous to SFG experiments under high-pressure of gases; gas chromatography was used to monitor reactant and product concentrations during the reaction so kinetics could be calculated.

Several reactions were carried out to determine the effect of structure on the reactions. The first case is ethylene hydrogenation. This is known to be a structure insensitive reaction. Ethylene hydrogenation was investigated on both Pt(111) and Pt(100). The effect of structure was investigated under both UHV conditions and high-pressure conditions. Under both pressure regimes, the results are substantially different, although the rate of ethane production is essentially the same on both surfaces.

The next reaction studied was the hydrogenation and dehydrogenation of cyclohexene on both Pt(111) and Pt(100). In general, dehydrogenation processes are surface-sensitive. Again, the effect of structure was investigated under UHV conditions and high-pressures and the results for both surfaces were very different. The rate of dehydrogenation was higher on the Pt(100) surface, and it was determined that the concentration of the active intermediate relative to the inactive intermediate was higher on this surface as compared to Pt(111).

The structure sensitivity of CO dissociation was also investigated by SFG on Pt(111), Pt(100), and Pt(557). It was determined that under high-pressures of CO, surface platinum atoms can become mobile. On Pt(111), the temperature at which platinum atom mobility begins is at a much higher temperature than the Pt(100) surface, which easily reconstructs. Because of this mobility, the coordination of platinum atoms decreases producing step and kink sites onto which platinum carbonyls can form. These platinum carbonyls are the precursor to CO dissociation. Because Pt(557) is essentially a Pt(111) surface with introduced steps, the temperature at which CO dissociation occurs is between the temperature observed for Pt(111) and Pt(100).

Carbon monoxide oxidation is known to be structure insensitive, although it was found that the temperature at which ignition occurs is structure sensitive. It was found that the trend in CO oxidation ignition temperatures was similar to the trend observed for CO dissociation, and so it was concluded that CO dissociation is an important step in catalytic ignition. To further support this idea, detailed CO oxidation studies were performed on Pt(557). CO dissociation could be observed *in situ* under CO oxidation conditions depending on the reaction conditions.

References

[1] G.A. Somorjai, "Introduction to Surface Chemistry and Catalysis", John Wiley & Sons, New York, 1994.

[2] G.A. Somorjai, *Surf. Sci.* 1994, **299/300**, 849.

[3] D.W. Goodman, *Chem. Rev*. 1995, **95**, 523.

[4] G. Ertl, *Surf. Sci.,* 1994, **299/300**, 742.

[5] Woodruff, D.P., and T.A. Delchar, "Modern Techniques of Surface Science", Cambridge University Press, New York, 1986.

[6] Blakely, D.W., Kozak, E., Sexton, B.A., and G.A. Sormorjai, *J. Vac. Sci. Technol.* 1976, **13**, 1091.

[7] Cabrera, A.L., Spencer, N.D., Kozak, E., Davies, P.W., and G.A. Somorjai, *Rev. Sci. Instrum*. 1982 **53**, 1888.

[8] Rupprechter, G., and G.A. Somorjai, *Catal. Lett.* 1997, **48**, 17.

[9] Davis, S.M., Zaera, F., and G.A. Somorjai, *J. Am. Chem. Soc.* 1982, **104**, 7453.

[10] Y.R. Shen, *Surf. Sci.* 1994, **299/300**, 551.

[11] Du, Q., Superfine, R., Freysz, E., and Y.R. Shen, *Phys. Rev. Lett.* 1993, **70**, 2313.

[12] Johal, M.S., Ward, R.N., and P.B. Davies, *J. Phys. Chem.* 1996, **100**, 274.

[13] Conboy, J.C., Messmer, M.C., and G.L. Richmond, *J. Phys. Chem.*1996, **100**, 7617.

[14] Y.R. Shen, *Nature* 1989, **337**, 519.

[15] Catalysis Research Waste Minimization Goals, Department of Energy, Available: http://www.catalysis.anl.gov/catalysis/waste.html.

[16] Catalysis Research, Department of Energy, Available: http://www.catalysis.anl.gov/.

[17] Vision 2020 Catalysis Report, The Council for Chemical Research, Available: http://www.ccrhq.org/vision/index/roadmaps/catrep.html.

[18] M. Boudart, *Adv. Catal.* 1969, **20**, 153.

[19] Zaera, F., and G.A. Somorjai, *J. Am. Chem. Soc*. 1984, **106**, 2288.

[20] Spencer N.O., Schoonmaker R.C, and G.A. Somorjai, *Nature* 1981, **294(5842)**, 643.

[21] Herz R.K., Gillespie W.D., Petersen E.E., and G.A. Somorjai, *J. Catal.* 1981, **67**, 371.

[22] Strongin, D.R., Carrazza, J., Bare, S.R., and G.A. Somorjai, *J. Catal.* 1987, **103**, 213.

[23] J.H. Sinfelt, *Catal. Lett.* 1991, **9**, 159.

[24] G.A. Somorjai, *8th International Congress on Catalysis. Proceedings. Vol. 1: Plenary Lectures*, 1984.

Chapter 2: Sum Frequency Generation (SFG)

Introduction

Sum frequency generation is a surface-specific vibrational spectroscopy with sub-monolayer sensitivity and pico-second time resolution. A visible laser beam at a fixed wavelength is overlapped with a tunable IR laser beam as shown in Figure 2.1. Vibrational spectra can be acquired by scanning the IR beam over the vibrational region of interest.

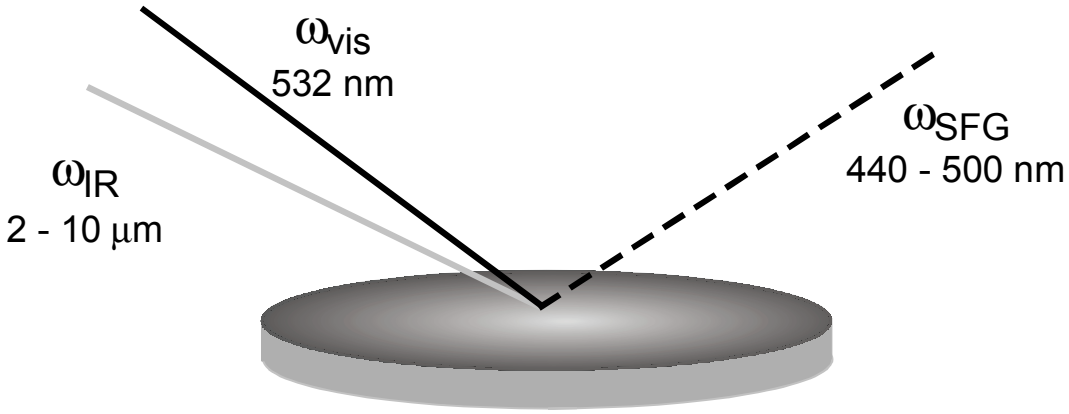

Figure 2.1 Overlap of the infrared and visible laser beams on a metal surface to produce the sum frequency beam.

SFG is powerful for investigating catalytic reactions on smooth surfaces such as those of a single crystal or an ordered material. Unfortunately, porous materials scatter the input beams so that only a weak SFG beam can be detected, and therefore the

applications of SFG to most typical solid catalysts are limited. Another disadvantage of SFG is that a spectrum may take anywhere from 10 minutes to an hour to obtain, depending on the number of laser shots averaged and width of frequency range investigated. Currently, the technique of broadband SFG is under development to allow the acquisition of spectra several hundred wavenumbers in width simultaneously with each laser shot, which will greatly reduce the acquisition time.

Theory Behind SFG

A discussion of the SFG process is presented here and more detailed descriptions can be found in the literature.[1,2,3,4,5] The principle of SFG is governed by second-order nonlinear optics, and the technique is made possible by the use of high-energy pulsed lasers. Under weak electric fields, the polarization of a material is described by

$$(1) \quad \vec{P} = \vec{P}^{(0)} + \vec{P}^{(1)}$$

$$(2) \quad \vec{P}^{(1)} = \varepsilon_0 \chi^{(1)} \vec{E}(r) \cos(\omega t)$$

where $\vec{P}^{(0)}$ is the static polarization, $\vec{P}^{(1)}$ is the first-order linear polarization, $\chi^{(1)}$ is the linear susceptibility, ε_o is the permittivity of free space, t is time, and $\vec{E}(r)$ cos(ωt) describes the electric field. In linear optics, as this equation indicates, the frequency of light is invariant as it passes through a medium, the frequency of the input beam is the same as the output beam. Under strong electric fields, such as those produced by lasers, second- and higher-order polarization terms must be added to eq. (1):

$$(3) \quad \vec{P} = \vec{P}^{(0)} + \vec{P}^{(1)} + \vec{P}^{(2)} + \vec{P}^{(3)} + \ldots$$

$$(4)\quad P_i^{(2)} = \varepsilon_0 \sum_{j,k} \chi_{ijk}^{(2)} \vec{E}_j(r)\cos(\omega_1 t)\vec{E}_k(r)\cos(\omega_2 t)$$

where $\chi^{(2)}$ is the second-order nonlinear susceptibility. The subscripts i, j, and k refer to the axes of the coordinate system. If the frequencies ω_1 and ω_2 are the same ($\omega_1 = \omega_2 = \omega$), $P_i^{(2)}$ can be rearranged by simple trigonometry to give the form

$$(5)\quad P_i^{(2)} = \tfrac{1}{2}\varepsilon_0 \sum_{j,k} \chi_{ijk}^{(2)} \vec{E}_j(r)\vec{E}_k(r)(1+\cos 2\omega t)$$

which indicates that a second frequency of light oscillating at 2ω can be generated from an oscillating dipole in the medium. This process is called second harmonic generation. If ω_1 and ω_2 are oscillating at different frequencies, then eq. (4) can be rearranged to the form

$$(6)\quad P_i^{(2)} = \tfrac{1}{2}\varepsilon_0 \sum_{j,k} \chi_{ijk}^{(2)} \vec{E}_j(r)\vec{E}_k(r)\left[\cos(\omega_1+\omega_2)t + \cos(\omega_1-\omega_2)t\right]$$

From the term in brackets of eq. 6, we see that there is now the possibility of generation by an oscillating dipole of frequencies at the sum and difference of ω_1 and ω_2. These two processes are known as SFG and difference frequency generation (DFG), respectively. In this work we focus on SFG although DFG also occurs.

The magnitude of the SFG signal is proportional to the absolute square of $\chi^{(2)}$ ($|\chi^{(2)}|^2$) which is made up of both a non-resonant susceptibility term ($\chi_{NR}^{(2)}$) and a

$$(7)\quad \chi^{(2)} = \chi_{NR}^{(2)} + \chi_{R}^{(2)}$$

resonant susceptibility ($\chi_R^{(2)}$) term. The non-resonant susceptibility term originates from the substrate surface and is typically invariant as the IR beam is scanned; it is

called the non-resonant background.

SFG is surface specific because $\chi^{(2)}$ is a third rank tensor whose element values depend on the properties of the medium under investigation. In a medium with inversion symmetry, $\chi^{(2)}$ should be invariant under inversion symmetry, however, the electric field and polarization must change sign as vectors. Thus, the inversion operation gives: $\chi^{(2)} = -\chi^{(2)}$ or $\chi^{(2)} = 0$ and therefore there is no SFG signal from a medium with inversion symmetry. In order for a medium to generate SFG signal, inversion symmetry has to be broken, which is only necessarily true at an interface or surface.

The resonant susceptibility, which originates from vibrational modes on the surface, is described by

$$(8)\quad \chi_R^{(2)} = N\chi_{i,j,k}^{(2)} \sum_{l,m,n} \left\langle (\hat{i}\cdot\hat{l})(\hat{j}\cdot\hat{m})(\hat{k}\cdot\hat{n}) \right\rangle \frac{A_q}{\omega_{IR} - \omega_q + i\Gamma_q} \Delta\rho_{gq}$$

where A_q is the strength of the qth vibrational mode, N is the number density of molecules on the surface, ω_{IR} the frequency of the infrared laser beam, ω_q the frequency of the qth vibrational mode, Γ_q the damping constant of the qth vibrational mode, and $\Delta\rho_{gq}$ is the population difference between the ground and fist excited states. The subscripts l, m, and n, refer to the axes for the molecular coordinate system and so the average, $\left\langle (\hat{i}\cdot\hat{l})(\hat{j}\cdot\hat{m})(\hat{k}\cdot\hat{n}) \right\rangle$, is the coordination transformation from molecular fixed coordinates to laboratory fixed coordinates averaged over molecular orientations. From eq.(8), it is observed that $\chi_R^{(2)}$ is at a maximum when $\omega_{IR} = \omega_q$, and hence a vibrational spectrum is acquired by scanning the IR frequency. The selection rules for

the SFG process are inferred from the equation

$$(9)\quad A_q = \frac{1}{2\omega_q}\frac{\partial \mu_n}{\partial q}\frac{\partial \alpha_{lm}^{(1)}}{\partial q}$$

where μ_n is the dipole moment and $\alpha_{lm}^{(1)}$ the polarizability. Hence, in order for $\chi_R^{(2)}$ to be non-zero, the vibrational mode of interest must obey both IR and Raman selection rules; there must be both a change in the dipole and a change in the polarizability. Because SFG is a second-order nonlinear process, only a medium without inversion symmetry can generate SFG signals under the electric-dipole approximation. Surfaces or interfaces lack inversion symmetry; therefore modes at surfaces and interfaces are SFG allowed. Centrosymmetric bulk materials and isotropic gas phases have centrosymmetry and are therefore SFG forbidden. Therefore, SFG is a surface-specific process. Because gas phases are isotropic and not SFG active, experiments can easily be performed from pressures of 1×10^{-10} Torr up to 10^3 Torr without the concern of gas phase interference.

The intensity of an SFG signal is also dependent on the ordering of the surface or interface. If molecules on the surface are randomly oriented, then $\chi^{(2)}$ becomes zero and SFG spectra will not be generated. Therefore, when examining a SFG spectrum, strong SFG features indicate that the surface adsorbates are well ordered.

Sum Frequency Generation from a Surface

As previously discussed, $\chi^{(2)}$ is a third rank tensor. It consists of 27 elements, whose values are a property of the medium under investigation and invariant under symmetry operations. The number of non-vanishing $\chi^{(2)}$ elements is often quite small

because the matrix elements depend on the symmetry of the medium. For an isotropic surface there are four nonequivalent, non-vanishing terms for $\chi^{(2)}$, as the others are equal to zero from considerations of rotational and mirror symmetries. The value of these four terms are: $\chi^{(2)}_{xxz} = \chi^{(2)}_{yyz}$, $\chi^{(2)}_{xzx} = \chi^{(2)}_{yzy}$, $\chi^{(2)}_{zxx} = \chi^{(2)}_{zyy}$, and $\chi^{(2)}_{zzz}$. They are determined by inserting the 27 possible combinations of (x, y, z) into the four-fold rotation operation: x' $\rightarrow$ y and y' $\rightarrow$ -x in combination with the two-fold rotation operation: x' $\rightarrow$ -x and y' $\rightarrow$ -y.

By using different polarization combinations for the IR, visible, and detected SFG light, information about molecular orientation on the surface may be obtained for non-metal surfaces.[6] For each polarization combination used during a SFG experiment, different susceptibility components are measured. The two incident beams in the SFG experiment can be brought onto the surface four different polarization combinations. Over an isotropic surface, these combinations determine the ratios of the different tensor elements, which provides information on the molecular orientations. By modeling these susceptibility components, it is then possible to determine the orientation of surface molecules. The (s,s) combination measures the $\chi^{(2)}_{zxx} = \chi^{(2)}_{zyy}$ elements and generates an out signal which is p-polarized. The notation for this polarization combination is PSS, where the polarizations represent the SF signal, incident visible and IR beams, respectively. The combinations of (s, p) and (p, s) mainly measure $\chi^{(2)}_{xxz} = \chi^{(2)}_{yyz}$, $\chi^{(2)}_{xzx} = \chi^{(2)}_{yzy}$ while (p, p) mainly measures $\chi^{(2)}_{zzz}$.

This polarization technique is not possible for the characterization of metal surfaces. Because of the metal-surface-selection rules (MSSR), an s-polarized IR beam

is canceled out due to the image field of the electrons in the metal. As a dipole parallel to the surface vibrates, a dipole opposite in sign oscillates at the same frequency. Therefore, an s-polarized IR beam cannot excite a dipole along a metal surface, and so when performing SFG experiments on a metal surface, the IR beam is always p-polarized. The visible beam may be either s- or p-polarized, but the signal is almost 40 times weaker for s-polarized visible light. Therefore, in the experiments reported here, both the IR and visible light were p-polarized, resulting in p-polarized SFG output.

References

[1] Y.R. Shen, *Surf. Sci.* 1994, **299/300**, 551.

[2] Du, Q., Superfine, R., Freysz, E., and Y.R. Shen, *Phys. Rev. Lett.* 1993, **70**, 2313.

[3] Johal, M.S., Ward, R.N., and P.B. Davies, *J. Phys. Chem.* 1996, **100**, 274.

[4] Conboy, J.C., Messmer, M.C., and G.L. Richmond, *J. Phys. Chem.*1996, **100**, 7617.

[5] Y.R. Shen, *Nature* 1989, **337**, 519.

[6] Hirose, C., Yamamoto, H., Akamatsu, N., and K. Domen, *J. Chem. Phys.* 1993, **97**, 10064.

Chapter 3: Experimental Considerations

Laser System

This work was performed using two different optical parametric generation/optical parametric amplification (OPG/OPA) laser setups used to generate the 532 nm visible green beam and the tunable IR beam. Both systems were driven by the fundamental output of a Nd:YAG laser. The laser operated at 20 Hz and provided a 20-ps pulse at a fundamental frequency of 1064 nm with 35 mJ of energy per pulse.

For the first laser system, just beyond the Nd:YAG laser, the beam was split into two separate beams. The first passed through a KD_2PO_4 (KD^*P) nonlinear crystal that doubled the frequency of the fundamental beam to 532 nm. This beam was used for the visible portion of the SFG experiment and had output energy of 400 μJ/pulse.

The second part of the fundamental beam passed through one of two angle-tuned optical parametric generation/optical parametric amplification (OPG/OPA) stages for the generation of the tunable IR source as shown in Figure 3.1.[1] A $LiNbO_3$ OPG/OPA stage was used to generate a tunable IR beam with frequencies between 2700 and 3600 cm^{-1}, which allowed investigation of the vibrational C-H stretching modes of adsorbed hydrocarbons. The maximum output of this stage was at 2850 cm^{-1} with 200 μJ of energy and a full width at half maximum (fwhm) of 12 cm^{-1}. The second OPG/OPA stage consisted of BaB_2O_4 (BBO) and $AgGaS_2$ (AGS) nonlinear

crystals to produce a tunable IR beam with frequencies between 1400 and 2300 cm^{-1} to probe vibrational modes associated

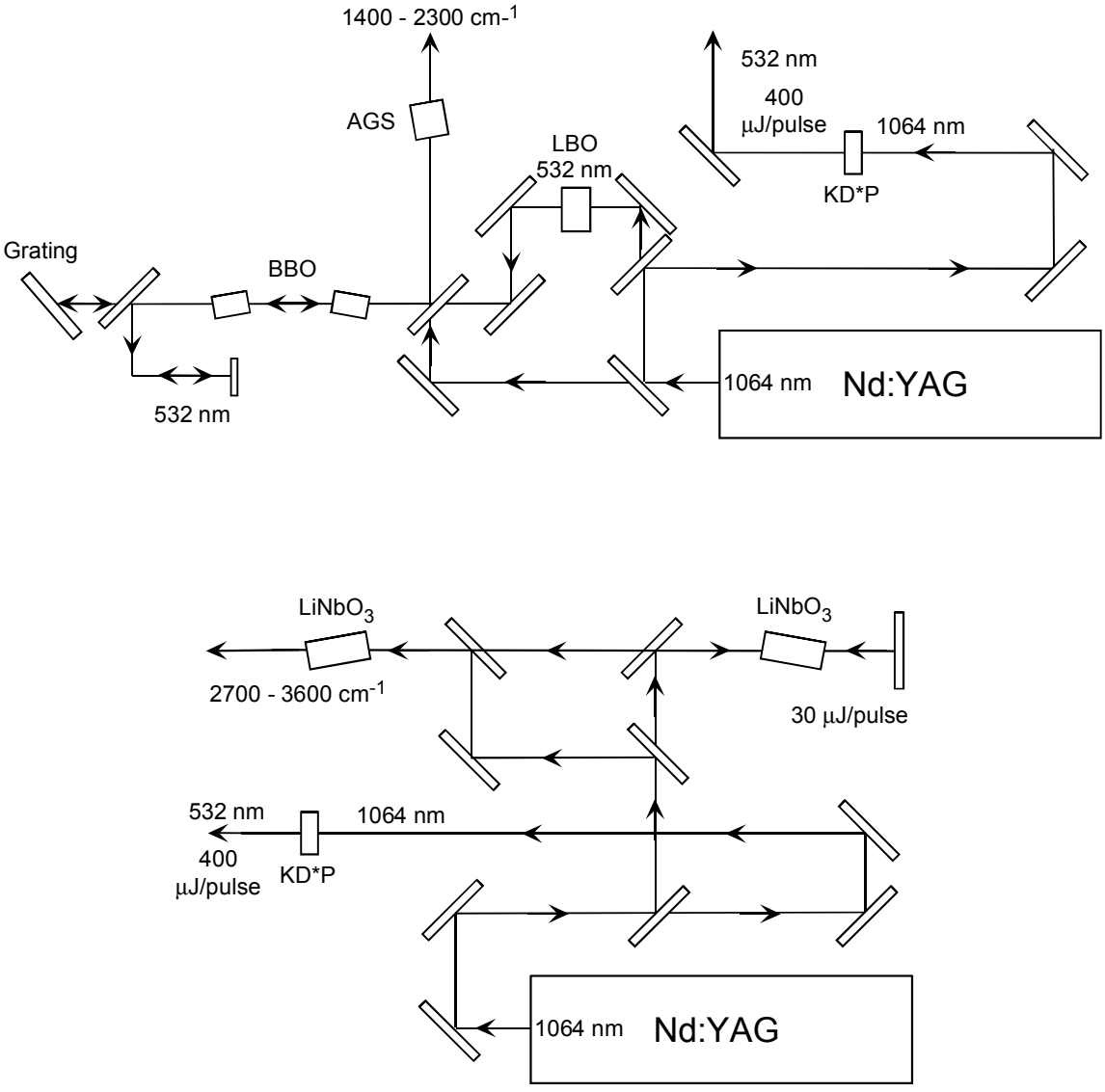

Figure 3.1 Schematic of two different OPG/OPA systems to generate laser beams used for SFG experiments. Tuning range is between 1400 –2300 cm^{-1} and 2700 – 3600 cm^{-1}.

with CO adsorbed in various coordination. The maximum output of this stage occurred at 2200 cm^{-1} with 120 μJ of energy and a fwhm of 8 cm^{-1}.

The second laser system was a commercially built OPG/OPA system provided by Laservision (Figure 3.2). The fundamental beam was passed through a KTP crystal to generate a 532 nm beam. This beam was then split, with a portion being used for the visible portion of the experiment and the second portion was sent to a OPG/OPA stage utilizing to counter rotating KTP crystals to generate a near IR beam between 720 and 870 nm. This near IR beam was then difference frequency mixed with a portion of the fundamental beam through two counter rotating KTA nonlinear crystals. This then generated a tunable IR beam between 2000 and 4000 cm^{-1}. The energy at 2875 cm^{-1} was 400 μJ with a fwhm of 10 cm^{-1}. By sliding in an $AgGaSe_2$ nonlinear crystal into

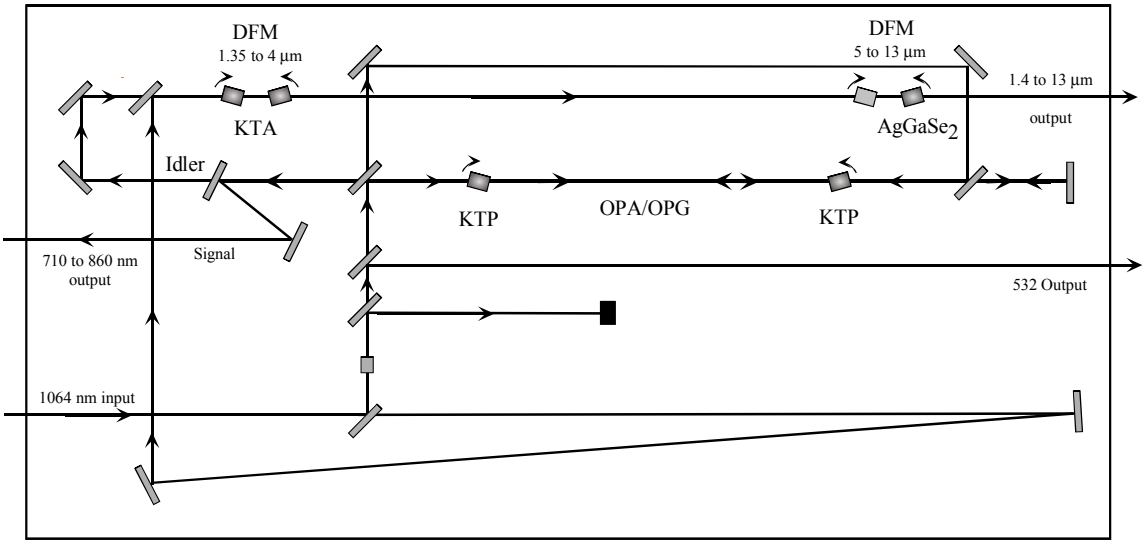

Figure 3.2 Schematic of LaserVision OPG/OPA system to generate laser beams for SFG experiments. Tunable between 1.4 and 13 μm.

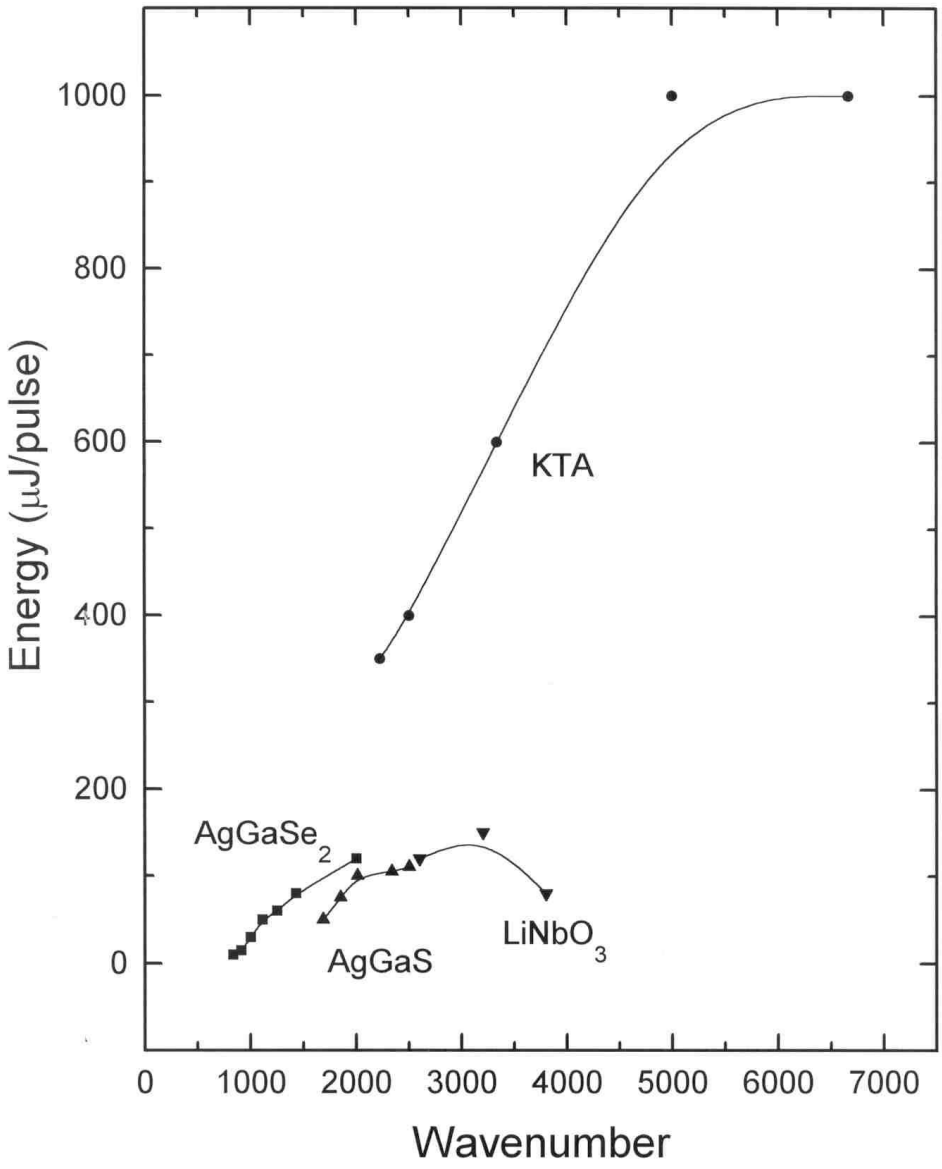

Figure 3.3 Comparison of the energy versus frequency curves for the OPG/OPA systems used in this work.

the signal and idler beams from the KTA crystals, a tunable beam between 1000 and 2000 cm^{-1} could be produced. The energy vs. frequency is shown in Figure 3.3 for both laser systems. The Laservision system provides a broader tunable range and also more energy.

Both the IR and visible beams are p-polarized and are both spatially and temporally overlapped on a single crystal mounted in a UHV chamber. The visible beam makes an angle of 50^{o} with respect to surface normal while the IR beam is at 55^{o} with respect to surface normal. The generated SFG beam is then sent through a monochrometer and the signal intensity is detected by a photomultiplier tube (Hamamatsu) and integrated by a gated integrator (Stanford Research).

Ultra High Vacuum System/High Pressure Reactor

Single crystal samples were mounted in a UHV/Reaction chamber pumped by a turbomolecular pump and an ion pump to a base pressure of 2×10^{-10} Torr. A schematic of the instrument is shown in Figure 3.4. The chamber was equipped with an Omicron rear view retarding field analyzer (RFA) for low energy electron diffraction (LEED) and Auger electron spectroscopy. A mass spectrometer was attached to the system to monitor the background gases under UHV conditions. By use of resistive heating, the sample could be heated up to a temperature of 1200 K, and cooled under vacuum with liquid nitrogen to 140 K. The crystals were cleaned in UHV by repeated cycles of Ar^{+} bombardment followed by exposure of 5×10^{-7} Torr of O_2 at 1125 K for two minutes. The sample was then annealed at 1135 K in UHV for one minute.

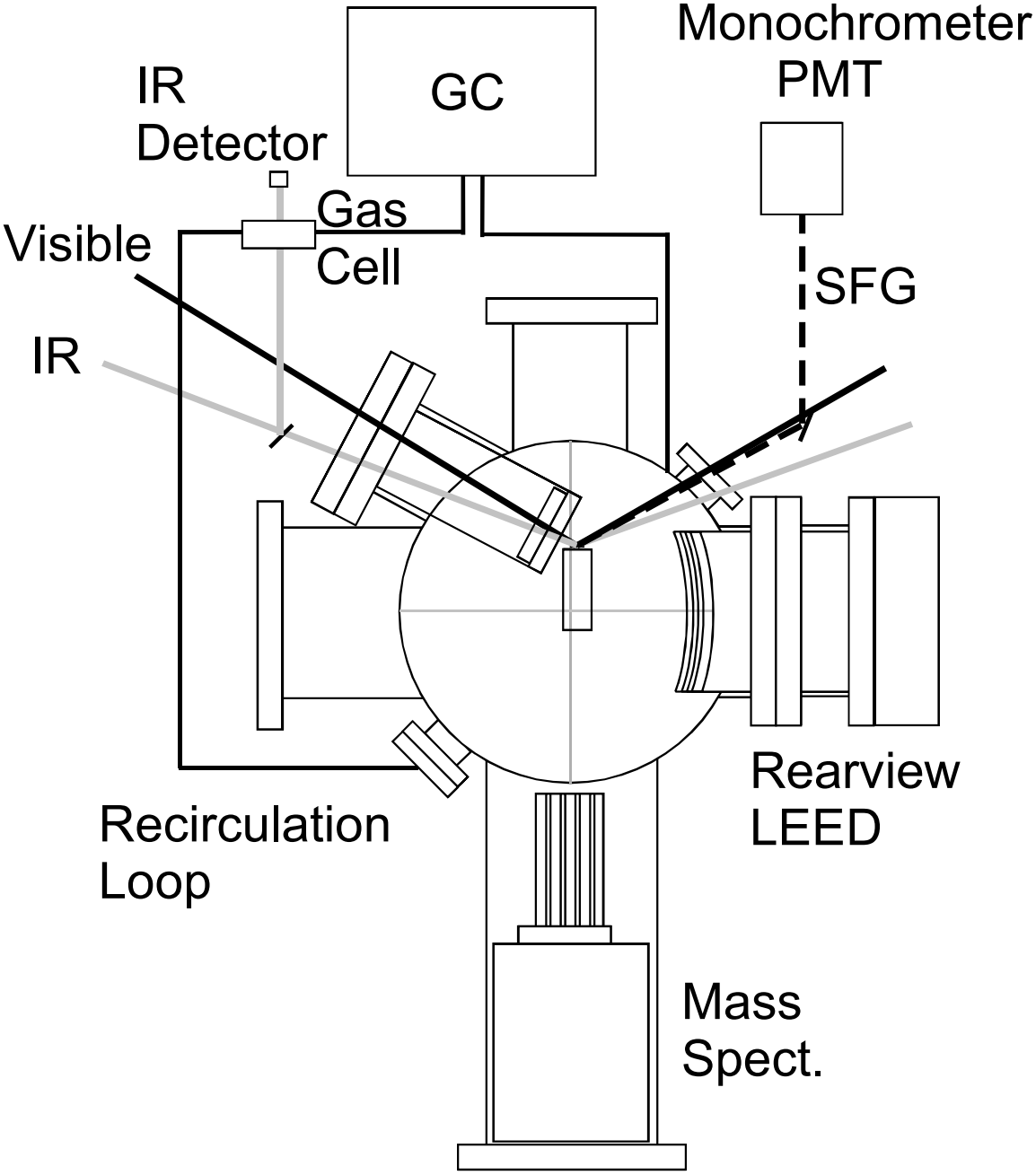

Figure 3.4 Top view schematic of the UHV and High-Pressure reaction system in which the single crystals were mounted.

During high-pressure catalytic reactions, the sample was isolated from the vacuum pumps by a gate valve. A recirculation loop delivered gases to a gas chromatograph to monitor the composition of the gas for the calculations of kinetics. For SFG experiments, the chamber had a window made of CaF_2 to allow the IR light to enter.

Platinum Single Crystals: Structure and Preparation

Three different platinum single crystals were used in this work. They are the (111), (100), and stepped (557) surfaces. The surface structures for the different surfaces are shown in Figure 3.5. The Pt(111) surface is cut to reveal a hexagonal surface structure. The most common sites in which molecules adsorb to the surface are the top-site (on top of a single platinum atom), bridge site (between two platinum atoms), and 3-fold hollow sites (between 3 platinum atoms). A Pt(100) surface is cut to reveal a square surface (1×1) structure. However, if a Pt(100) surface is properly cleaned and annealed, the outermost surface atoms will reconstruct to what is known as a pseudo-hexagonal (5×20) structure similar to the (111) surface.[2,3,4] The phase transition from the (1×1) to the (5×20) structure occurs above 400 K, so as the crystal is cooled after it is cleaned and annealed, the surface is (5×20). Once molecules such as CO or NO are adsorbed on the surface, the surface reconstruction relaxes back to the (1×1) structure. Thus, the (5×20) surface is lower in energy than the (1×1) under vacuum. The Pt(557) surface is prepared by cutting a platinum single crystal 9.5^{o} relative to the (111) orientation.[5,6,7] This prepares a stepped surface with 6 atom wide

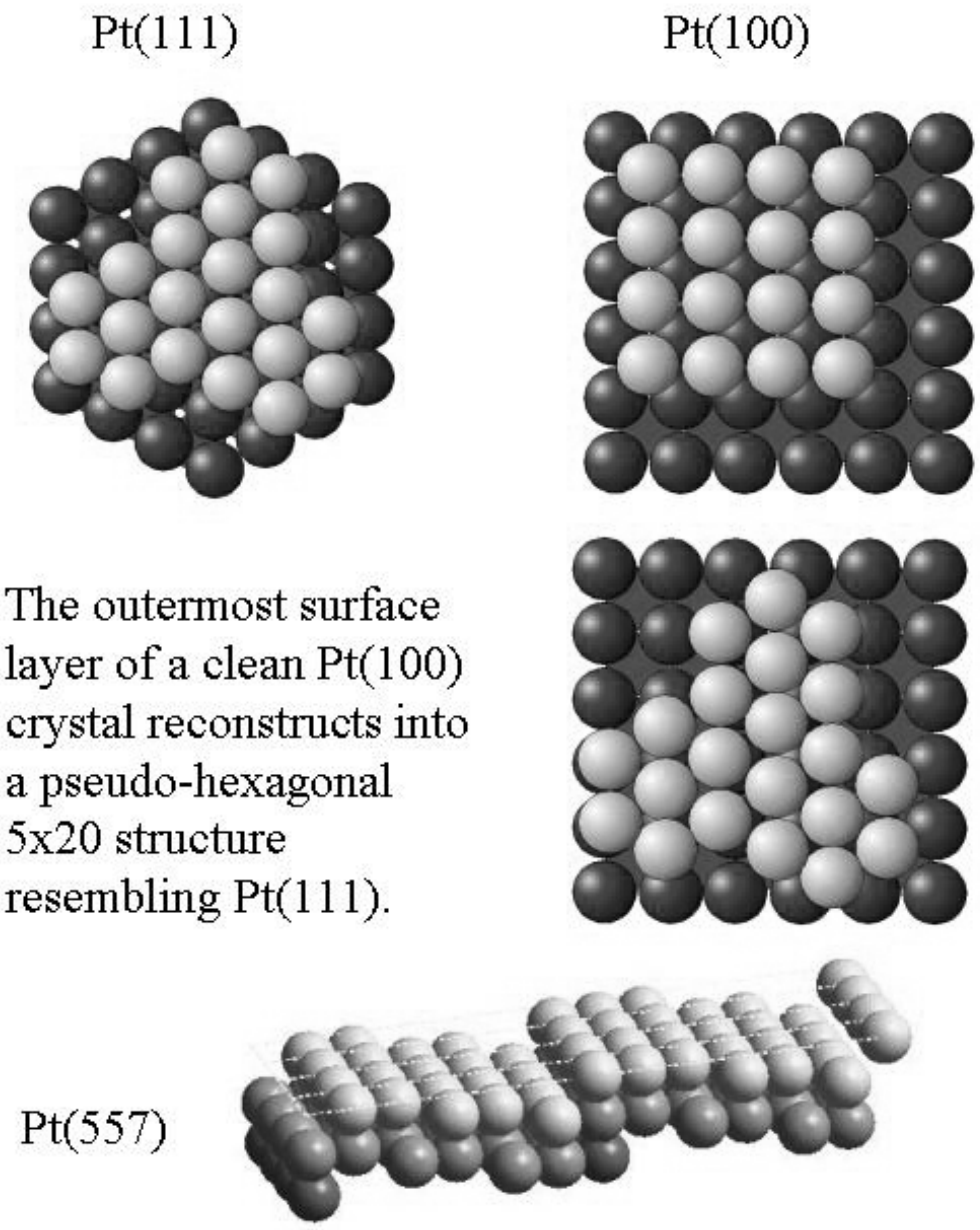

Figure 3.5 Structure of the Pt(111), Pt(100), and Pt(557) single crystal surfaces.

terraces of (111) orientation with single atom high steps. In addition to the sites already mentioned for the Pt(111) surface, the Pt(557) surface also has step sites.

Once the crystal was mounted in the chamber, it was first heated to 1123 K for 30 minutes to outgas the sample and sample holder. The crystal was then cleaned by argon ion sputtering to remove any contaminants on the surface. Argon gas was leaked into the chamber through a leak valve to a pressure of 3×10^{-5} Torr and an electron gun operating at 1200 eV then ionized argon atoms, which then bombarded the surface. The ion sputtering would last for 12 minutes and the sample was then flashed to 1123 K and sputtered again. After the second sputtering step, the sample was exposed to 5×10^{-7} Torr of O_2 and heated to 1123 K for 2 minutes to oxidize any carbon left on the surface. The sample was then cooled and the system was evacuated to below 1×10^{-9} Torr. Next, the sample was annealed at 1133 K for 1 minute and slowly cooled to room temperature. The sample was then checked by Auger spectroscopy to determine whether the surface was clean. If the surface was clean, gasses were introduced either at low or high-pressures depending on the experiment through a gas manifold system.

Auger Electron Spectroscopy

Auger electron spectroscopy is a technique that gives elemental analysis of contaminants on a surface. Not only can it give elemental identity, it can be used analytically to determine the concentration of surface contaminants. The amount of carbon and oxygen are of interest in the experiments to be discussed. Auger electron spectroscopy is a surface sensitive technique because of the limited depth of penetration

of the incident electron beam and because of the high probability of inelastic scattering that electrons exhibit below 2000 eV.[8] The energy of the input electrons was approximately 1500 eV, but the electrons detected by the retarding field analyzer (RFA) were below 600 eV. Because we are detecting such low energy electrons, the electrons could not have penetrated deep into a surface.

During an Auger electron spectroscopy experiment, high-energy electrons (1500 eV) are accelerated toward a surface. These electrons lose their energy by inelastic scattering as the atoms which make up the solid are ionized by the loss of a core electron. An ion that is generated by an incoming electron loses some of its potential energy by filling the vacant core hole with an electron from a shallower level. The electron that relaxes into the core hole must release energy, which is emitted either through a photon or to kinetic energy given to another shallow electron, or an Auger

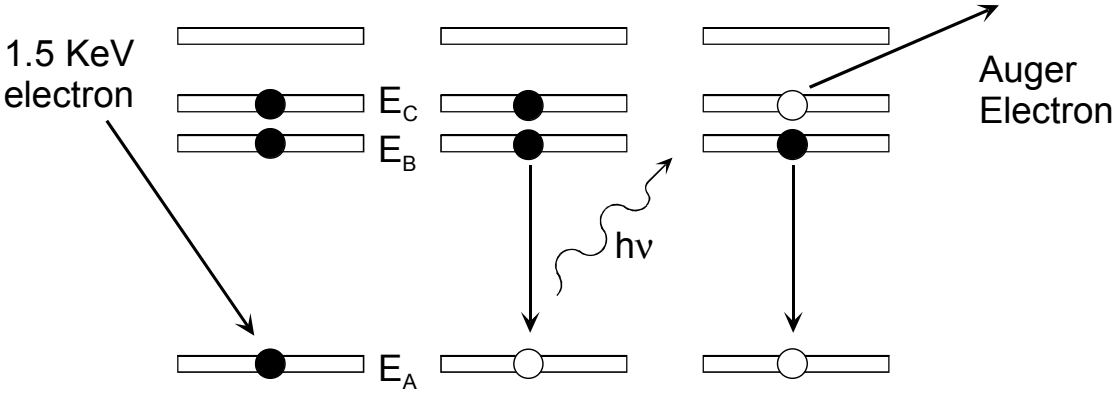

Figure 3.6 Diagram demonstrating the difference between X-ray fluorescence and the Auger effect.

electron. The first process is known as X-ray fluorescence while the second competing process is known as the Auger effect. Figure 3.6 demonstrates the difference between these two processes.

The energy of a photon released during X-ray fluorescence can be described by: $h\nu = E_A - E_B$. The energy of the Auger electron is described by: $KE = E_A - E_B - E_C$. Thus, Auger electron spectroscopy is the technique of measuring the energy of Auger electrons by the use of an energy Analyzer.

Normalization of SFG Spectra

As previously discussed, sum frequency generation signal is generated specifically at a surface or interface, and is therefore surface specific. However, this does not mean that the media the laser beams must pass cannot interfere with an SFG spectrum. The intensity of a sum frequency signal is proportional to the magnitude of the input electric fields as seen in equation 2.6. A spectrum is highly dependent on the intensity of the IR beam, and so if the gas phase in the reactor absorbs the IR light at a particular frequency, the magnitude of the IR beam at the surface will decrease as it is tuned over a vibrational mode of a gas phase molecule. This affects the intensity of the SFG signal, and therefore gas phase artifacts can be seen in the SFG spectrum. If the absorbance is large and the SFG background is large, a gas phase IR spectrum can actually appear in the SFG spectrum giving artificial SFG peaks making assignments difficult.

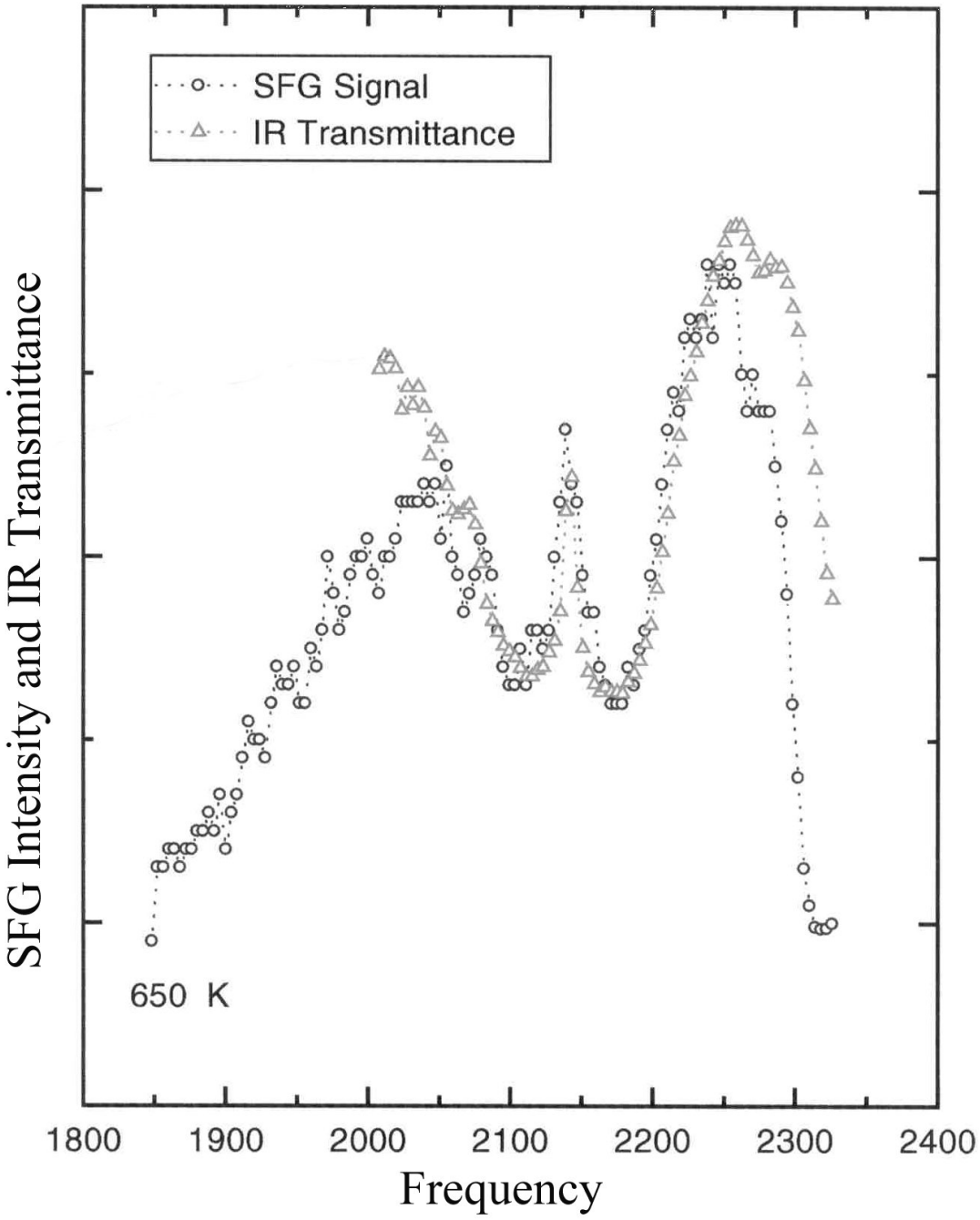

Figure 3.7 SFG spectrum of Pt(100) under oxidizing conditions and IR transmittance spectrum of 40 Torr of CO. Several features are observed in the SFG spectrum that are attributed to gas phase attenuation of the IR beam.

An example of how extreme this problem can be is demonstrated in the SFG and IR spectra shown in Figure 3.7. The SFG spectrum was acquired from a Pt(100) crystal during a CO oxidation experiment that increased the SFG background. The pressure of CO was 40 Torr, and the gas phase path length was 15 cm. It first appears that there are several peaks centered near 2040, 2143, and 2275 cm^{-1}. For all practical purposes, the peaks appear as if they were real, although, upon close inspection, the peaks are artificial as shown in the IR gas phase spectrum. This gas phase spectrum was acquired by passing the IR beam through a 10 cm long cell containing 40 Torr of CO. Essentially, the SFG and IR gas phase spectra show the same features, indicating that the cause of the peaks in the SFG spectrum is due to the attenuation of the IR beam by the CO causing a decrease in the SFG intensity corresponding to vibrational modes. The decrease above 2275 cm^{-1} is due to CO_2 in the atmosphere attenuating the IR beam.

Another example is shown during and ethylene hydrogenation experiment on Pt(100) under 40 Torr of ethylene. In Figure 3.8, a SFG spectrum and a gas phase IR spectrum are shown together in a single plot. In the SFG spectrum, two real peaks are observed at 2865 and 2905 cm^{-1} and two artificial peaks are seen at 2985 and 3040 cm^{-1}. When the gas phase IR spectrum is compared to the SFG spectrum, it is clear that the peaks at 2985 and 3040 cm^{-1} are not real SFG features. Thus, it is extremely important to normalize SFG spectra and to and reduce the attenuation of the IR beam to properly study catalysis *in situ*.

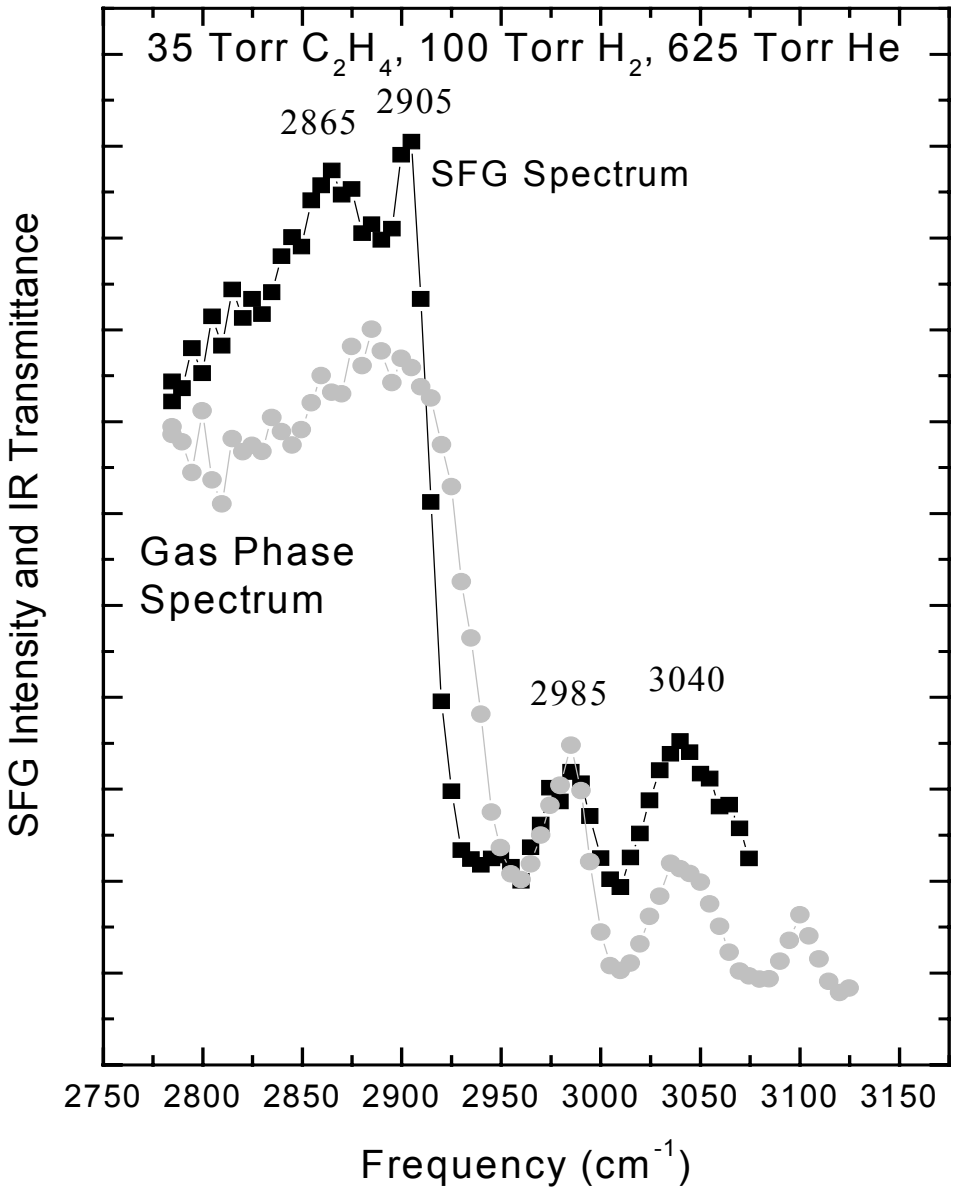

Figure 3.8 SFG spectrum of Pt(100) during ethylene hydrogenation and IR transmittance spectrum of 35 Torr of ethylene. The peaks at 2985 and 3040 are artificial caused by the attenuation of the IR beam by the gas phase ethylene in the chamber.

The major problem causing this attenuation is the long path length that the IR beam is required to pass through the gas phase medium. The original chamber used to acquire Figures 3.7 and 3.8 had a path length of 15 cm. It is possible to normalize for the IR attenuation by taking a gas phase IR spectrum of the same path length and same pressure. The gas phase artifacts can be removed by dividing the SFG spectrum by the gas phase spectrum. The problem with using a chamber with such a large path length is that the IR beam can be completely attenuated by the time it reaches the sample making it impossible to properly normalize an SFG signal. Thus, it is necessary to reduce the path length to be able to properly normalize SFG spectra.

For these experiments, assembling a new chamber reduced the IR gas phase path length. The original chamber had a CaF_2 window attached to a 2.75" flange 15 cm from the center of the chamber where the single crystal is mounted. To decrease the path length, a 6 inch flange was welded to a different bell jar and an inverted flange was built with a CaF_2 window attached on the inside as shown in Figure 3.4. This shortened the path length to less than 4 cm^{-1}. The effect of this modification is shown in Figure 3.9. The SFG spectrum of an ethylene hydrogenation experiment on Pt(100) under similar condition as to Figure 3.8 is shown. In this experiment, the artificial peaks are not observed. To show the high-pressure capability of this new system with proper normalization, the un-normalized and normalized SFG spectra of high pressures of CO are shown in Figure 3.10 and

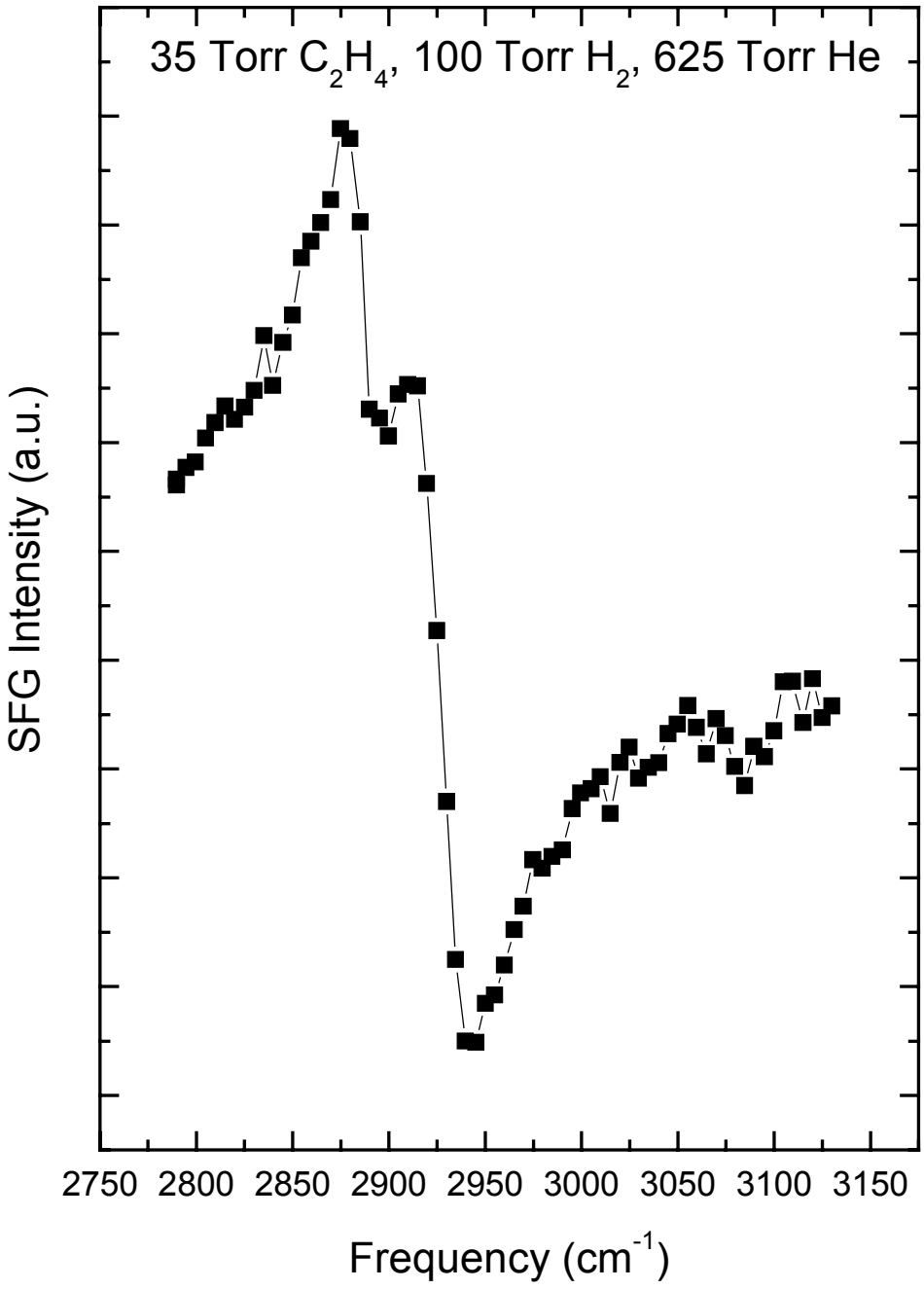

Figure 3.9 SFG spectrum of Pt(100) under ethylene hydrogenation reaction conditions. Gas phase artifacts are absent in this spectrum.

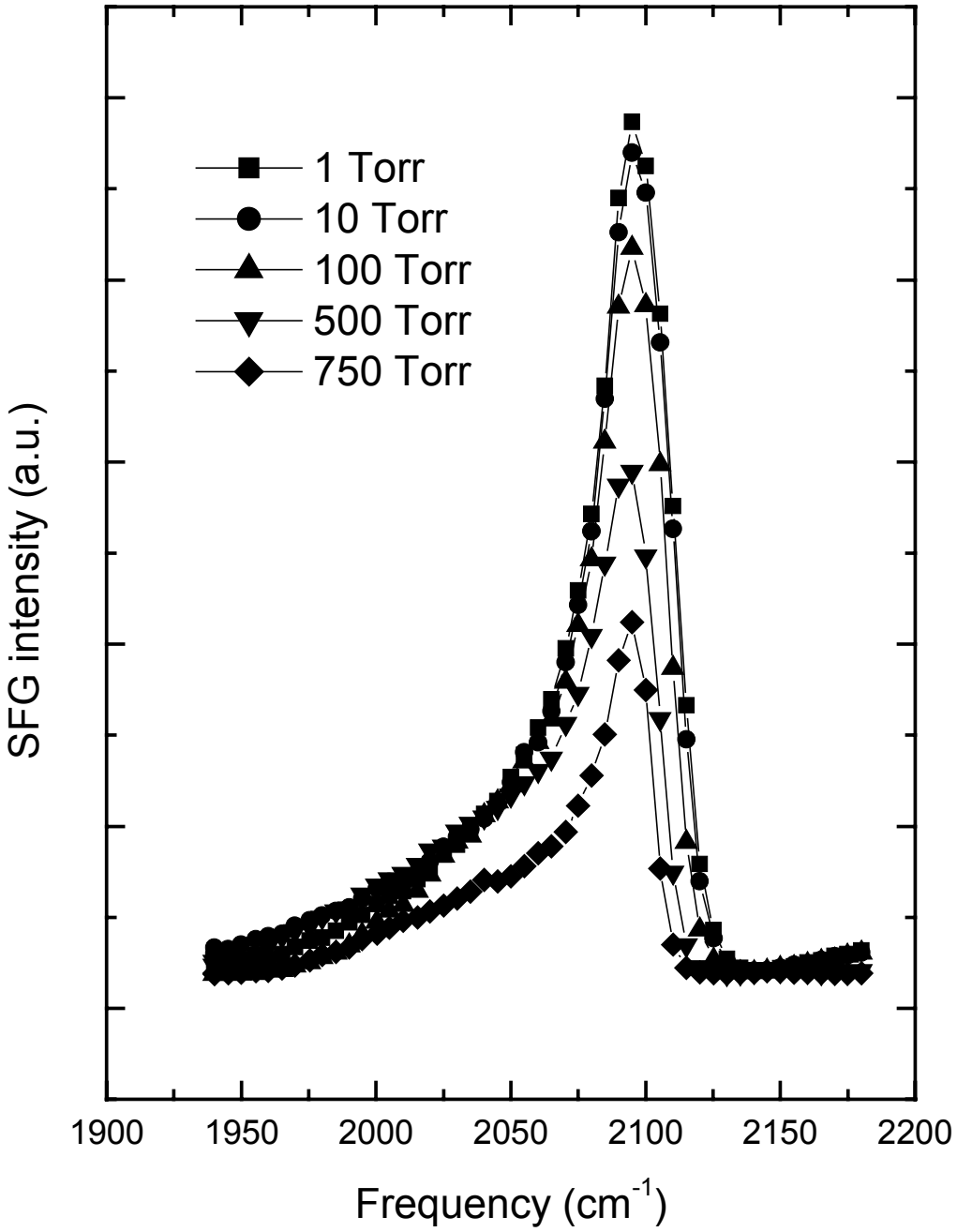

Figure 3.10 SFG spectra of high-pressures of CO. The spectra are not normalized and the intensity of the top-site CO peak decreases as a function of pressure.

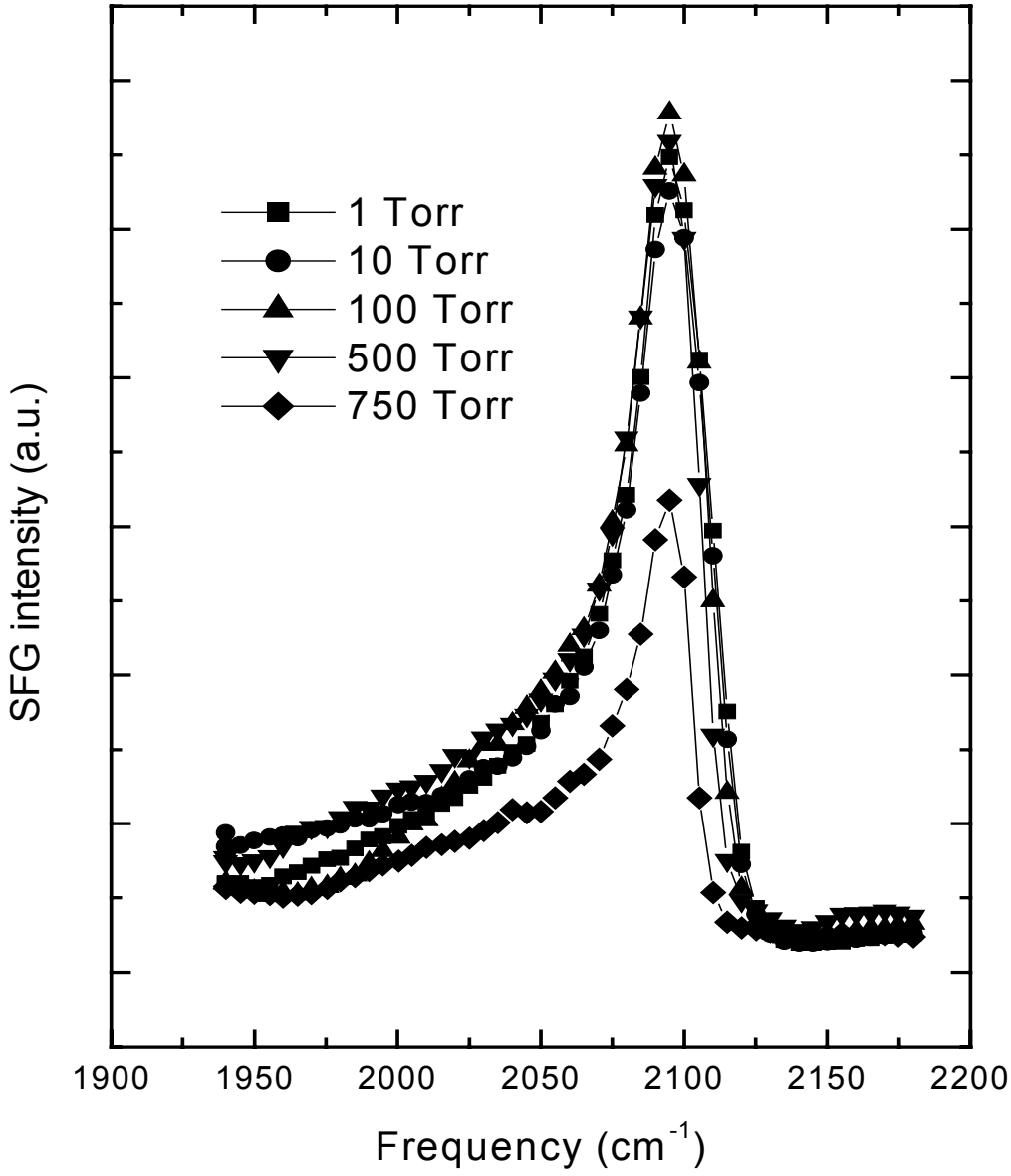

Figure 3.11 Data from Figure 3.10 normalized. The intensity of the top-site CO peak remains the same up to 500 Torr.

Figure 3.11, respectively. The intensity of the top-site CO peak for the un-normalized

spectra slowly decreases as the CO pressure is increased, whereas the intensity remains essentially the same for the normalized data up to 500 Torr.

References

[1] Zhang, D., Huang, J., Shen, Y. R., and C. Chen, *J. Opt. Soc. Am.* 1993, **10**, 1758.

[2] Heilmann, P., Heinz, K., and K. Muller, *Surf. Sci.* 1979, **83** 487.

[3] Morgan, A.E., and G.A. Somorjai, *Surf. Sci.* 1968, **12,** 405.

[4] Broden, G., Pirug, G., and H.P. Bonzel, S*urf. Sci.* 1978, **72,** 45.

[5] Lin, T.H., and G.A. Somorjai, *Surf. Sci.* 1981, **107,** 573.

[6] Ohno, Y., Sanchez, J.R., Lesar, A., Yamanaka, T., and T. Matsushima, *Surf. Sci*. 1997, **382**, 221.

[7] Somorjai, G.A., Joyner, R.W., and B. Lang, *Proc. R. Soc. Lond. A*. 1972, **331**, 335.

[8] Woodruff, D.P., and T.A. Delchar, "Modern Techniques of Surface Science", Cambridge University Press, New York, 1986.

Chapter 4: Ethylene Hydrogenation: A Structure Insensitive Case

Introduction

The first mechanism proposed for the hydrogenation of the simplest olefin, ethylene, on a platinum surface was that of Horiuti and Polanyi, reported in the 1930's.[1] According to their model, ethylene adsorbs on a clean platinum surface by breaking one of the C=C double bonds and then forming two σ-bonds with the metal surface. This intermediate is known as di-σ bonded ethylene. One of the metal-carbon bonds is then presumed to be hydrogenated with adsorbed hydrogen, creating an ethyl intermediate, allowing ethane production through the final hydrogenation of the remaining metal-carbon bond.

Surface techniques such as ultraviolet photoemission spectroscopy (UPS) were later used under UHV conditions to investigate the mechanism of ethylene hydrogenation on platinum single crystals. It was shown that at temperatures below 52 K, ethylene physisorbs through the π-bond, referred to as π-bonded ethylene.[2] As the temperature is heated above 52 K, the π-bond is broken, and di-σ bonded ethylene is formed.[3] Ethylidyne ($M{\equiv}CCH_3$) is formed as di-σ bonded ethylene is dehydrogenated and transfers a hydrogen atom from one carbon atom to the other.[4] As the surface is heated further, ethylidyne decomposes into graphitic precursors.[5]

Ethylidyne is not believed to be a reaction intermediate in ethylene hydrogenation. Davis et al.[6] showed ethylidyne hydrogenation was several orders of magnitude slower than the overall hydrogenation of ethylene to ethane. Furthermore, Beebe et al.[7], using *in-situ* IR transmission spectroscopy, showed that the reaction rate was the same on a supported Pd/Al_2O_3 catalyst, whether or not the surface was covered with ethylidyne. These results of these investigations indicate that ethylidyne is a spectator species that is not directly involved in ethylene hydrogenation.

To determine the importance of π-bonded ethylene and di-σ bonded ethylene, Mohsin et al.[8] using transmission IR spectroscopy, showed that both species are hydrogenated on a Pt/Al_2O_3 catalyst as hydrogen flows over the surface. In addition, Mohsin et al. showed that only di-σ bonded ethylene is converted to ethylidyne in the absence of hydrogen when the catalyst is heated. These studies, however, were not performed under actual high-pressure reaction conditions because gas phase ethylene interferes with IR experiments. Since-gas phase ethylene does not generate a SFG signal, SFG is an ideal technique to characterize ethylene hydrogenation *in-situ* under high-pressure reaction conditions.

The (111) and (100) crystal faces of platinum were used to determine, at high reactant pressures (0.1 – 1 atm) the rates of ethylene hydrogenation using gas chromatography. Simultaneously, SFG vibrational spectroscopy was utilized to monitor the surface species, some of which were surface reaction intermediates. We found that strongly bound ethylidyne and di-σ bonded ethylene are not the active species which turnover during ethylene hydrogenation. The reaction rate was the same for ethylene hydrogenation on both Pt(111) and Pt(100) indicating the reaction is

structure insensitive. Weakly bound species such as π-bonded ethylene and ethyl are the most likely species which turnover, although they are only observed under certain reaction conditions.

Possible surface species observed under high-pressure reaction conditions.

During an ethylene hydrogenation reaction, there are several different species that can exist on the surface. These species are separated into two categories, strongly adsorbed species and weakly bound species. The strongly bound species can exist under both UHV conditions and high-pressure conditions whereas weakly bound species can exist only under high-pressure conditions as they quickly desorb under vacuum. The two most common strongly adsorbed species are ethylidyne and di-σ bonded ethylene. The structures of these two species are shown in Figure 4.1.

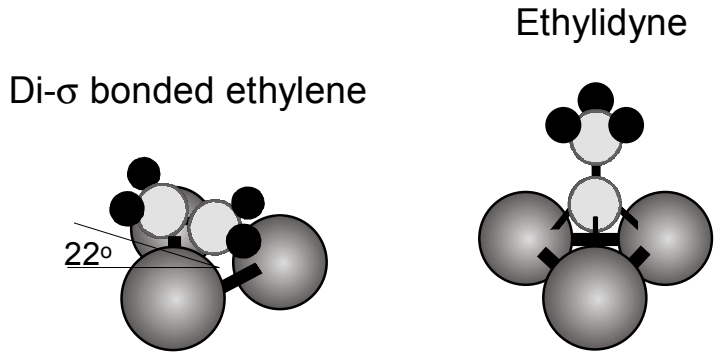

Figure 4.1 Structures of strongly adsorbed species: di-σ bonded ethylene and ethylidyne.

Through LEED experiments, the adsorption structures of both ethylidyne and di-σ bonded ethylene have been solved for Pt(111). When ethylene is introduced to a Pt(111) crystal above 240 K, ethylene will go under dehydrogenation to form

ethylidyne on the surface. Ethylidyne adsorbs in 3 fold hollow sites and in a (2 × 2) structure.[9] Ethylidyne is the most stable species on the Pt(111) surface and is therefore not likely to partake in ethylene hydrogenation reactions because of its high stability on the surface.[10] Since ethylidyne is found to adsorb in 3-fold hollow sites, it is not a stable species on the unreconstructed Pt(100) surface which does not have 3-fold hollow sites. The (1 × 1) structure is the expected surface for Pt(100) once adsorption occurs.

When Pt(111) is exposed to ethylene under UHV conditions below 240 K, di-σ bonded ethylene will adsorb on the surface. This species bonds with the C-C centers above both fcc and hcp 3-fold hollow sites with a tilt angle of about 22°.[11] Again, because the Pt(100) (1 × 1) structure does not have 3-fold hollow sites, di-σ bonded ethylene is not as stable on Pt(100) as compared to Pt(111).

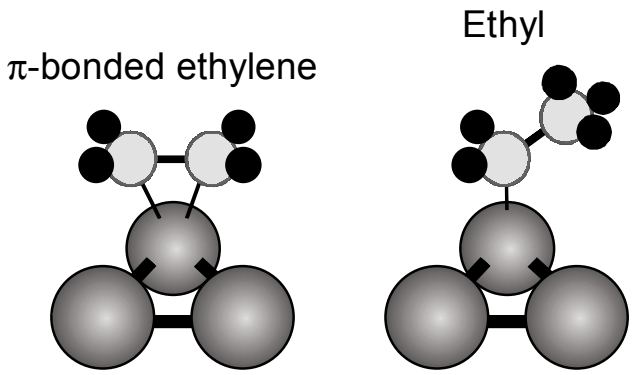

Figure 4.2 Possible structures for the weakly bonded species π-bonded ethylene and ethyl.

The structures of weakly bonded species π-bonded ethylene and ethyl are shown in Figure 4.2. Because of the low adsorption energies that these species have,

they are not easily detectable under UHV conditions but are present under high-pressure conditions.

Experimental

The Pt(111) and Pt(100) single crystal were mounted and cleaned as described in the previous chapter. Once the crystals were determined to be clean by Auger electron spectroscopy, ethylene was either introduced under or low or high-pressure conditions. Ethylene adsorption studies were first performed on both crystal surfaces to help in the assignment of peaks observed under high-pressure reaction conditions.[12] Once the surface was characterized under low ethylene pressures, the crystal was clean again and high-pressures of ethylene and H_2 were introduced into the chamber. The progress of the ethylene hydrogenation reaction was then monitored with gas chromatography while the surface was analyzed with SFG.

Results and Discussion

UHV Adsorption and Low-Pressure Experiments

Ethylene adsorption studies were first performed on both crystal surfaces to help in the assignment of peaks observed under high-pressure reaction conditions.[12] Di-σ bonded ethylene was formed on Pt(111) by exposing the surface to 4 L of ethylene at 243 K as seen by a single resonance at 2903 cm^{-1} (Figure 4.3). As this surface is annealed to higher temperatures, di-σ bonded ethylene dehydrogenates to ethylidyne

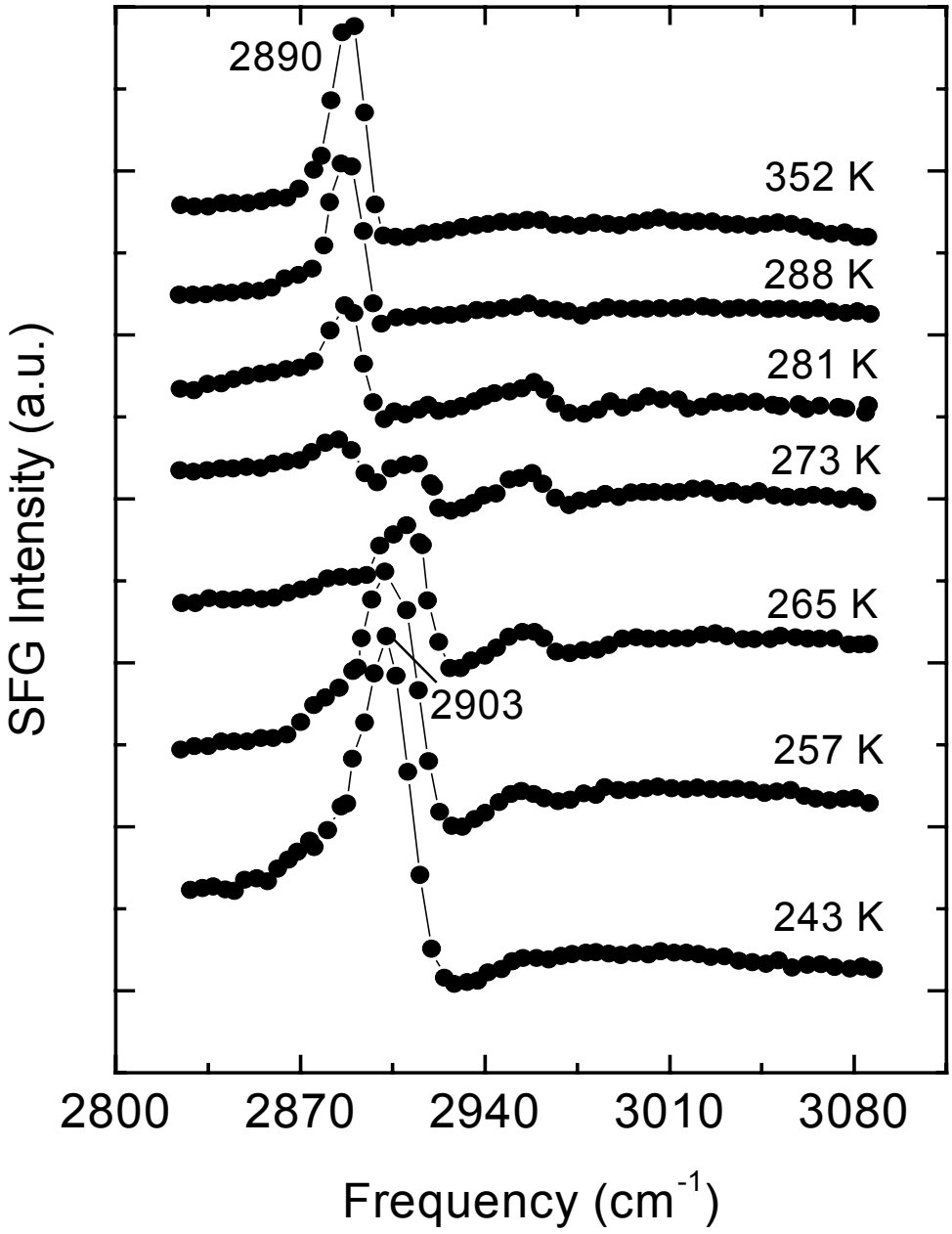

Figure 4.3 Pt(111) exposed to 4L of ethylene at 243 K. Di-σ bonded ethylene is formed and upon heating, the di-σ bonded ethylene dehydrogenates to produce ethylidyne.[13]

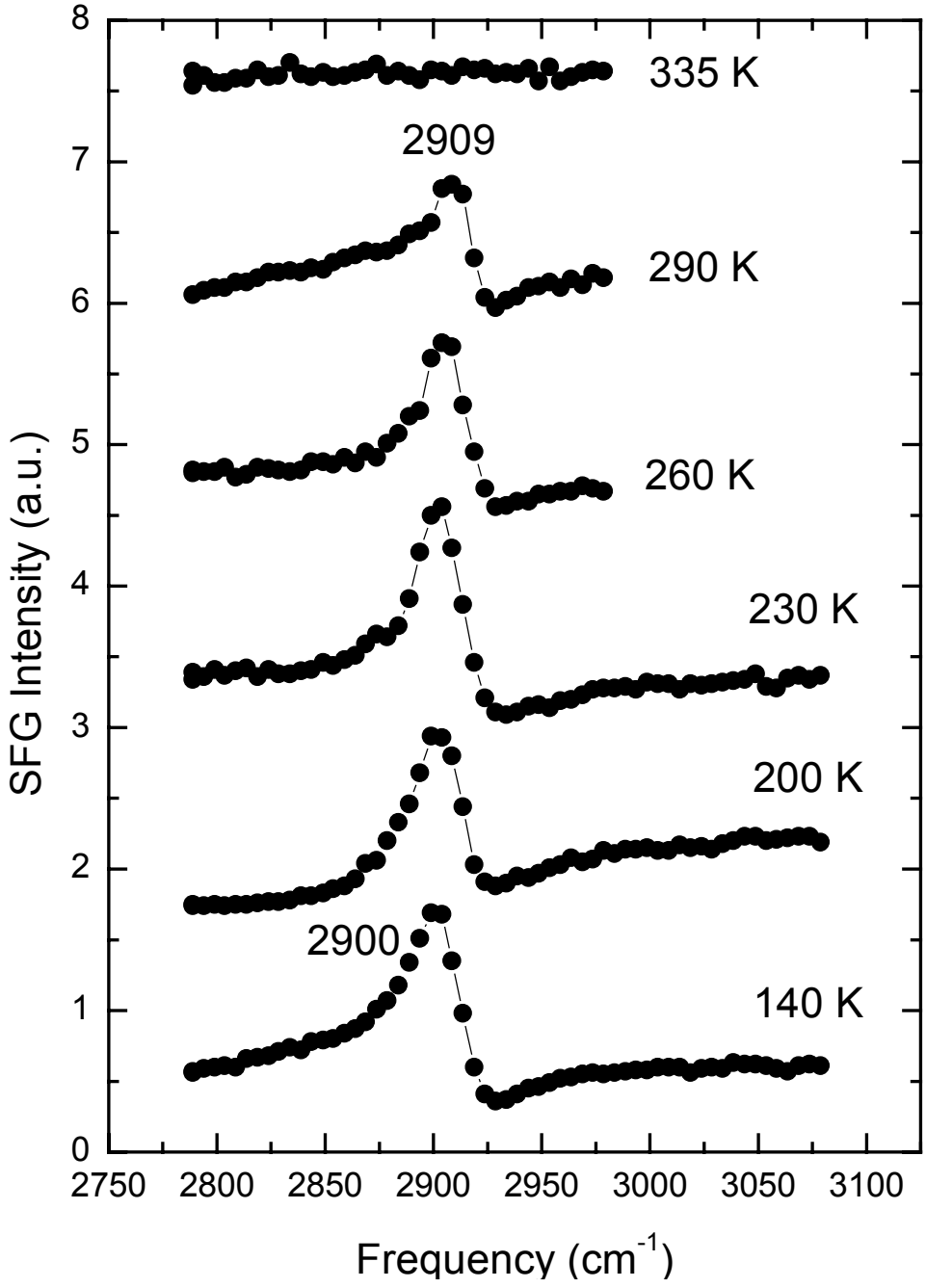

Figure 4.4 Pt(100) exposed to 4L of ethylene at 140 K. Di-σ bonded ethylene is formed and upon heating, the intensity of the peak decreases. Ethylidyne is not formed

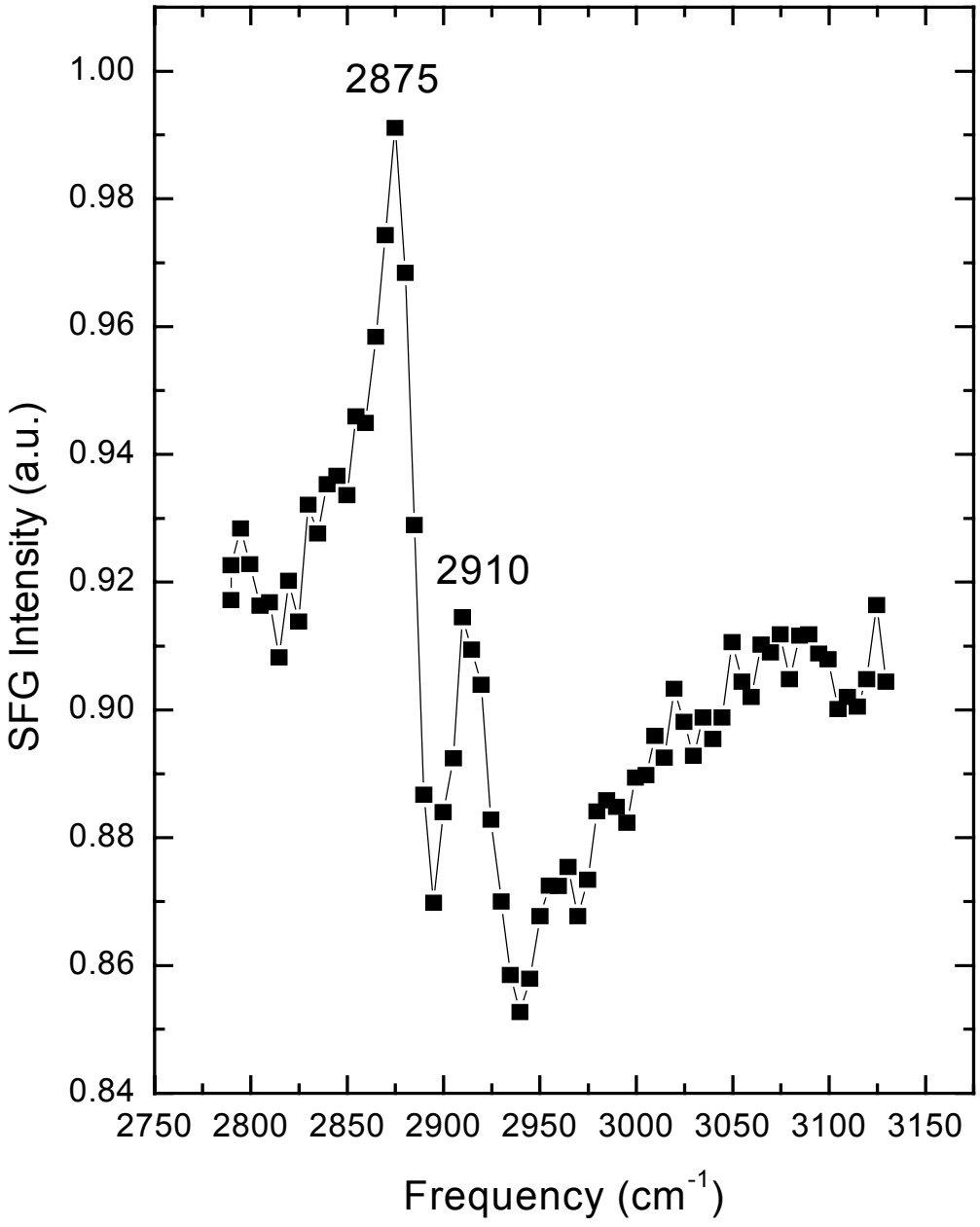

Figure 4.5 Pt(100) exposed to 5×10^{-7} Torr of ethylene at 300 K. Both di-σ bonded ethylene and ethylidyne are formed.

around 280 K and a single resonance corresponding to ethylidyne is observed at 2890 cm^{-1}.[13] If a Pt(100) surface is exposed to 4 L of ethylene at 140 K, di-σ bonded ethylene is formed with a single resonance at 2900 cm^{-1} (Figure 4.4). However, unlike Pt(111), the di-σ bonded ethylene will not dehydrogenate to ethylidyne when the sample is heated. The peak corresponding to di-σ bonded ethylene shifts to 2090 cm^{-1} and the intensity of the di-σ bonded ethylene decreases as a function of temperature until it is gone without any evidence of the formation of ethylidyne. At 140 K, di-σ bonded ethylene adsorbs in 3-fold hollow sites on the Pt(100) (5 × 20). It is likely at higher temperatures, as the di-σ bonded ethylene is dehydrogenated, the (5 × 20) structure reconstructs back to the (1 × 1) structure prohibiting the re-adsorption of either di-σ bonded ethylene or ethylidyne since these species require 3-fold hollow sites for adsorption. Only under a static pressure of ethylene above 5×10^{-7} Torr will both di-σ bonded ethylene and ethylidyne form on Pt(100) as shown in Figure 4.5.

On both Pt(111) and Pt(100), the ethylidyne stretching frequency was observed around 2880 cm^{-1} and the di-σ bonded ethylene stretching frequency was observed at 2910 cm^{-1}. Both ethylidyne and di-σ bonded ethylene were previously found to sit in fcc 3-fold hollow sites LEED with molecular axis of di-σ bonded ethylene is tilted with respect to the surface plane by about 22^{o}.[14,11] The surface of the Pt(100) crystal face reconstructs to a pseudo-hexagonal structure, known as Pt(100)(5x20), resembling the hexagonal structure of Pt(111) when properly cleaned. As the Pt(100)(5x20) surface was exposed to 1×10^{-7} Torr of ethylene, the surface structure was monitored with LEED, and the surface was observed to reconstruct back to the 1x1 structure. This is

interesting considering ethylidyne and di-σ bonded ethylene sit in fcc 3-fold sites. Because it appears that the C-H bond of di-σ bonded ethylene is unperturbed on the Pt(100) surface as compared with the Pt(111) surface, it is likely that ethylidyne and di-σ bonded ethylene hold the 3-fold site in place as it first adsorbs on the Pt(100)(5x20) surface.

High Pressure Ethylene Hydrogenation

High pressure ethylene hydrogenation reactions were performed on both the Pt(111) and Pt(100) surfaces by introducing 100 Torr of H_2, 35 Torr of ethylene, and 625 Torr of He. The temperature of the crystal was maintained at room temperature as SFG spectra were acquired and gas phase analysis was measured using GC. The measured turnover rates were measured to be 11±1 and 12±1 molecules/site/second for Pt(111) and Pt(100), respectively. The fitted SFG spectra for ethylene hydrogenation on Pt(111) and Pt(100) are shown in Figure 4.6[12] and Figure 4.7, respectively. Both ethylidyne and di-σ bonded ethylene are the main features on both crystal faces. The measured strengths of the vibrational mode (A_q) are shown in parenthesis at the end of the indicated species names next to the peaks. From the values of A_q, it is observed that the ratio of ethylidyne to di-σ bonded ethylene is different on the two crystal surfaces. On Pt(111), the values of A_q for ethylidyne(4.0) and di-σ bonded ethylene(5.0) are roughly the same, where as the value of A_q for di-σ bonded ethylene(2.1) on Pt(100) is roughly three time as large as ethylidyne(5.7). This indicates that the relative concentration of ethylidyne and di-σ bonded ethylene are different on the two surfaces, essentially demonstrating that there is a higher concentration of ethylidyne on the

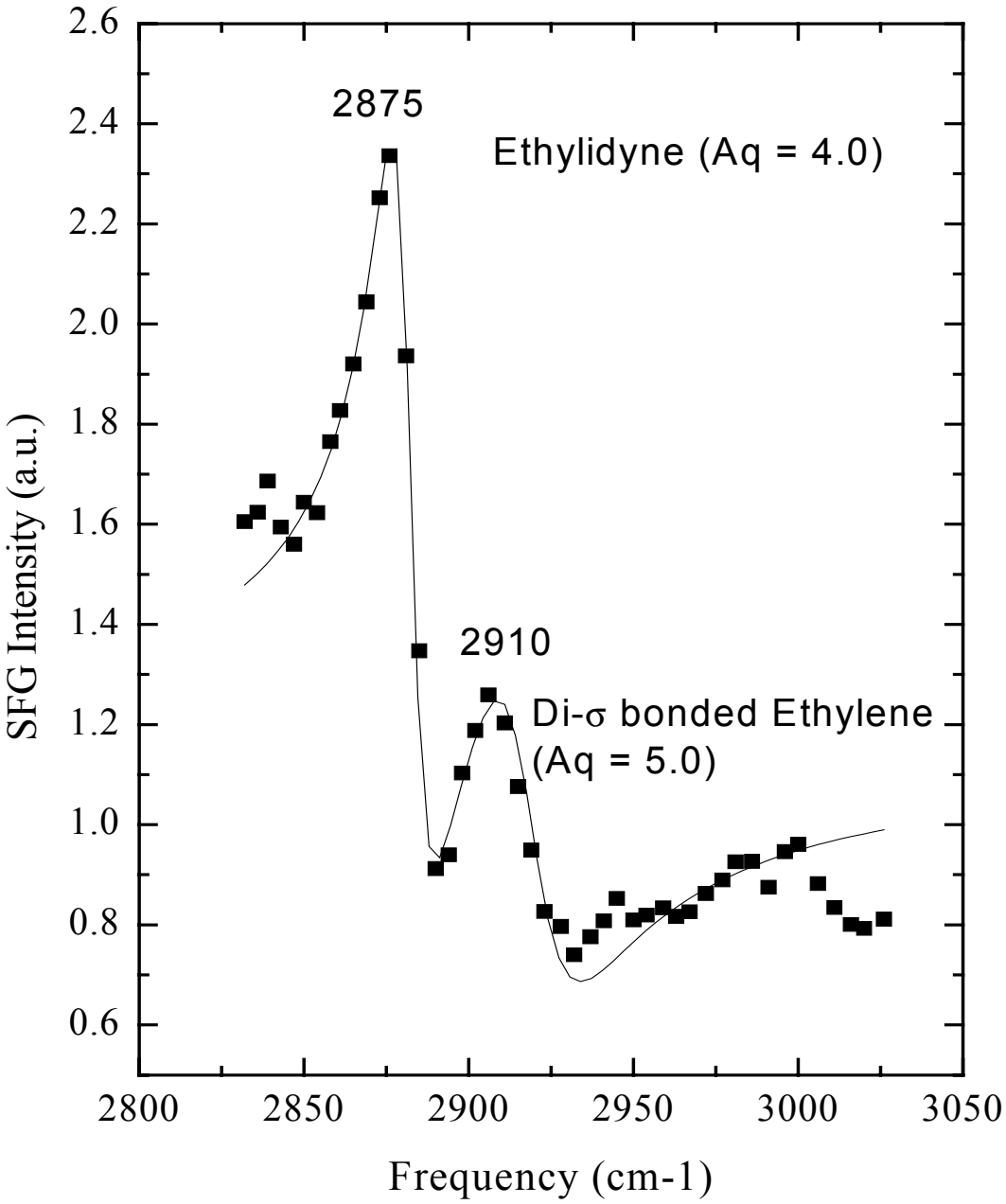

Figure 4.6 SFG spectrum of Pt(111) under ethylene hydrogenation conditions: 35 Torr of ethylene, 100 Torr of H_2, and 635 Torr of He. Aq is the value of the fitted amplitude for the peak.[12]

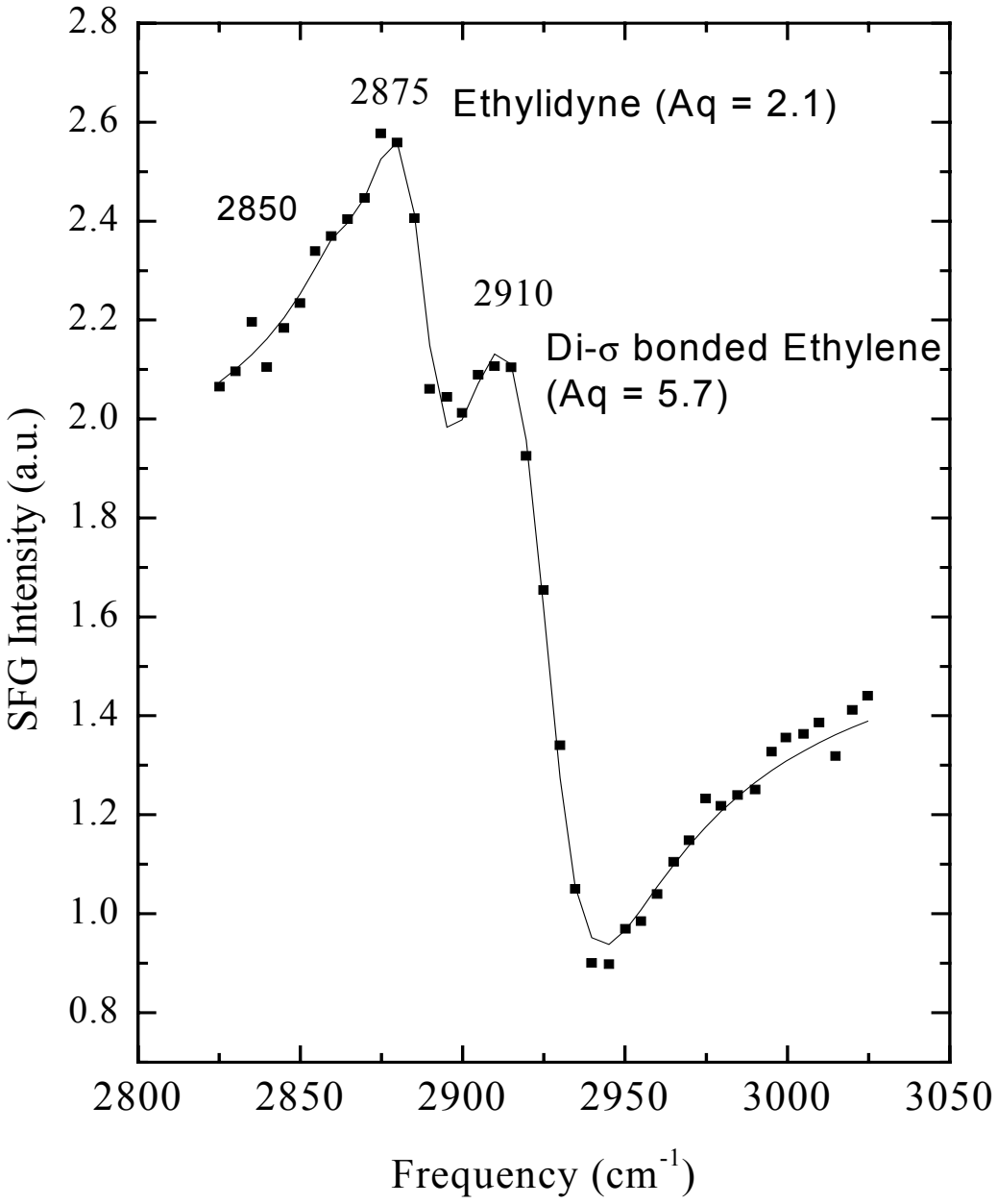

Figure 4.7 SFG spectrum of Pt(100) under ethylene hydrogenation conditions: 35 Torr of ethylene, 100 Torr of H_2, and 635 Torr of He. Aq is the value of the fitted amplitude for the peak.

Pt(111) surface. Noticing that the relative concentrations of these species are different for the two crystal faces while their turnover rates are essentially the same, indicates that neither ethylidyne or di-σ bonded ethylene are the reactive intermediates on the surface.

The most likely reactive intermediates for ethylene hydrogenation are weakly bound species such as π-bonded ethylene and ethyl. Under the conditions reported above, the only evidence of a weakly bound species is a shoulder at 2850 cm^{-1} on both surfaces, which corresponds to the fermi resonance of an ethyl species. The combined coverage of ethylidyne and di-σ bonded ethylene is approximately 35% of a monolayer, or between 60 and 70% of a saturation coverage. Because there is a high concentration of ethylidyne and di-σ bonded ethylene, the concentration of the active surface intermediates may be at the detection limits of SFG. It is important to note that the concentration of the reactive intermediates are most likely the same on both surfaces since the reaction rate for ethylene hydrogenation is the same on both surfaces.

SFG spectra during ethylene hydrogenation with high pressures of H_2 and high temperatures show stronger evidence that ethyl species (2925 cm^{-1}) and π-bonded ethylene (3000 cm^{-1}) exist under reaction conditions as shown in Figure 4.8. At these pressures, the rate of hydrogenation is substantially higher and so the concentration of surface intermediates must be higher. Clearly, in the spectra for both Pt(111) and Pt(100), the concentration of di-σ bonded ethylene and ethylidyne are considerably smaller as shown in Figure 4.6 and Figure 4.7 and so there is a larger number of sites

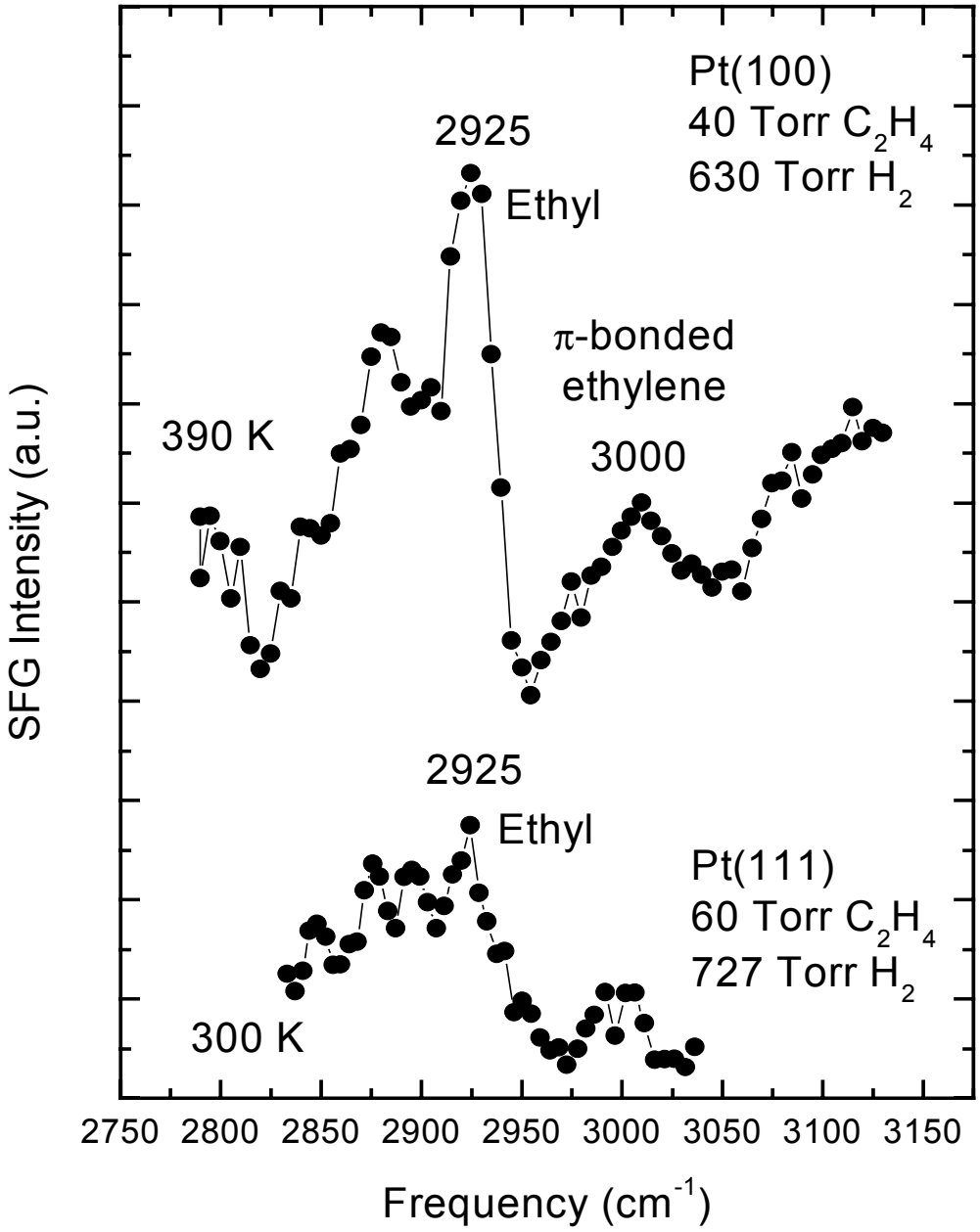

Figure 4.8 SFG spectra of Pt(111)[12] and Pt(100) under high-pressure ethylene hydrogenation conditions. Weakly bonded species π-bonded ethylene and ethyl are observed.

available for ethylene hydrogenation. From the data presented, the proposed reaction pathway for ethylene hydrogenation is shown in Figure 4.9.

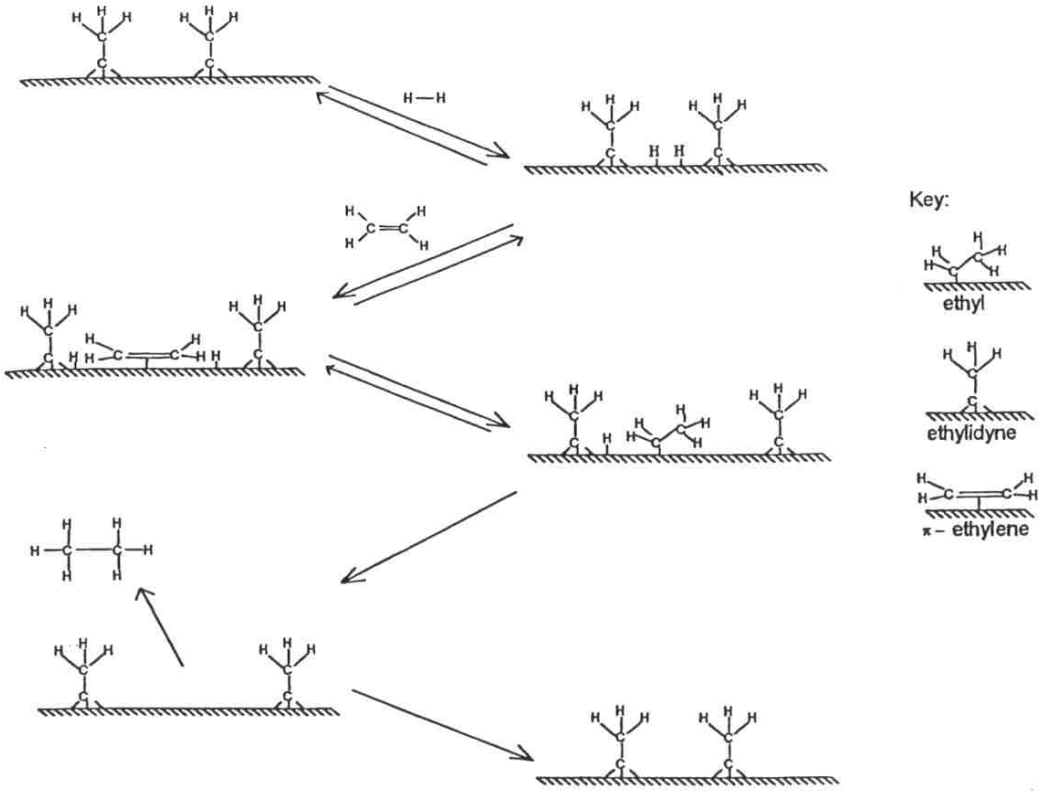

Figure 4.9 Proposed reaction pathway for ethylene hydrogenation. The active reaction intermediates are ethyl and π-bonded ethylene.[12]

Conclusions

In the results discussed above, it is clear that SFG is a unique tool that allows the detection of vibrational spectra of adsorbed molecules present on single crystal surfaces under catalytic reaction conditions. Not only is it possible to detect active surface intermediates, it is also possible to detect spectator species which are not responsible for the measured turnover rates. By correlating high-pressure SFG spectra under reaction conditions and GC kinetic data, it is possible to determine which species are important under reaction intermediates.

Because of the flexibility of this technique for studying surface intermediates, it is possible to determine how the structures of single crystal surfaces affect the observed rates of catalytic reactions. As an example of a structure insensitive reaction, ethylene hydrogenation was explored on both Pt(111) and Pt(100). The rates were determined to be essentially the same. It was observed that both ethylidyne and di-σ bonded ethylene were present on the surface under reaction conditions on both crystals, although in different concentrations. This result shows that these two species are not responsible for the measured turnover rate, as it would be expected that one of the two crystals would be more active than the other, since the concentration of the surface intermediate would be different on the two crystals. The most likely active intermediates are weakly adsorbed molecules such as π-bonded ethylene and ethyl. These species are not easily detected because their concentration lies at the detection

limit of SFG. The SFG spectra and GC data essentially show that ethylene hydrogenation is structure insensitive for Pt(111) and Pt(100).

SFG has proven to be a unique and excellent technique for studying adsorbed species on single crystal surfaces under high-pressure catalytic reactions. Coupled with kinetic data obtained from gas chromatography measurements, it can give much insight into how the structure of a single crystal surface affects the chemistry of a catalytic reaction by detecting surface species under reaction conditions.

References

[1] Horiuti, I., and M. Polanyi, *Trans. Faraday Soc*. 1934, **30**, 1164.

[2] Cassuto, A., Kiss, J., and J. White, *Surf. Sci.* 1991, **255**, 289.

[3] Ibach, H., and S. Lehwald, *Surf. Sci.* 1982, **117**, 685.

[4] Cremer, P., Stanners, C., Niemantsverdriet, J., Shen, Y., and G.A. Somorjai, *Surf. Sci.* 1993, **328**, 111.

[5] Land, T., Michely, T., Behm, R., Hemminger, J., and G. Comsa, *J. Chem. Phys.* 1992, **97**, **9**, 6774.

[6] Davis, S., Zaera, F., Gordon, B., and G.A. Somorjai, *J. Catal.* 1985, **92**, 250.

[7] Beebe, T., and J. Yates, *J. Am. Chem. Soc.* 1986, **108**, 663.

[8] Mohsin, S., Trenary, M., and H. Robota, *J. Phys. Chem.* 1988, **92**, 5229.

[9] Starke, U., Barbieri, A., Materer, N., Van Hove, M.A., and G.A. Somorjai, *Surf. Sci.* 1993, **286**, 1.

[10] Ditlevsen, P.D., Van Hove, M.A., and G.A. Somorjai, *Surf. Sci.* 1993, **292**, 267.

[11] Döll, R., Gerken, C.A., Van Hove, M.A., and G.A. Somorjai, *Surf. Sci.* 1997, **374**, 151.

[12] Cremer, P.S., Su, X., Shen, Y.R., and G.A. Somorjai, *J. Am. Chem. Soc.* 1996, **118**, 2942.

[13] Cremer, P., Stanners, C., Niemantsverdriet, J.W., Shen, Y.R., and G.A. Somorjai, *Surf. Sci.* 1995, **328**, 111.

[14] Starke U., Barbieri A., Materer N., Van Hove M. .A., and G.A. Somorjai, *Surf. Sci.* 1993, **286**, 1.

Chapter 5: Cyclohexene Dehydrogenation: A Structure Sensitive Case

Introduction

Before the advent of SFG, there have been many different types of spectroscopies used to study the adsorption of cyclohexene on Pt surfaces. These spectroscopic methods include EELS, HREELS, and IRAS.[1,2,3,4,5] The results of these studies show that cyclohexene dehydrogenates to form benzene through a C_6H_9 intermediate. The techniques used in these studies are limited to low-pressure studies and it possible that there are different reactive intermediates on Pt surfaces under high-pressure catalytic reaction conditions. Because of this limitation, it was not possible to investigate the effect of the surface structure during cyclohexene dehydrogenation under reaction conditions. In order to determine the effect of structure, a high-pressure technique such as SFG is needed.

Using SFG, a comparison between cyclohexene hydrogenation and dehydrogenation over Pt(111) and Pt(100)(5x20) single crystals at high pressures and temperatures is made to determine how the surface structure influences these reactions. In addition, as a reference to high-pressure experiments, cyclohexene on Pt UHV experiments were performed on both crystals to determine how structure affects adsorption of cyclohexene. Under high-pressure reaction conditions, cyclohexene

dehydrogenation and hydrogenation occurred through 1,3-cyclohexadiene and 1,4-cyclohexadiene surface intermediates whose relative concentration changed with platinum surface structure. Since the rate of cyclohexene dehydrogenation was faster through 1,3-cyclohexadiene, and 1,3-cyclohexadiene was the dominant species on the (100) crystal face of platinum, the rate of benzene formation was greater on that catalyst surface. The Pt(111) surface had both 1,3-cyclohexadiene and 1,4-cyclohexadiene present under reaction conditions.

Experimental

The single crystals were cleaned as described in Chapter 3. Once the surface was determined to be clean by Auger electron spectroscopy, both UHV adsorption and high-pressure reactions were performed. UHV adsorption experiments were performed to correlate SFG results with previous vibrational spectroscopy results on Pt(111) and Pt(100). Also, UHV results are useful for understanding spectra obtained under high-pressure reactions. These UHV experiments consisted of dosing 20 L of cyclohexene, which was first purified by the freeze-pump-thaw method, at 130 K. SFG spectra were then acquired at 130 K and then the sample was incrementally flashed to higher temperatures and cooled back to 130 K for further SFG experiments. For high-pressure experiments, the bell jar was sealed off from the pumps, and 10 Torr of cyclohexene, 100 Torr of hydrogen, and 650 Torr of He were introduced into the chamber. After the initial room temperature SFG spectra and GC data was acquired, the sample was then

heated in 25 degree increments up to 600 K while monitoring spectroscopic changes of surface species using SFG and monitoring the gas composition.

Results and Discussion

UHV Adsorption Experiments

A clean Pt(111) crystal was exposed to 20 L of cyclohexene at 130 K, and a SFG spectrum was acquired. The sample was then annealed to consecutively higher temperatures and allowed to cool back to 130 K, after which SFG spectra were taken. The results are shown in Figure 5.1.[6] At 130 K, the SFG spectrum is similar to the IR/Raman spectra of liquid-phase cyclohexene.[7] The peaks at 2875 and 2958 cm^{-1} are assigned to C-H stretch modes, and the peak at 2918 cm^{-1} is assigned to a Fermi resonance ($\nu_s + 2\nu_{def}$) of the bending mode of C-H groups.

As a free molecule, cyclohexene has a double bond and a half-chair conformation with C_2 symmetry.[8,7] Cyclohexene adsorbs by donating its π-electron density to the metal as it bonds to the surface. As a result of the different electronic coupling with the carbon ring, the equatorial C-H appears at a higher stretching frequency than the axial C-H.[9,10] Except for a small shift in frequencies, this spectrum is also nearly identical to the Raman spectrum of deuterated cyclohexene 3,3,6,6-d_4.[7] In the deuterated molecule, the vibrational features arise from CH_2 groups at the C_4 and C_5 positions, and therefore the peaks observed in the SFG spectra are assigned to C-H bonds at C_4 and C_5. Because features corresponding to C_3 and C_6 C-H bonds were not observed, it is believed that these bonds are parallel to the surface and not observed

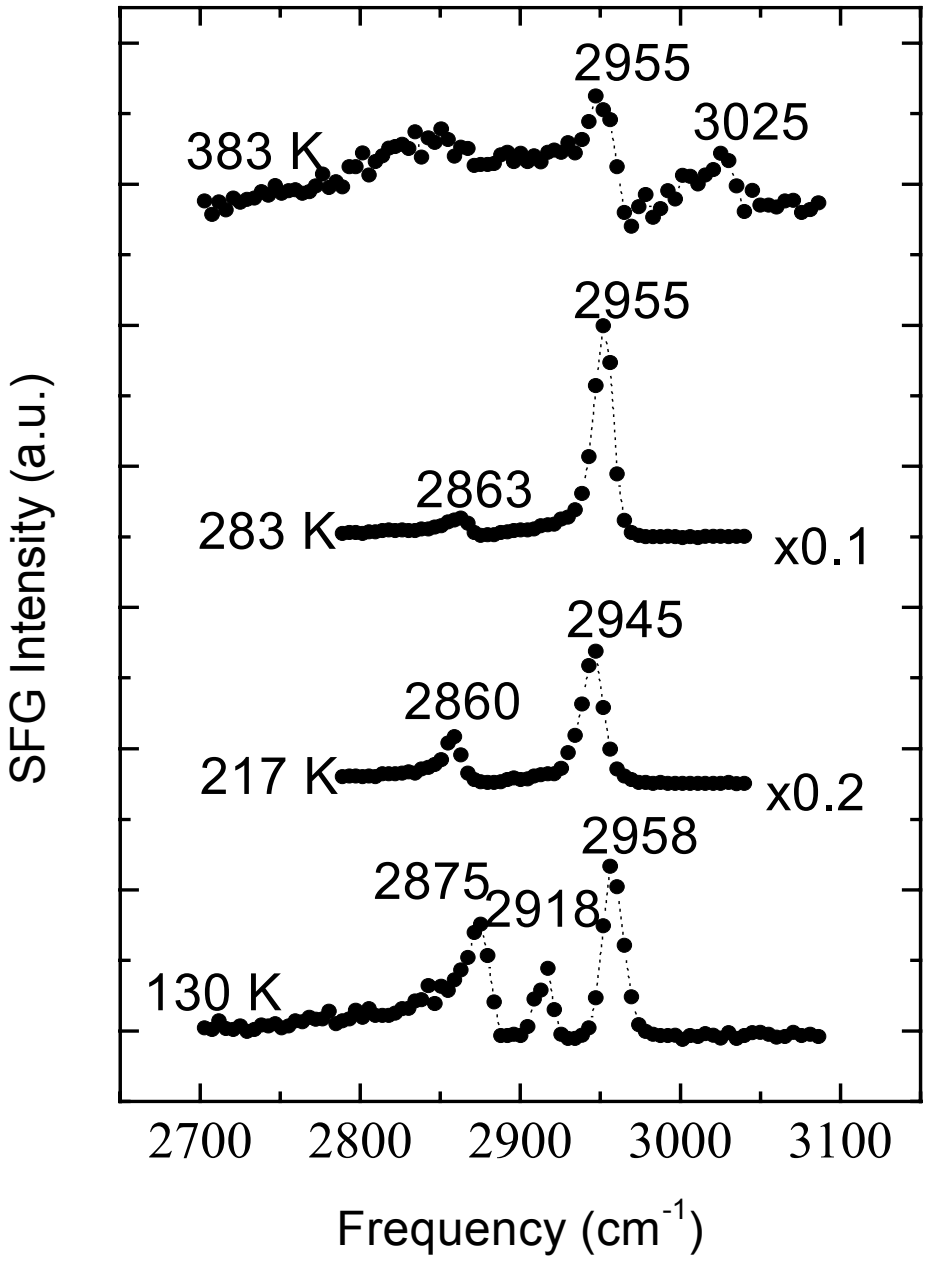

Figure 5.1 SFG spectra of Pt(111) after being exposed to 20 L of cyclohexene.[6]

because of the metal surface selection rule. Furthermore, because the SFG spectrum appears to be that of a molecular species it is believed that cyclohexene is π/σ hybridized as it adsorbs.

As the sample was heated, the π/σ hybridized cyclohexene was up to a temperature of 200 K, where upon a change in the SFG spectrum was observed. At 217 K, two new peaks with slightly higher intensity were observed, at 2860 and 2945 cm^{-1}. Others have observed a similar change in the spectrum,[1] and is explained as the conversion of the π/σ bonded species to a di-σ bonded cyclohexene. The shift in the two species is probably due to the electronic effect as the hybridization of the double bond has changed from sp^2 to sp^3. The higher intensities of these two peaks relative to those of the previous example probably result because the di-σ bonded species is more nearly perpendicular to the metal surface than its π/σ bonded predecessor.

The SFG spectra recorded at temperatures above 217 K remained relatively unchanged until about 283 K, where upon the two spectral features shifted to 2955 and 2863 cm^{-1}. Dehydrogenation of the di-σ bonded cyclohexene species is inferred to have occurred, and the new peaks are believed to be associated with a π-allyl c-C_6H_9 species, as observed by others.[1,4,5] The strong feature at 2955 cm^{-1} is attributed to the equatorial C-H stretching in the c-C_6H_9 species. The proposed C_6H_9 structure shows the equatorial C-H on C_4 and C_6 as perpendicular to the surface, and this structure explains the high intensity of this peak.

The C_6H_9 intermediate was observed on the surface up to a temperature of 371 K, and at higher temperatures more dehydrogenation occurred, as evidenced by the

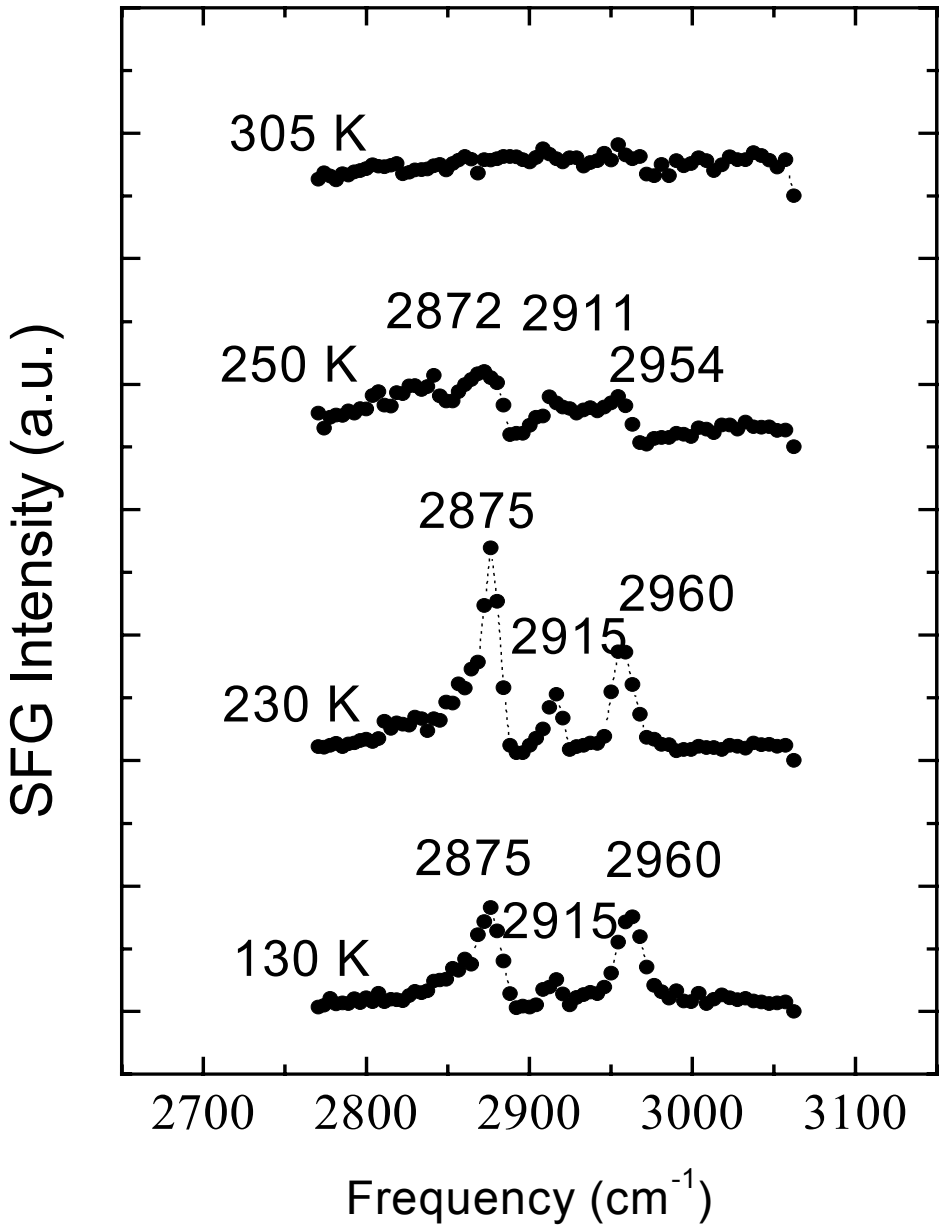

Figure 5.2 SFG spectra of Pt(100) after being exposed to 20 L of cyclohexene.

greatly attenuated spectral intensity and the appearance of a feature at 3025 cm^{-1}. This

new feature is indicative of a sp^2-hybridized CH stretch and may arise from benzene or other decomposition products on the surface. The dehydrogenation temperature in this investigation was slightly higher than those reported previously, and the difference suggests site blocking effects associated with the relatively high coverage of cyclohexene used in this investigation. Only at higher temperatures will desorption and decomposition occur, freeing up active dehydrogenation sites.

A similar experiment was performed on a Pt(100)(5x20) single crystal exposed to 4 L of cyclohexene at 130 K (Figure 5.2). The SFG spectrum observed at this temperature is practically identical to those observed with the Pt(111) crystal; cyclohexene adsorbs through the double bond in a π/σ hybridization. Again, the peaks at 2875 and 2960 cm^{-1} correspond to ν(CH) at C_4 and C_5, and the feature at 2915 cm^{-1} may indicate a Fermi resonance ($\nu_s + 2\nu_{def}$). As the sample was heated to temperatures above 200 K, differences were seen between the SFG spectra of the adsorbates on Pt(111) and Pt(100). In contrast to the peak shift observed for the species on Pt(111), the peaks at 2875 and 2960 cm^{-1} representing the species on Pt(100) did not shift their positions. Furthermore, on the Pt(111) surface, the feature at 2918 cm^{-1} disappeared, whereas the feature at 2915 cm^{-1} in the spectrum of the species on Pt(100) actually became more intense. Bradshaw et al.[3] used IR spectroscopy to observe the same effect on a Pt(100)(5x20) crystal. On the basis of EELS data representing the same surface, Bradshaw et al. believe that cyclohexene undergoes a conformational change from the half-chair to the half-boat structure. With this conformational change, the axial hydrogen atoms at the C_3 and C_6 become perpendicular to the metal surface, and

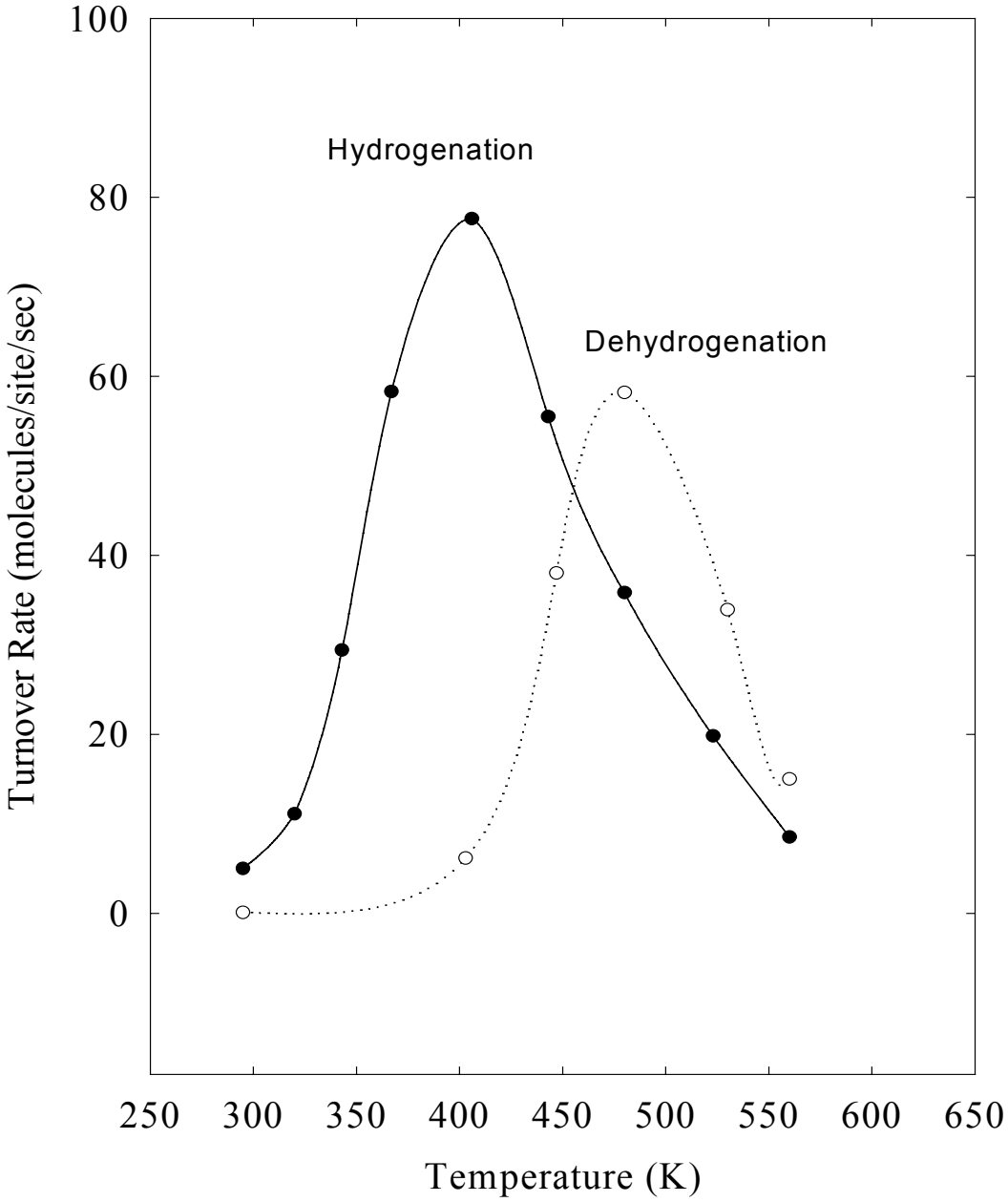

Figure 5.3 The temperature dependence of cyclohexene hydrogenation and dehydrogenation turnover rates under 10 Torr cyclohexene, 100 Torr of H_2, and 650 Torr He on Pt(111).[6]

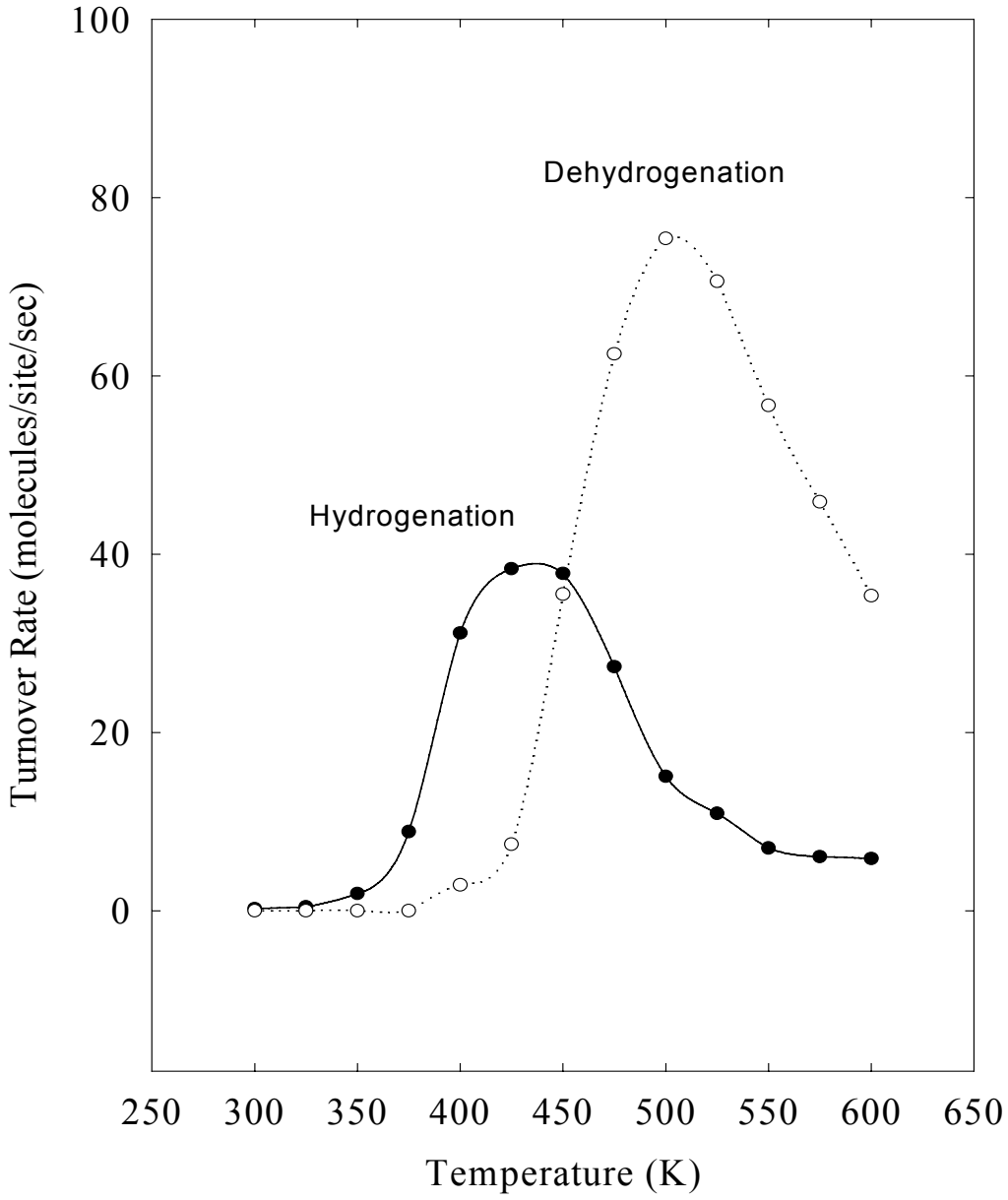

Figure 5.4 The temperature dependence of cyclohexene hydrogenation and dehydrogenation turnover rates under 10 Torr cyclohexene, 100 Torr of H_2, and 650 Torr He on Pt(100).

therefore the corresponding peaks in the vibrational spectra become more intense. As the Pt(100) crystal was heated to about 300 K, there were no more features observed in the SFG spectrum, and the surface was probably covered with benzene.

High Pressure Cyclohexene Hydrogenation and Dehydrogenation

To mimic a high-pressure industrial reaction, a platinum single crystal was placed into a UHV chamber/batch reactor and cleaned by conventional methods. Into the reactor, 10 Torr of cyclohexene, 100 Torr of hydrogen, and 650 Torr of He were introduced.[6] The sample was heated to temperatures between 300 and 600 K while changes in the spectra of surface species were monitored by using SFG, and the gas composition was monitored by gas chromatography. Turnover rates were determined from the chromatographic data at each temperature, as shown in Figure 5.3 and Figure 5.4 for cyclohexene on Pt(111) and Pt(100), respectively. At 300 K, the hydrogenation and dehydrogenation TORs were found to be negligible. Upon heating of the crystal sample, the hydrogenation TOR increased and reached a maximum of 78 molecules per platinum site per second at 400 K for Pt(111) and a maximum of 38 molecules per platinum site per second at 425 K for Pt(100). Near the temperature of the maximum hydrogenation TOR on either crystal, the dehydrogenation TOR began to increase while the hydrogenation rate began to decrease with increasing temperature. On Pt(111), the maximum dehydrogenation TOR is 58 molecules per platinum site per second at 475 K, and on Pt(100), the maximum dehydrogenation TOR was 75 molecules per platinum site per second at 500 K.

Assuming that the dehydrogenation TOR is negligible in the region of increasing hydrogenation TOR, the activation energies for cyclohexene hydrogenation

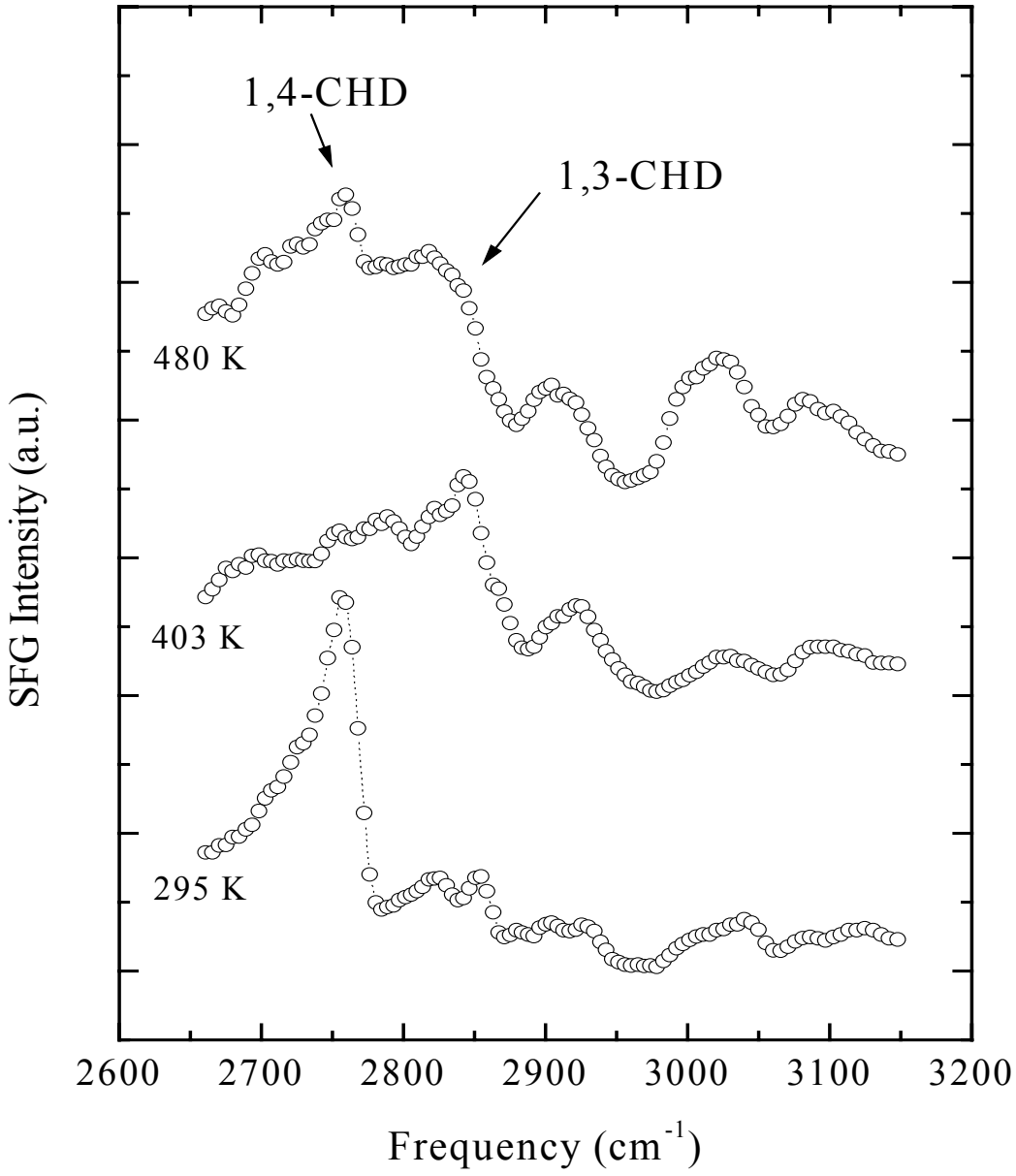

Figure 5.5 SFG spectra of reaction intermediates adsorbed on Pt(111) during cyclohexene hydrogenation and dehydrogenation under 10 Torr cyclohexene, 100 Torr of H_2, and 650 Torr He.[6]

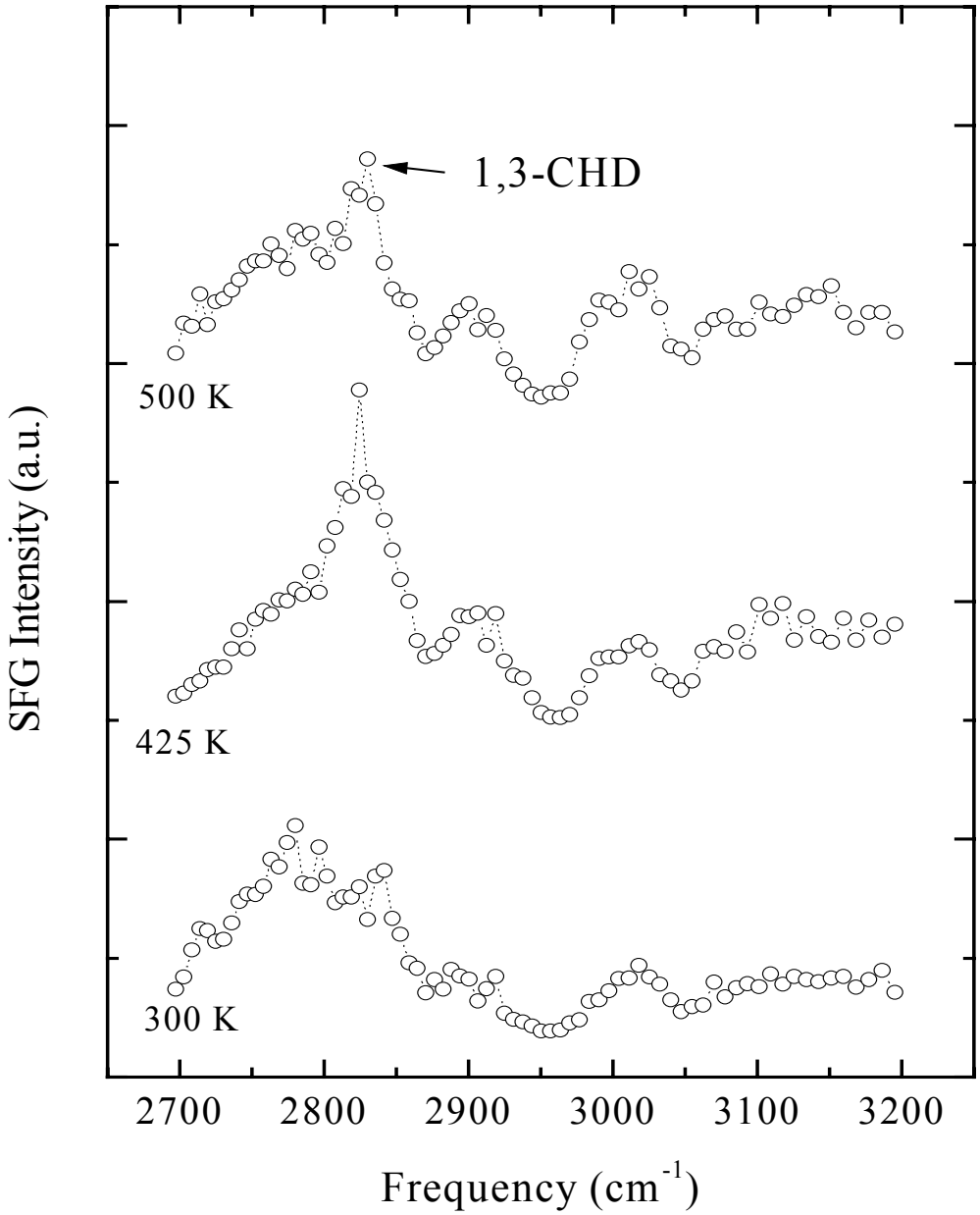

Figure 5.6 SFG spectra of reaction intermediates adsorbed on Pt(100) during cyclohexene hydrogenation and dehydrogenation under 10 Torr cyclohexene, 100 Torr of H_2, and 650 Torr He.

were calculated to be 8.9 and 15.5 kcal/mol for Pt(111) and Pt(100) respectively. As the temperature was increased above the cyclohexene hydrogenation rate maximum, the hydrogenation rate decreased as the dehydrogenation rate increased. This result may indicate that the numbers of active surface sites for the two processes change or the concentration of hydrogen on the surface changed. Otherwise, the hydrogenation reaction rate would obey the Arrhenius law over the entire temperature range.

While the catalytic reactions were being performed, SFG spectra were collected. Figure 5.5 and Figure 5.6 shows the SFG spectra for the temperature at which the gases were introduced into the chamber, the spectra for the maximum hydrogenation TOR, and the spectra for the maximum dehydrogenation TOR. In the spectrum of the adsorbates on Pt(111) (Figure 5.5) at 295 K, a sharp feature was observed at 2755 cm^{-1}. This feature at 2755 cm^{-1} is assigned to 1,4-cyclohexadiene. We stress that there is no evidence of a c-C_6H_9 intermediate species, as was observed under UHV conditions. The major features of the species on Pt(100) at 300 K(Figure 5.6), are assigned to 1,3-cyclohexadiene; a weak accompanying feature at about 2780 cm^{-1} is assigned to 1,4-cyclohexadiene.

At the maximum hydrogenation TOR, at 403 K and 425 K for Pt(111) and Pt(100), respectively, the two similar SFG spectra indicate the presence of 1,3-cyclohexadiene as the major surface species. This spectral evidence indicates that cyclohexene hydrogenation proceeds through a 1,3-cyclohexadiene intermediate. As the temperature was increased to the maximum of the dehydrogenation TOR, the SFG spectra of adsorbates on the two crystal surfaces again became different from each other. The spectrum of the species on Pt(111) indicates the presence of both 1,3- and

1,4-cyclohexadiene, whereas only 1,3-cylcohexadiene was observed on Pt(100). Considering the differences in the two SFG spectra and the difference of the TORs for the maximum dehydrogenation, reaction pathways are proposed for dehydrogenation on each platinum surface. On Pt(111), cyclohexene dehydrogenation can proceed through either a 1,3- or 1,4-cyclohexadiene intermediate, whereas on Pt(100) dehydrogenation only occurs through a 1,3-cyclohexadiene intermediate. Figure 5.7 shows the difference of the reaction pathways for the two surfaces.

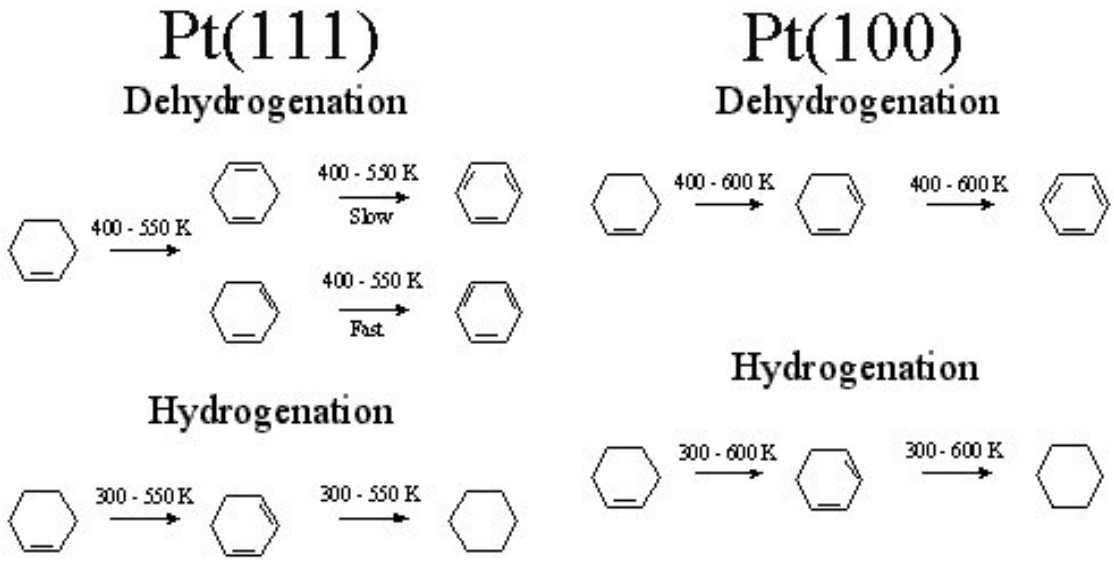

Figure 5.7 Reaction pathways for high-pressure cyclohexene hydrogenation and dehydrogenation for Pt(111) and Pt(100).

Because cyclohexene dehydrogenation occurs faster on Pt(100) than on Pt(111), and because 1,4-cyclohexadiene is absent from the Pt(100) surface, it is believed that 1,4-cyclohexadiene inhibits dehydrogenation on the Pt(111) surface. This inference is

reasonable considering that 1,4-cyclohexadiene conceivably must isomerize to 1,3-cyclohexadiene before it is completely dehydrogenated to form benzene.

Conclusions

Under UHV conditions, cyclohexene is dehydrogenated to benzene through a C_6H_9 intermediate, but under high-pressure conditions, this reaction intermediate is not observed. By comparing the structure sensitivity of cyclohexene hydrogenation and dehydrogenation on Pt(111) and Pt(100) at high-pressure, SFG data and corresponding kinetics data showed that hydrogenation occurs on both surfaces through a 1,3-cyclohexadiene intermediate. Dehydrogenation occurs faster on Pt(100) than on Pt(111), and from an examination of the SFG spectra, it became clear that both 1,3-cyclohexadiene and 1,4-cylcohexadiene exist on Pt(111), whereas only 1,3-cyclohexadiene exists on Pt(100). The evidence shows that dehydrogenation occurs faster through the 1,3-cyclohexadiene species than through the 1,4-cyclohexadiene species, and it may explain why the Pt(100) surface gives a higher TOR. There are not active sites blocked by 1,4-cyclohexadiene on Pt(100), but there are on Pt(111). The structure sensitivity can be explained by the predominance of one of the two reaction intermediates, which provides a more rapid reaction pathway than the other reaction intermediate.

References

[1] Bussell, M.E., Henn, F.C., and C.T. Campbell, *J. Phys. Chem.* 1992, **96**, 5965.

[2] Rodriguez, J.A., and C.T. Campbell, C. T., *J. Phys. Chem.* 1989, **93**, 826.

[3] Lamont, C.L.A., Borbach, M., Martin, R., Gardner, P., Jones, T. S., Conrad, H., and A.M. Bradshaw, *Surf. Sci.* 1997, **374**, 215.

[4] Land, D.P., Erley, W., and H. Ibach, *Surf. Sci.* 1993, **289**, 773.

[5] Martin, R., Gardner, P., Tushaus, M., Bonev, C. H., and A.M. Bradshaw, and T.S, Jones, *J. Electron Spectrosc. Relat. Phenom.* 1990, **54/55**, 773.

[6] Su, X., Kung, K., Lahtinen, J., Shen, Y.R., and G.A. Somorjai, *Catal. Lett.* 1998, **54**, 9.

[7] Lespade, L., Rodin, S., Cavagnat, D., and S. Abbate, *J. Phys. Chem.* 1993, **97**, 6134.

[8] N. Neto, *Spectrochimica Acta.* 1967, **23A**, 1763.

[9] Haines, J., and D.F.R. Gilson, *J. Phys. Chem.* 1990, **94**, 4712.

[10] Caillod, J., Saur, O., and J.C. Lavalley, *Spectrochim. Acta.* 1980, **36A**, 185.

Chapter 6: Structure Sensitivity of CO Dissociation

Introduction

Much of our knowledge of carbon monoxide structure and bonding on transition metal surfaces comes from high vacuum or low-pressure studies using low energy electron diffraction surface crystallography[1,2,3] and electron[4,5] and vibrational spectroscopies.[6] Simple rules were proposed that divided transition metal surfaces into two groups; one that dissociates CO and the other that does not.[7] Platinum was placed in the group that does not dissociate CO. As early as 1976 there was evidence for CO dissociation on a kinked surface of platinum from x-ray photoelectron spectroscopy indicating CO dissociation is surface structure sensitive.[8] It is well known that many transition metals form stable carbonyl compounds at high-pressures of CO. Some of these (e.g., $Fe(CO)_5$ and $Ni(CO)_4$) have high vapor pressures and are stable gas phase species.[9] Platinum also forms carbonyls that have been synthesized and their structures have been determined.[10] It is clear from reviewing the literature that the interaction of CO with platinum at high CO pressures will be very different as compared to its low pressure adsorption on the Pt(111) crystal face where it occupies top sites and bridge sites. In fact STM studies at high CO pressures and at 300 K detected the formation of a (5 x 1) CO surface structure corresponding to an incommensurate CO overlayer that has not been seen at low pressures.[11]

In this work we report on CO adsorption and dissociation at high (40 Torr) CO pressure and as a function of temperature on three different single crystal surfaces of platinum, Pt(111), Pt(557) and Pt(100). We find that CO dissociation occurs on all three crystal faces with decreasing temperature at 673 K, 548 K, and 500 K, respectively. Dissociation occurs by the Boudouard reaction $2CO \rightarrow C + CO_2$ and carbon deposition is readily observed on the three metal surfaces. There is evidence for platinum-carbonyl compound formation and for roughening of the platinum surface at the temperatures where CO dissociation occurs. It appears that the onset of CO dissociation coincides with the onset of platinum atom mobility inducing the formation of surface defects, steps and kinks, which become the sites for CO dissociation. The reaction is surface structure sensitive, with the (100) platinum surface dissociating CO at the lowest temperature, followed by the stepped (557) surface that has terraces of (111) orientation, and then the (111) crystal face.

Experimental

As described in Chapter 3, the samples were cleaned in UHV by repeated cycles of Ar^+ bombardment followed by exposure of 5×10^{-7} Torr of O_2 at 1125 K for two minutes. The sample was then annealed at 1135 K for one minute. After the sample was determined to be clean by Auger spectroscopy, CO (Scott Specialty) was introduced through a gas manifold system. The CO had an initial purity of 99.99% and was further purified by passing it through a zeolite trap cooled with liquid nitrogen. During high-pressure catalytic reactions, the sample was isolated from the vacuum

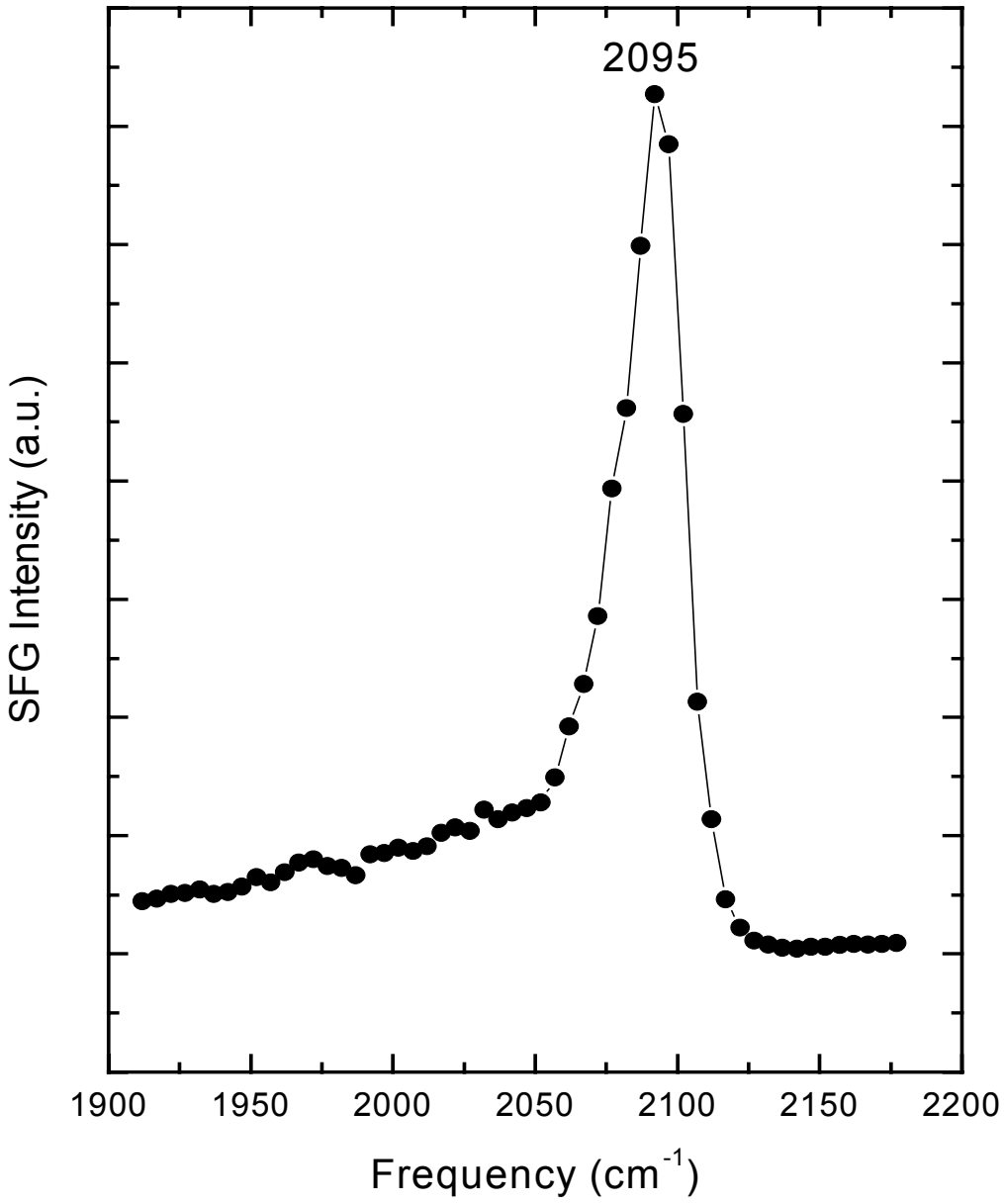

Figure 6.1 SFG spectrum of Pt(111) after a 4L exposure of CO.

pumps by a gate valve. For SFG experiments, the chamber had input and output

windows made of CaF_2 to allow the IR light to enter the chamber.

After the sample was cleaned, the single crystal of interest was exposed to 4 L of CO and sum frequency generation (SFG) spectra were acquired and averaged to compare with previous low-pressure results. Once the low-pressure spectra were acquired, the sample was then exposed to 40 Torr of CO at 300 K. SFG spectra were then acquired as a function of temperature as the sample was heated.

Results

CO adsorption and decomposition on Pt(111)

Before any high-pressure studies are performed by SFG, control experiments under UHV conditions are first performed to reproduce results previously observed under UHV conditions. A Pt(111) single crystal was mounted into the UHV chamber and cleaned as described earlier. Once the crystal was shown to be clean by Auger spectroscopy, the surface was exposed to 4 L (1 L = 10^{-6} Torr/sec) of CO. An SFG spectrum was acquired and is shown in Figure 6.1. A single resonance was observed at 2095 cm^{-1} and agrees with previous results.[12,13] This resonance is assigned to a c(4 × 2) array of CO adsorbed linearly on top site platinum sites.

An advantage of SFG over other vibrational spectroscopy techniques is that the gas phase does not contribute to the SFG signal. This means that single crystal surfaces can be probed with SFG while they are exposed to high-pressure CO as long as the SFG signal is properly normalized with a gas phase IR spectrum to take into account IR

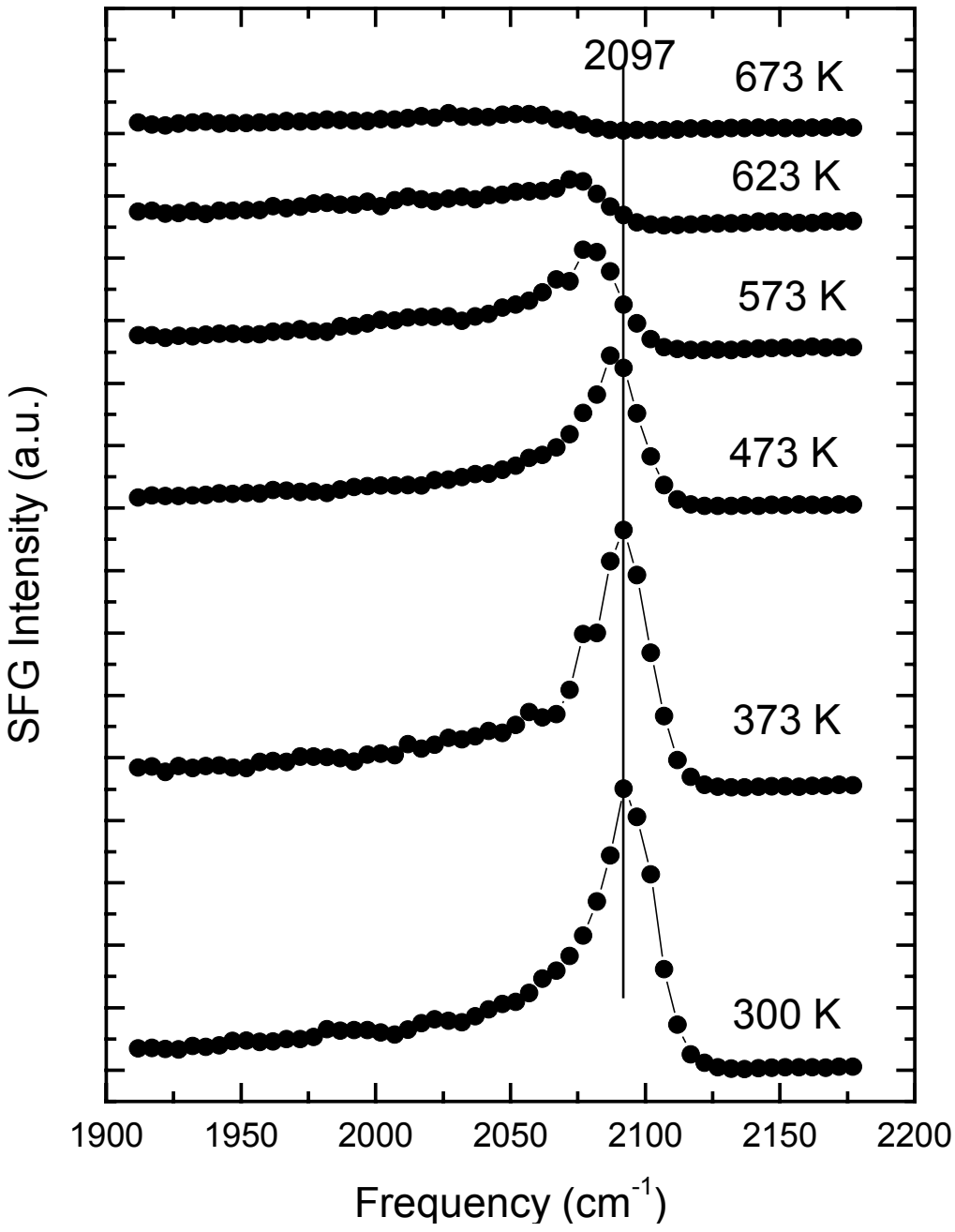

Figure 6.2 SFG spectra of Pt(111) as a function of temperature under 40 Torr of CO.

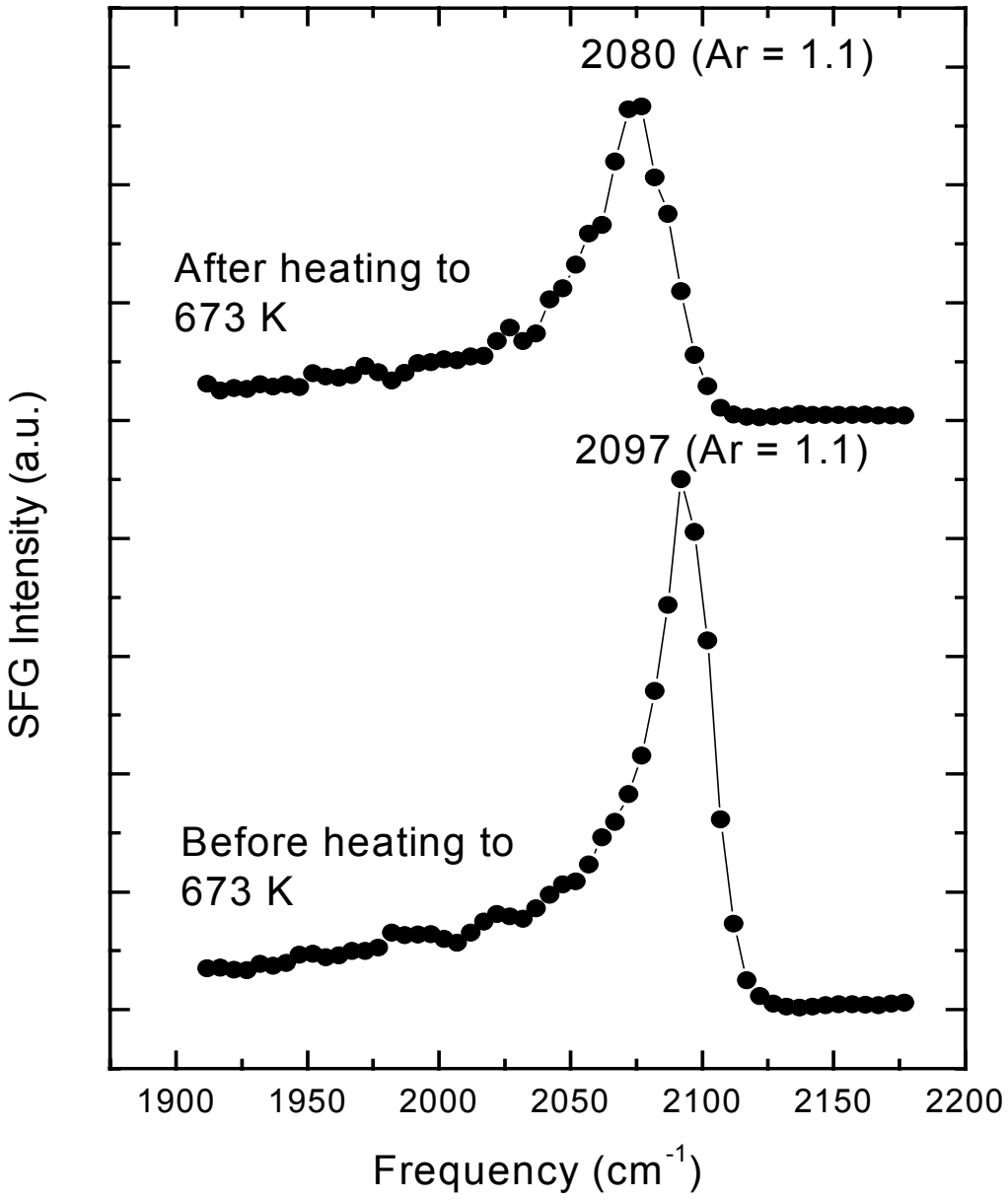

Figure 6.3 SFG spectra of Pt(111) under 40 Torr of CO at 300 K. The top spectrum is after heating to 673 K, showing an irreversible change in the heating and cooling cycle.

beam absorption by CO gas. After the Pt(111) surface was characterized under UHV conditions, 40 Torr of CO was introduced into the chamber. At 300 K under a pressure of 40 Torr of CO, a single resonance is observed in the SFG spectrum (Figure 6.2). This resonance is observed at 2097 cm^{-1}. The surface was then gradually heated sequentially to higher temperatures at which time SFG spectra were acquired. Each spectrum shown is the average of three scans unless noted otherwise. As the sample is heated up to 623 K, the spectrum slowly shifts to 2081 cm^{-1}. If the sample is cooled back down to 300 K after being heated to 623 K, the CO peak recovers with the same frequency and intensity as observed before the heating cycle. When the sample is heated to 673 K, the SFG spectra evolves with time by shifting to 2052 cm^{-1} and decreasing in intensity with consecutive spectra. The sample was then cooled back down to 300 K. As shown in Figure 6.3, the CO peak does not recover to the same frequency as compared to the CO spectra before the temperature cycle, but the amplitudes relative to the 4L spectrum are the same. This shows that there is an irreversible change in the heating and cooling cycle when the sample is heated to 673 K. After heating to 673 K, the chamber was quickly evacuated to 5×10^{-8} Torr, and an Auger spectrum of the Pt(111) surface was acquired. The Auger spectrum was dominated by carbon at 273 eV. From these results, it seems clear that Pt(111) is capable of dissociating CO to leave carbon on the surface under high temperatures and high-pressures of CO.

CO adsorption and decomposition on Pt(557)

A Pt(557) single crystal surface was also studied for CO dissociation properties. This is a stepped Pt surface in which there are 6 atom wide terraces of (111) orientation and

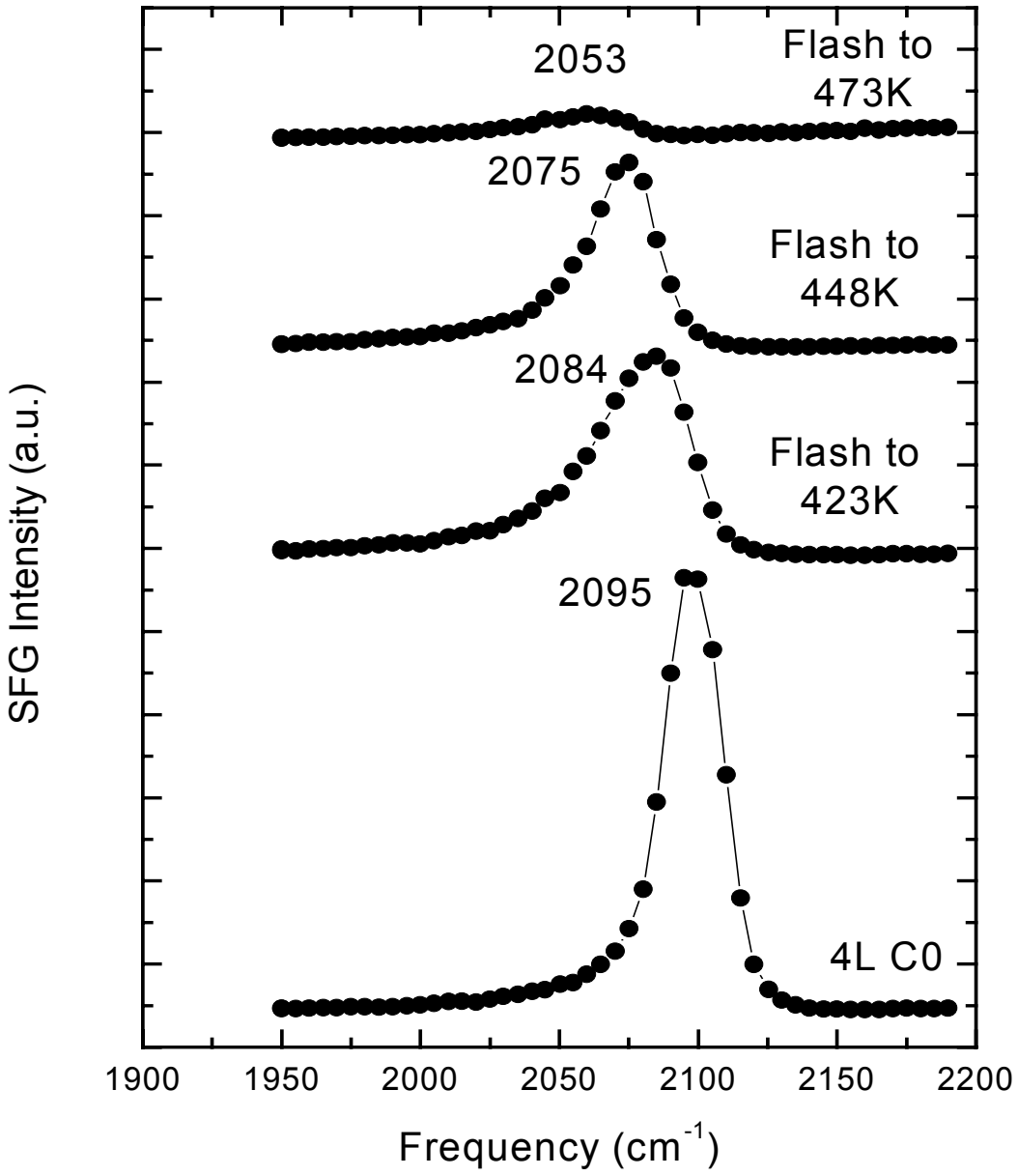

Figure 6.4 SFG spectra of a 4L exposure of CO on Pt(557). The sample was flashed to the temperatures noted to reveal CO adsorbed on either terrace or step sites.

single atom high steps of (100) orientation.[14,15,16] This surface was chosen since various stepped platinum surfaces have been shown to dissociate CO under UHV conditions.[8,17,18] It was expected that the stepped Pt(557) surface would dissociate CO at lower temperatures than was observed for Pt(111) when exposed to 40 Torr of CO.

A Pt(557) crystal was mounted into the vacuum system and cleaned as described earlier. After the surface was shown to be clean by Auger spectroscopy, the crystal was to exposed 4 Langmuir (L) of CO at 293K. Three SFG spectra were acquired and averaged. After fitting the averaged spectrum with equation 1, a single resonance at 2095 cm^{-1} with a fwhm of 11 cm^{-1} was observed (Figure 6.4). It is known that CO adsorbs on both terrace sites and on step edges on Pt(557) as revealed by temperature programmed desorption experiments. CO is observed to desorb at 423K for the terrace sites, and at 498K for step sites.[19,15] Since only one feature is observed in the SFG spectrum at saturation coverage, the SFG spectrum is indicative of a two-dimensional domain composed of CO molecules adsorbed at both step and terrace sites.[20] To determine whether just CO adsorbed on stepped edges could be observed by SFG, the surface was flashed sequentially to higher temperatures and cooled back down to 293K at which point SFG spectra were acquired (Figure 6.4). The sample was flashed to 423K, the desorption temperature of CO on terrace sites, and immediately cooled back down to 293K. The fitted SFG spectrum shows a single feature at 2084 cm^{-1} with a fwhm of 17 cm^{-1}. The lower frequency and broad peak may indicate that there was not a total desorption of terrace site CO. Incomplete desorption would leave both two-dimensional domains of CO adsorbed on terrace sites and one-dimensional domains of CO adsorbed on the step edges. The SFG spectrum is believed to be

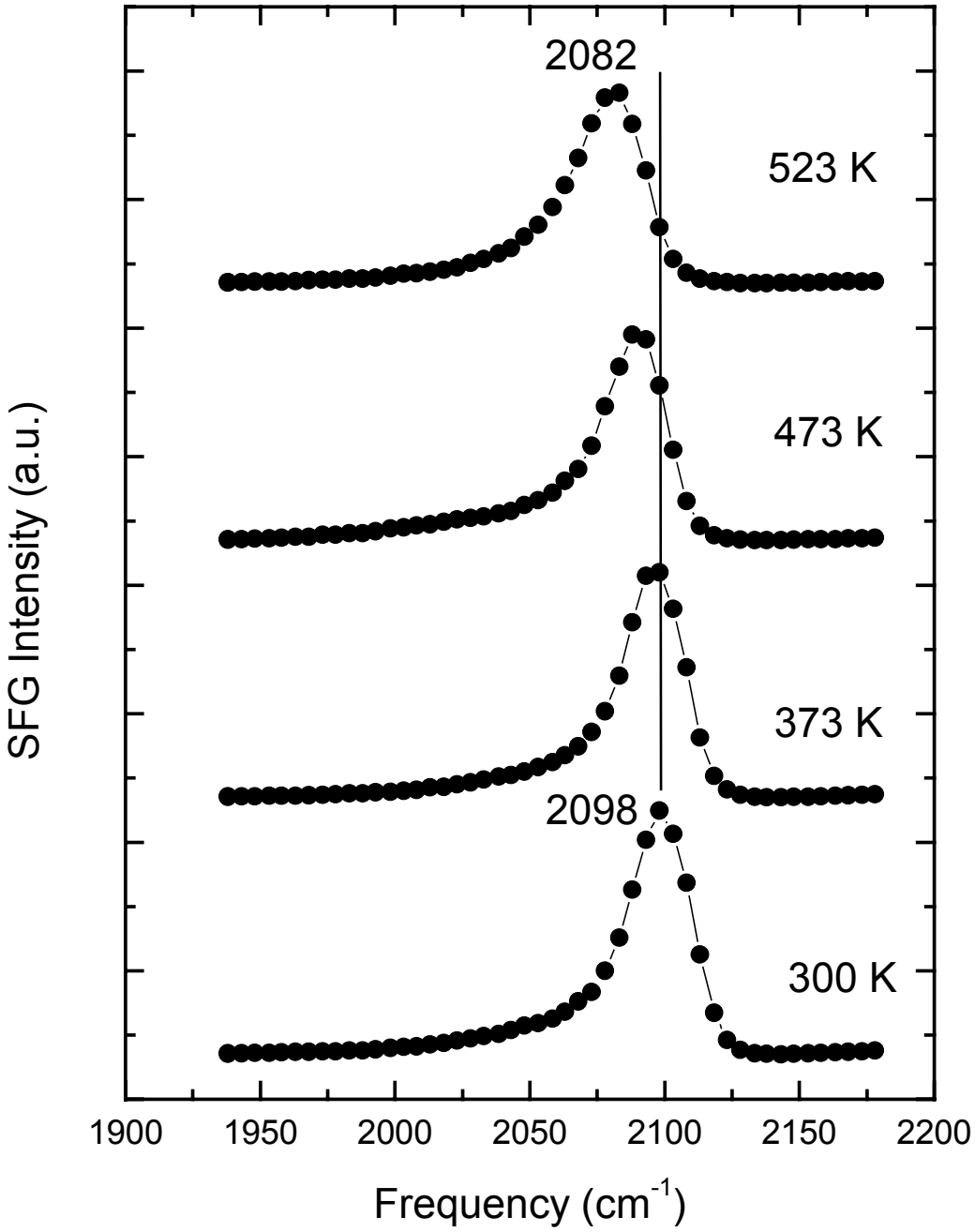

Figure 6.5 SFG spectra of Pt(557) as a function of temperature under 40 Torr of CO.

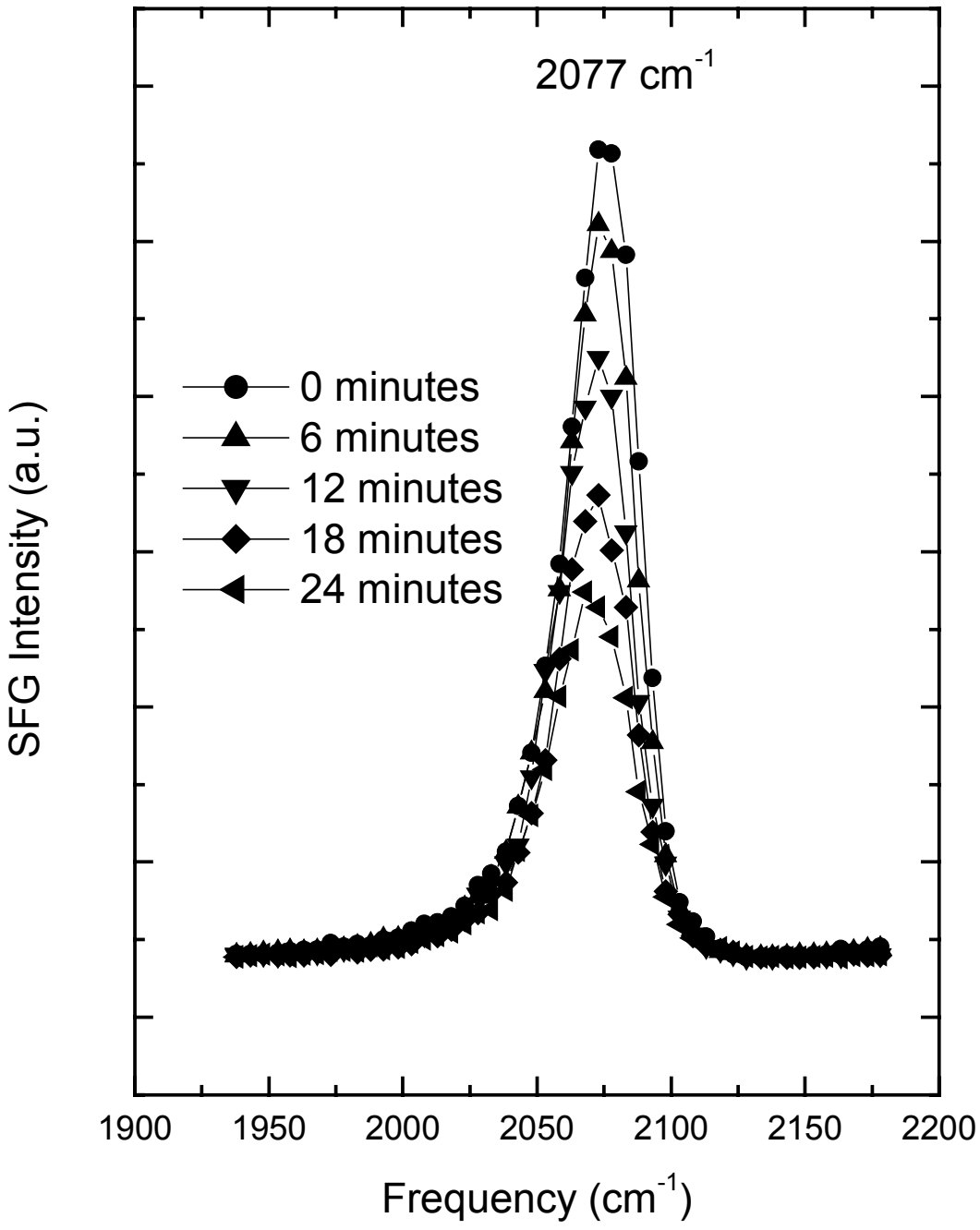

Figure 6.6 SFG spectra of Pt(557) under 40 Torr of CO at 548 K. The CO top-site peak decreases as a function of time.

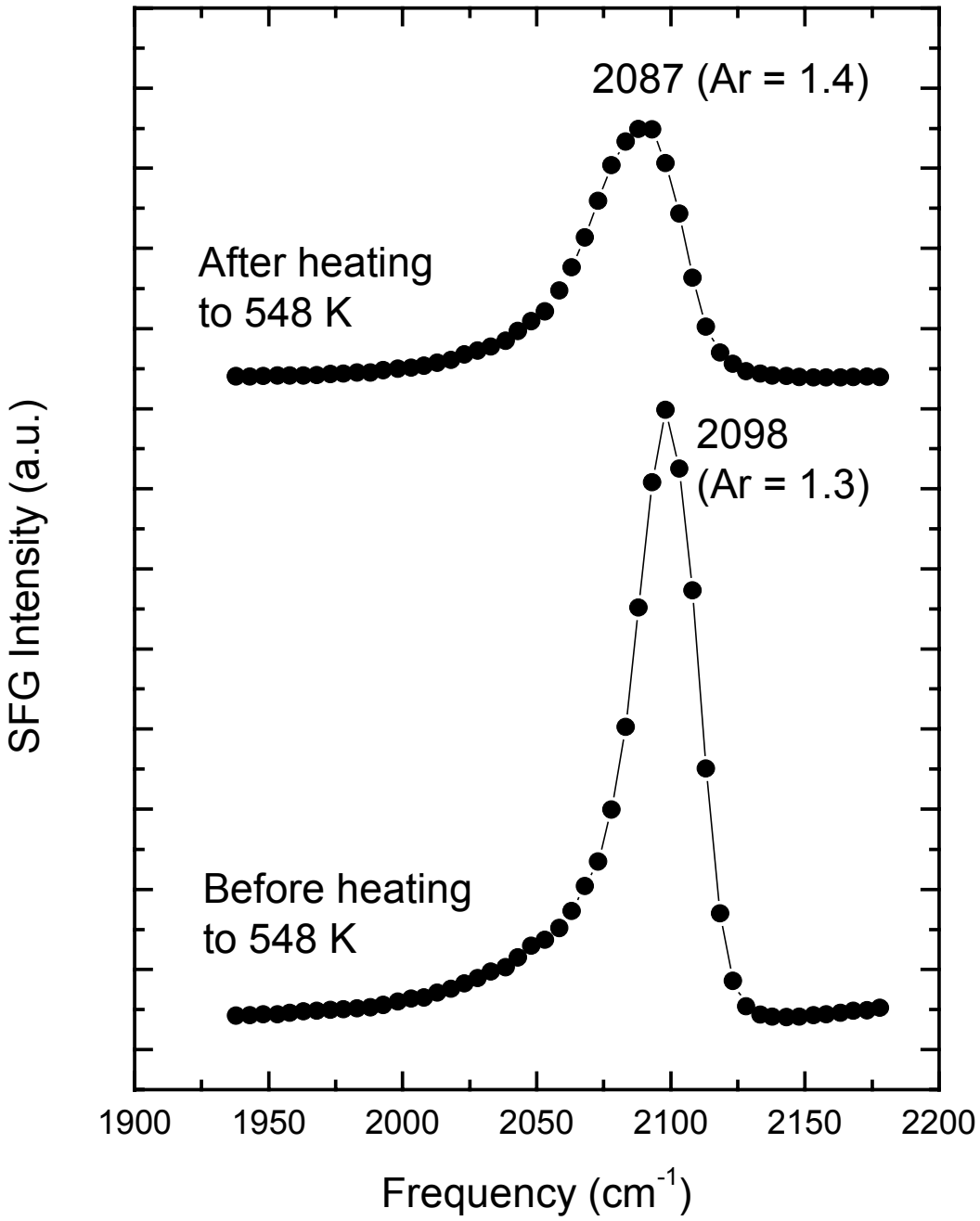

Figure 6.7 SFG spectra of Pt(557) under 40 Torr of CO at 300 K. The top spectrum is after heating to 548 K, showing an irreversible change in the heating and cooling cycle.

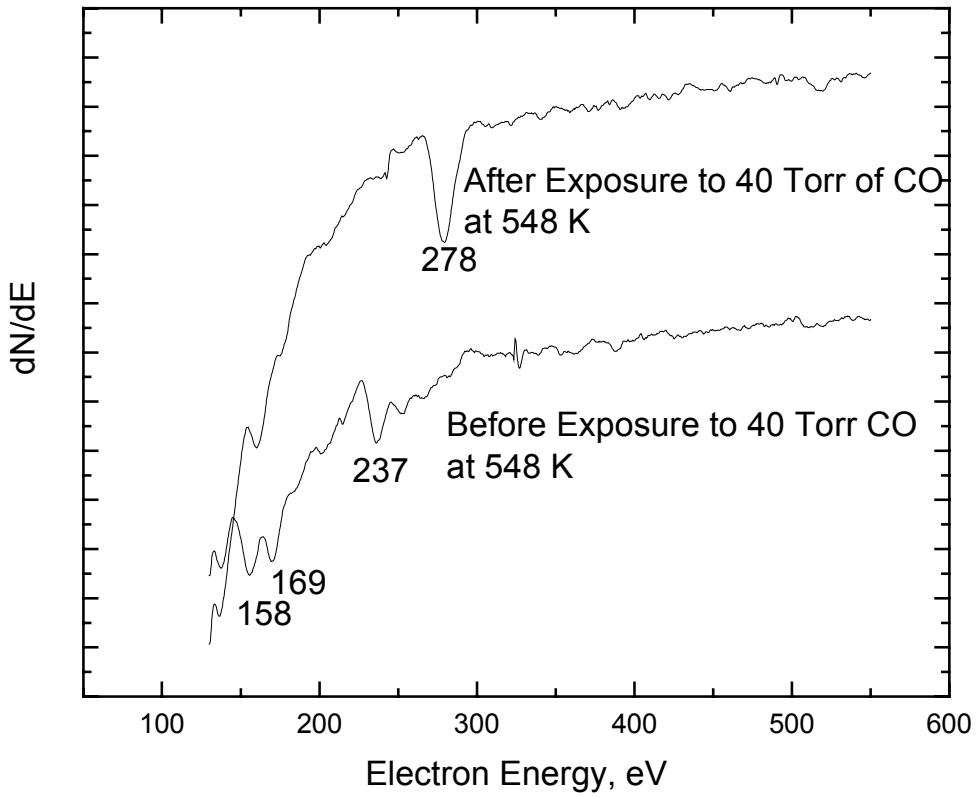

Figure 6.8 Auger spectra of Pt(557) before and after heating to 548 K in 40 Torr of CO.

composed of two peaks that are not resolved due to the resolution of the instrument. This could explain why the peak is broader than the peak observed directly after the 4L exposure.

The crystal was then flashed to higher temperatures. After flashing to 448 K, a feature at 2075 cm^{-1} is observed with a fwhm of 12 cm^{-1}. This spectrum indicates that there is now complete desorption of CO from the terrace sites, leaving just 1 dimensional domains of adsorbed CO at the step edges.[20] This spectrum remains

unchanged at higher temperatures until 498K, the desorption temperature of CO adsorbed at step edges, where the peak intensity and position change dramatically. A small peak is observed at 2053 cm^{-1}, and this frequency is due to the low coverage of CO at this temperature. If the crystal is heated above 498K, no resonance is observed. Auger spectroscopy then reveals a clean Pt(557) surface and no evidence of CO decomposition is observed.

For high-pressure CO studies, the Pt(557) single crystal was cleaned, and then exposed to 40 Torr of CO. After the CO was introduced into the chamber, an SFG spectrum was acquired. A single resonance at 2100 cm^{-1} is observed at 300K (Figure 6.5). As the sample is heated up to 523K, the resonance shifts to 2082 cm^{-1} with a slight decrease in intensity. When the sample is heated to 548 K, a dramatic effect is observed in the spectra (Figure 6.5). The peak position shifts to 2077 cm^{-1}, and as the sample is held at 548 K, the peak position remains unchanged, but the peak intensity decreases significantly over time. The crystal was then cooled back to room temperature, and a single resonance is observed at 2090 cm^{-1}. The amplitudes relative to the 4L spectrum are essentially the same (Figure 6.7) before and after the heating and cooling cycle. An irreversible change was also observed for the heating and cooling cycle on Pt(557). The chamber was then quickly pumped down to 5×10^{-8} Torr and an Auger electron spectrum was acquired. The Auger spectrum was completely dominated by a carbon peak at 279 eV (Figure 6.8). Similar to the results on Pt(111), CO also appears to dissociate on Pt(557) under 40 Torr of CO, but at a lower temperature.

CO adsorption and dissociation on Pt(100)

Pt(100) was also used to explore the dissociation of CO. When a Pt(100) surface is cleaned and prepared properly, the outermost layer of Pt atoms will reconstruct to form what is known as a pseudo-hexagonal Pt(100)-(5 × 20) structure.[21,22,23] Once the surface coverage of CO increases to above 0.5 ML, this hexagonal surface reconstructs back to the Pt(100)-(1 × 1) square surface structure.[24,25]

A Pt(100) surface was mounted into the UHV chamber and cleaned as described earlier. Once the surface was shown to be clean with Auger spectroscopy, the surface was observed to be the reconstructed (5 x 20) hex Pt(100) by LEED. The surface was then exposed to 4L of CO. A single resonance at 2092 cm^{-1} was observed and is shown in Figure 6.9. This frequency is assigned to atop (4 x 2) CO phase on unreconstructed (1 x 1) Pt(100).

The Pt(100) surface was then exposed to 40 Torr of CO. At 298 K, a single resonance at 2100 cm^{-1} was observed (Figure 6.10). The sample was then gradually heated to 450 K and a slight shift to 2086 cm^{-1} was observed with little change in intensity (Figure 6.10). If the sample was then cooled from this temperature back down to 300 K, the CO peak recovers to 2100 cm^{-1} and so the heating cycle shows reversibility up to 450 K. The surface was heated to 500 K and a dramatic change in the SFG spectra is observed. The peak immediately red shifts 20 cm^{-1} to 2065 cm^{-1} with a slight decrease in intensity. With consecutive SFG spectra at 500 K, the peak is observed to quickly lose its intensity as a function of time (Figure 6.11) and shifts to 2055 cm^{-1}. The Pt(100) crystal was then cooled back to 300 K, and again, an

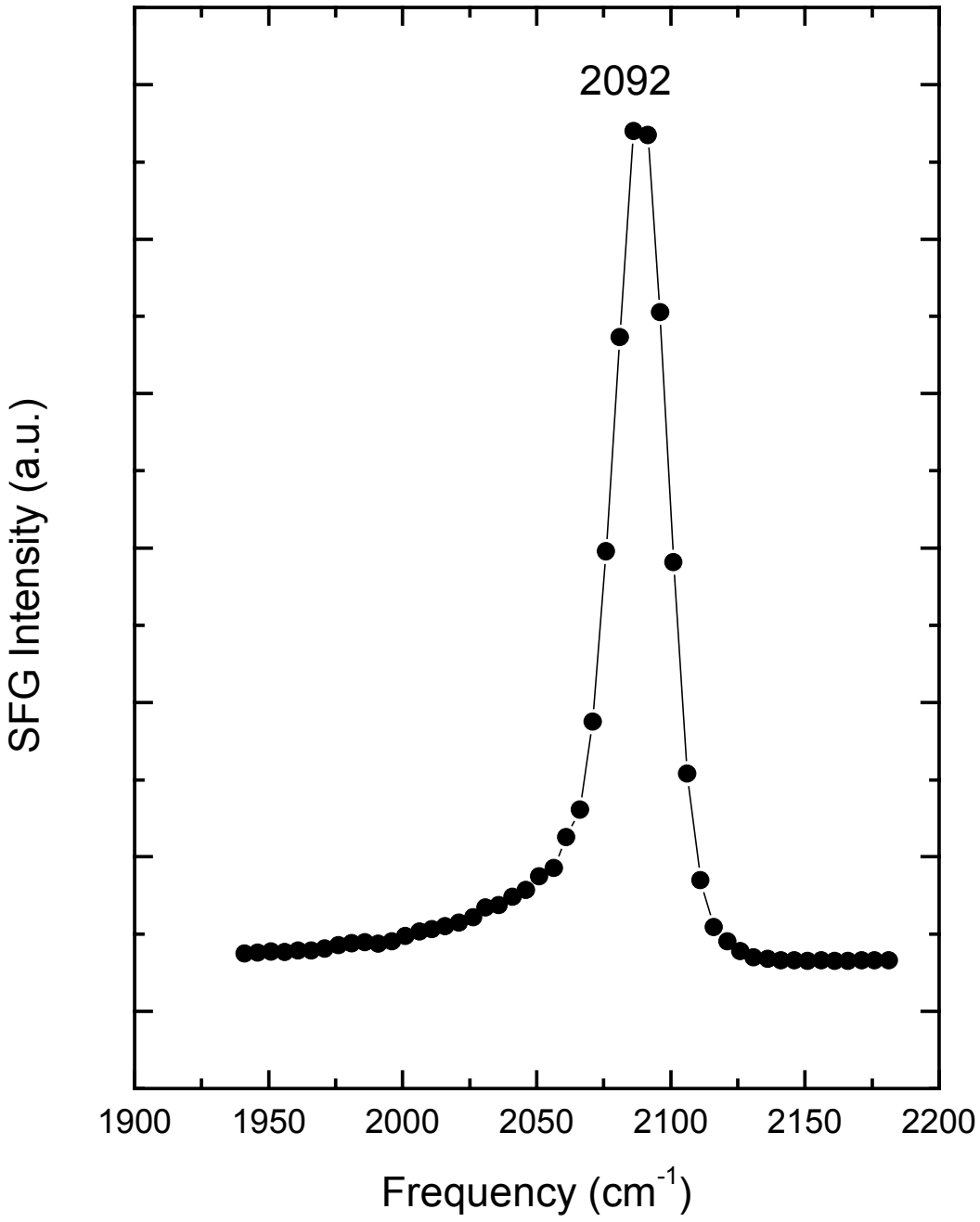

Figure 6.9 SFG spectrum of Pt(100) after a 4L exposure of CO.

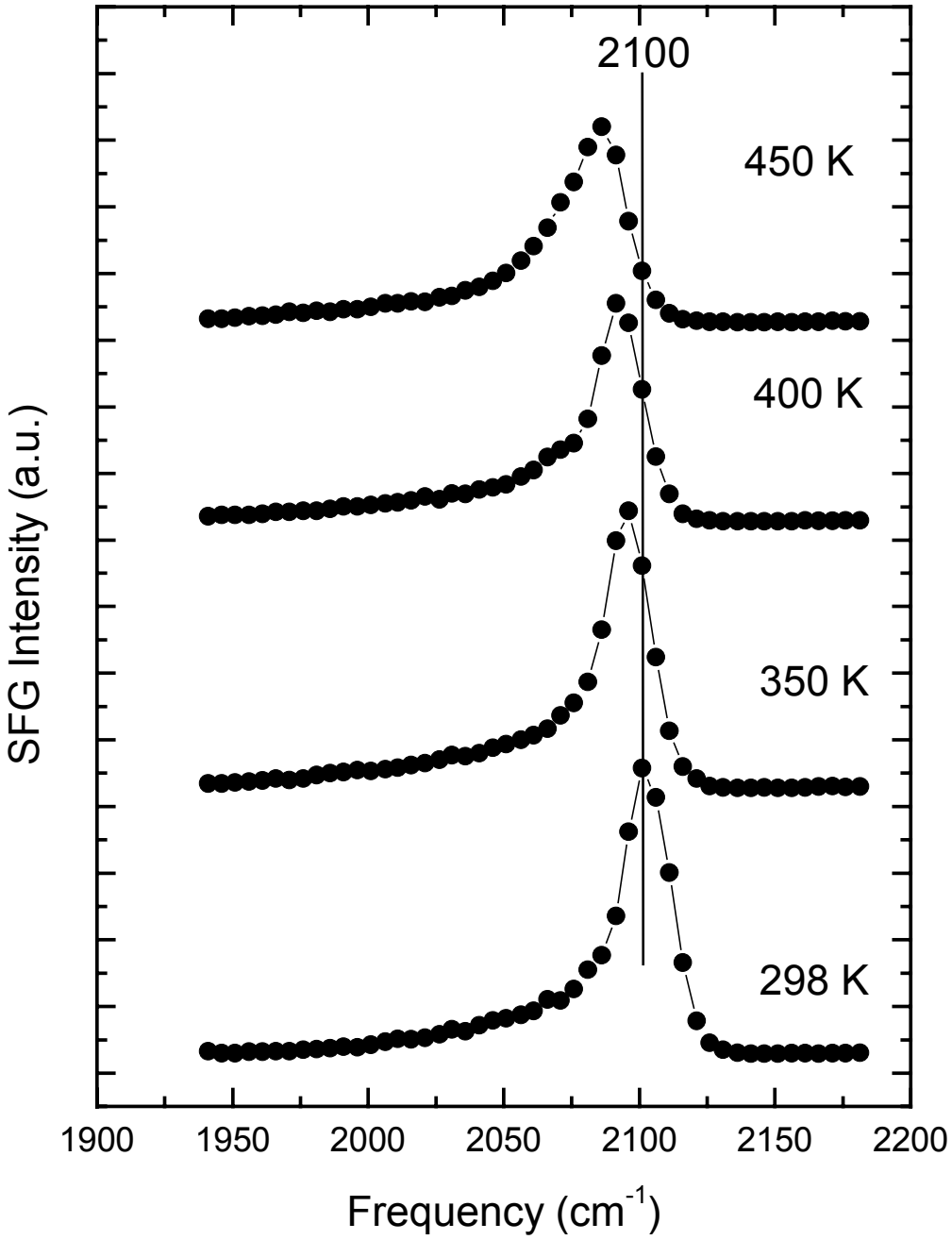

Figure 6.10 SFG spectra of Pt(100) as a function of temperature under 40 Torr of CO.

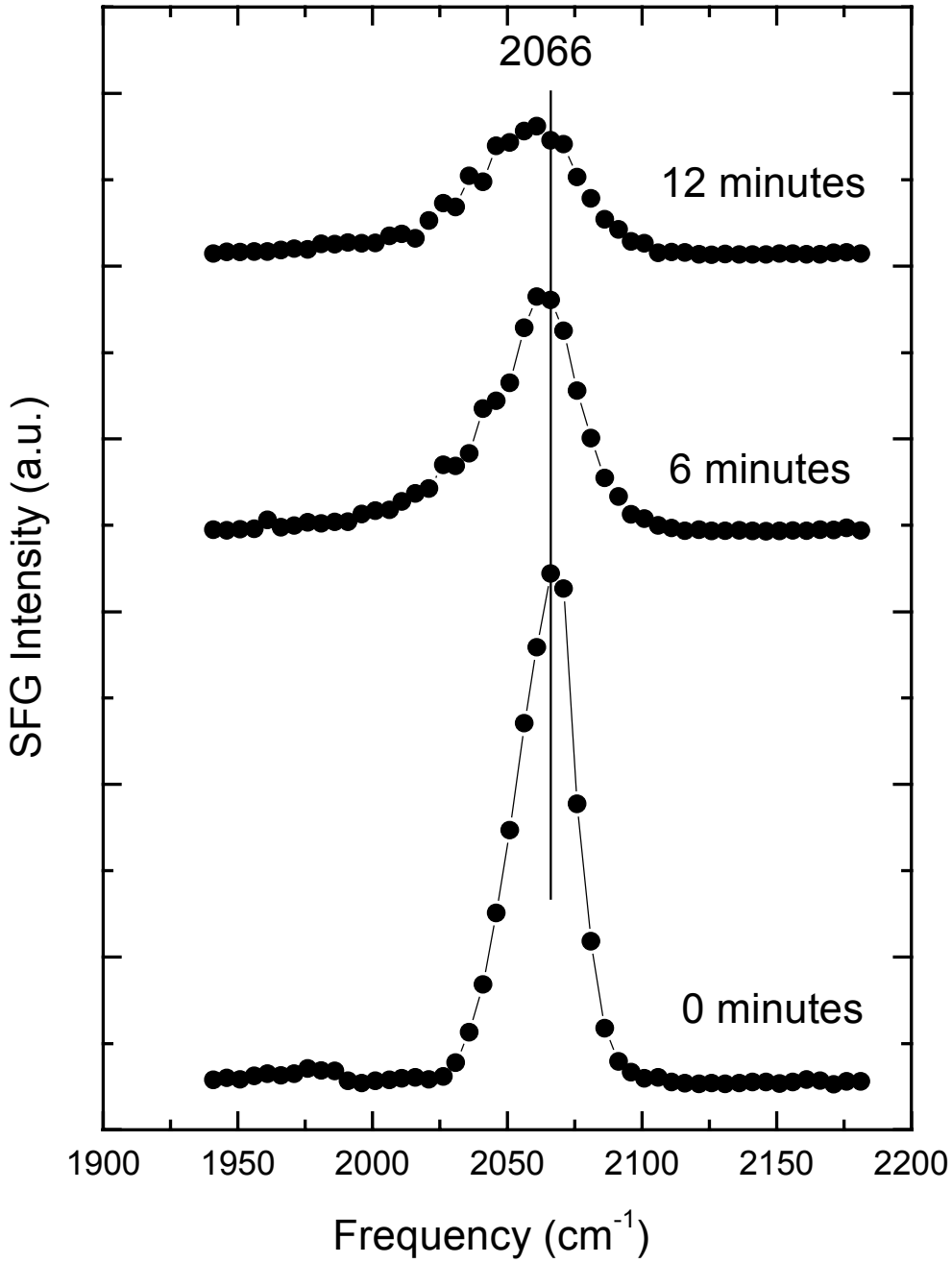

Figure 6.11 SFG spectrum of Pt(100) under 40 Torr of CO at 500 K. The peak shifts and decreases as a function of time.

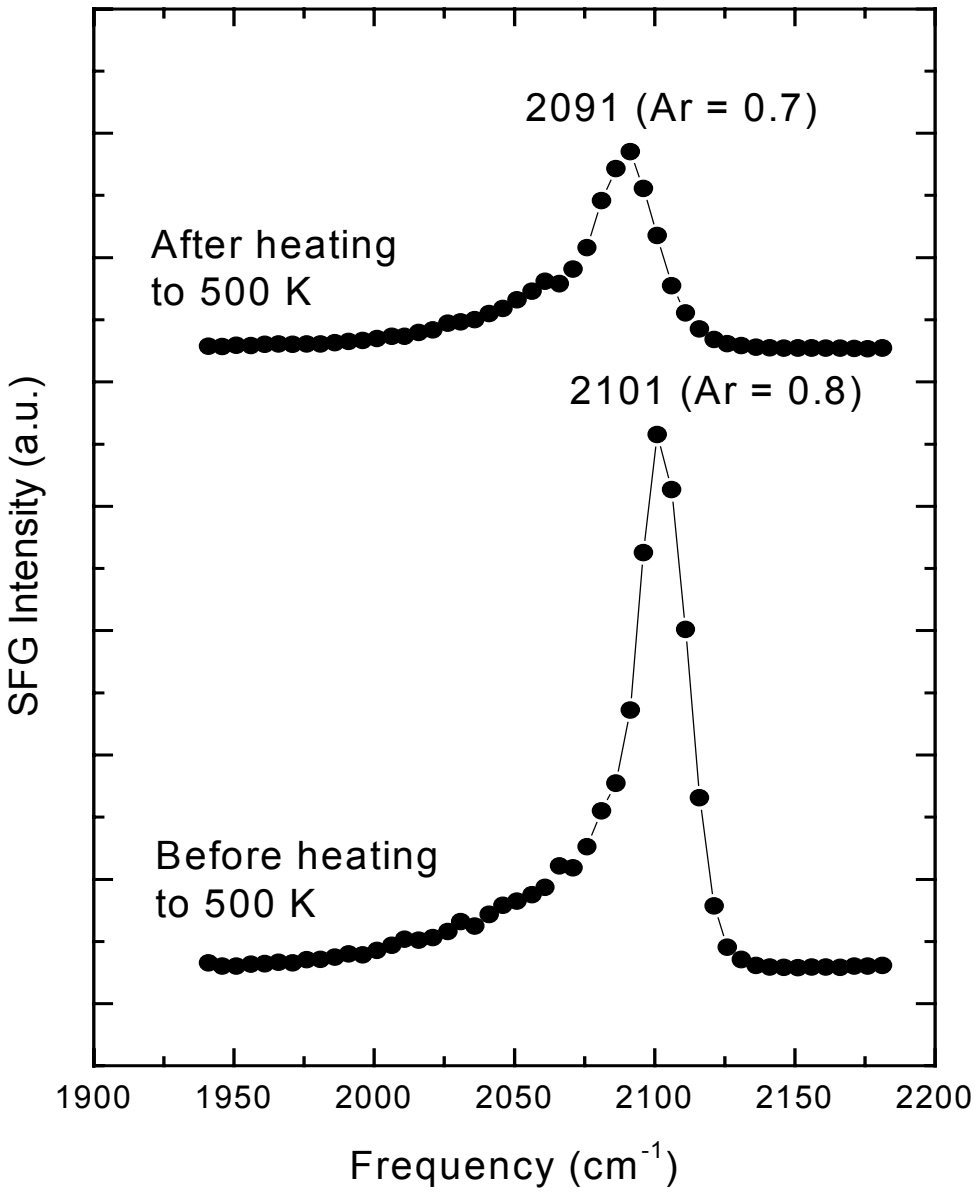

Figure 6.12 SFG spectra of Pt(100) under 40 Torr of CO at 300 K. The top spectrum is after heating to 500 K, showing an irreversible change in the heating and cooling cycle.

irreversible change is observed (Figure 6.12). The spectrum after the heating and cooling cycle is red shifted to 2091 cm^{-1} and is much broader, but the amplitude is about the same. The chamber was then evacuated and an Auger spectrum was acquired revealing the surface was covered with carbon. Pt(100) also dissociates CO under high-pressure, but at a considerably lower temperature as compared to Pt(111) and Pt(557).

Discussion

From the results presented above, when a platinum single crystal is exposed to 40 Torr of CO, the CO SFG peak is observed to red shift to lower frequency as a function of increasing temperature. Once a critical temperature is reached, the CO peak intensity will decrease rapidly as a function of time, and if heated long enough, the peak will disappear completely. The CO top-site frequency is plotted against the heating temperature in Figure 6.13 for these three surfaces. As evident from this dissociation trend, Pt(111) is the least active for dissociating CO as the dissociation occurs at the highest temperature (673 K). Pt(100) is the most active as it has the lowest temperature for CO dissociation (500 K). The activity of the Pt(557) crystal lies between the activity of the Pt(111) and Pt(100) crystal.

There have been many studies that investigated the interaction of CO and platinum single crystals under UHV conditions and most of these studies agree that CO will not dissociate on low miller index surfaces of platinum. However, there have been studies that have shown evidence of CO dissociation on platinum surfaces that contain

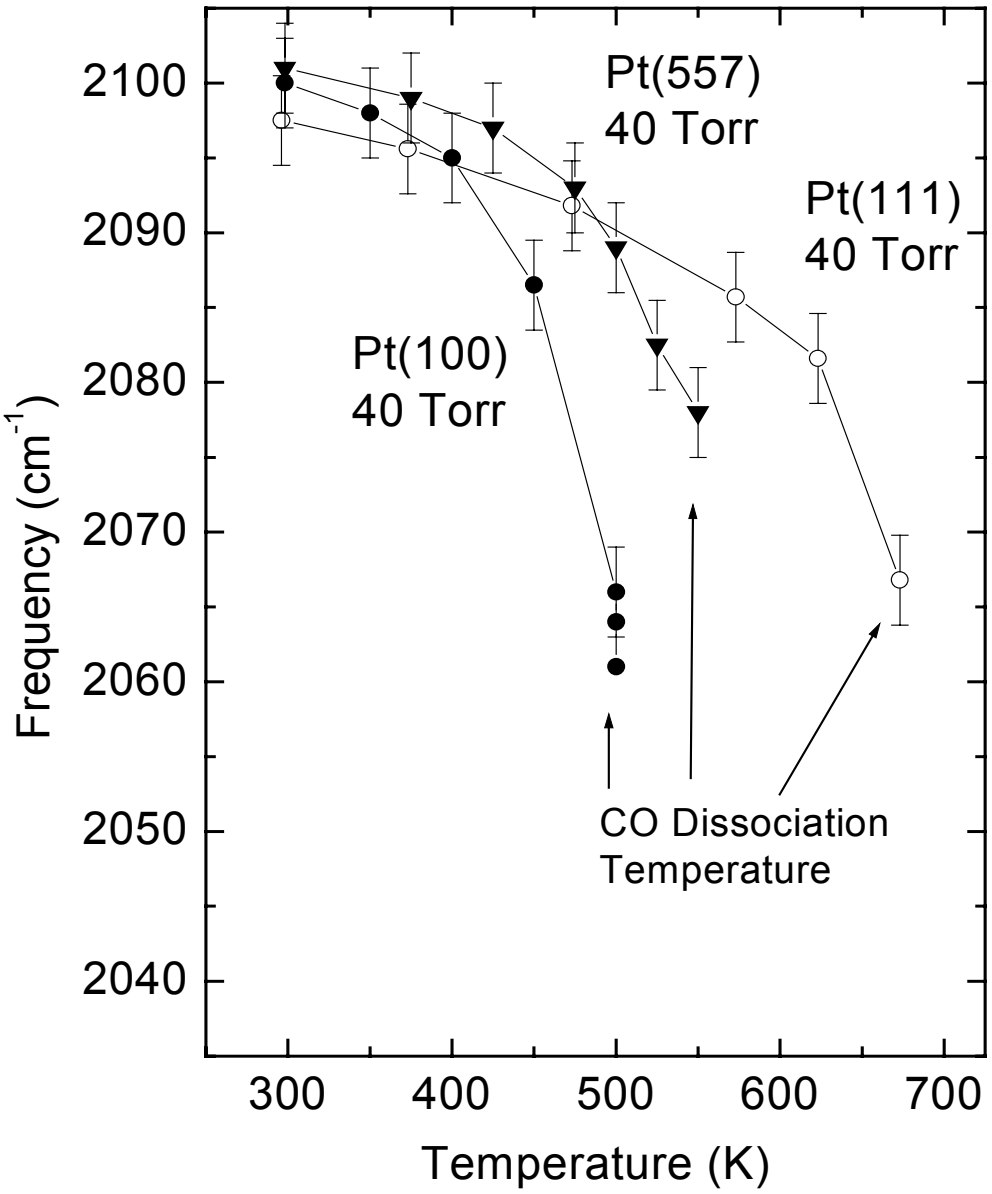

Figure 6.13 CO top-site frequency as a function of temperature for Pt(111), Pt(557) and Pt(100) under 40 Torr of CO.

step and kink sites.[8,17,18] There are several different adsorption sites available on Pt

single crystal surfaces with kink and step sites. Using vibrational spectroscopy to probe the stretching frequency of CO adsorbed on these stepped and kinked surfaces, it has been found that the CO stretching frequency is lower if it is adsorbed on stepped or kink sites than CO on terrace sites.[20] This observation means that CO is more strongly bound to these sites, which inherently causes the C≡O bond to weaken. This makes it easier to break the CO bond and deposit carbon on the surface.

Iwasawa and coworkers showed using X-ray photoelectron spectroscopy (XPS) that adsorbed CO dissociates on a stepped Pt(6(111) × (710)) surface.[8] Using a spherical single crystal, Li and coworkers showed CO dissociated on various surfaces of the sphere with step edges and kink sites.[17] For the Pt(210) face of the sphere, the observed CO dissociation begins around 380 K. Park and coworkers used XPS to observe CO dissociation on Pt(410) around 450 K.[18]

From these adsorption studies on Pt, it becomes clear that step and kink sites are needed to dissociate CO. Thus, a low Miller index crystal face will not dissociate CO under UHV conditions. With the advent of high-pressure surface sensitive techniques such as sum frequency generation surface vibrational spectroscopy (SFG), it is now possible to observe the behavior of CO dissociation from UHV pressures to near atmospheric pressures. Previously in this group, it was found using SFG and Auger electron spectroscopy that CO does dissociate on Pt(111) under high pressure (400 Torr) and high temperature (~673 K).[26] It was shown that high-pressures of CO could roughen or anneal the surface depending on the surface temperature.

In this previous study of Pt(111) under the presence of 400 Torr of CO, a red shift was observed for the top site CO peak as the sample was heated. It was explained

that this red shift was most likely due to anharmonic coupling to the frustrated translation mode.[27,28] This model explains that a temperature dependent red shift could result from vibrational dephasing, which is due to a rapid energy exchange between low frequency modes of the adsorbed molecule and substrate that are anharmonically coupled to the top site vibrational mode. Essentially, because of the mobility of CO molecules at high-temperatures, dephasing of the harmonic coupling occurs.

In this current study under 40 Torr, a similar red shift for the top-site CO frequency was also observed for each crystal, although, the red shift was not as large for the Pt(557) crystal. It is likely that anharmonic coupling to the frustrated translational mode is only partly responsible for the observed red shift. Surface roughening could also account for a portion of the red shift that was observed. Brandt and coworkers showed that the CO frequency is not only dependent on the harmonic coupling between CO molecules; it is also dependent on the coordination number (n) of platinum atoms in which the top-site CO is adsorbed.[29] For n=9, which corresponds to platinum atoms on (111) terraces, and a coverage of 0.33 ML, Brandt and coworkers calculated a top-site CO frequency of 2098 cm^{-1}. For n=6, which corresponds to platinum atoms at kink sites, they calculate a top-site CO frequency of 2076 cm^{-1}. As the coordination number decreases below 6, the data extrapolates to even lower frequencies. It is possible that as the temperature is raised in the presence of high pressures of CO, the surface slowly roughens, decreasing the coordination to a point where platinum binary carbonyls can form to facilitate the dissociation of CO.

It is believed that the red shift observed at temperatures up to the CO dissociation temperature is due to anharmonic coupling to the frustrated vibration

mode. At the temperature at which CO dissociation begins to occur, the surface is roughened to form step and kink sites through the production of platinum carbonyls. The frequency shift at this temperature is then believed to be a result of a decrease in the coordination number of platinum surface atoms.

Dipole coupling has been ruled out as a possible explanation for the observed red shift. The dipole coupling argument explains that the observed CO top site stretching frequency is a function of coverage.[30,31] As the coverage increases, the frequency increases. The dipole coupling argument was ruled out because the fitted amplitudes, which depend partly on the CO coverage, did not change by more than 10%. This indicated the coverage at high temperatures was close to the same as the coverage at low temperatures. The specifics for CO dissociation over each crystal will now be discussed.

Pt(111)

Under 40 Torr of CO on Pt(111), the SFG spectrum changed as a function of temperature up to 623 K. This change was mainly a red shift in the frequency of the top-site CO peak and a slight decrease in the fitted amplitude of the peak. These results are very similar to results obtained on Pt(111) under 400 Torr of CO pressure and it is believed that the frequency shift is due to anharmonic coupling to the frustrated translational mode.[27,28]

At 673 K, the SFG spectra changed as a function of time with the top site peak red shifting to 2052 cm^{-1} and becoming broader. The CO top-site frequency observed is very similar to platinum carbonyls ($Pt(CO)$, $Pt(CO)_2$, $Pt(CO)_3$, which have been observed to exhibit CO stretching frequencies near 2055 cm^{-1}.[10] Most likely at 673 K,

platinum carbonyls are being formed which could explain surface roughening. In order for platinum carbonyls to form, surface platinum atoms must be extracted from the surface array, which then decreases the coordination number of that platinum atom. The production of platinum carbonyls could be the driving force for surface roughening under high-pressure CO and high temperatures. Once this roughened surface is formed, CO dissociation can then occur on defect sites.

When the crystal is cooled back down to 300 K, an irreversible change in the heating and cooling cycle is observed. The frequency of the top site CO is now observed at 2080 cm^{-1}, a 17 cm^{-1} red shift from the frequency observed before the heating cycle at 300 K. The fitted amplitude is essentially the same but the line width is broader, so it appears that CO is now adsorbed on a modified Pt(111) surface. The system was then pumped down to 5 x 10^{-8} Torr, and Auger spectroscopy revealed a carbon-covered surface. The lower frequency and broader peak is due to CO co-adsorbed with carbon on the surface.

Pt(557)

CO dissociation occurs at a lower temperature on Pt(557) than on Pt(111) (548 vs. 673 K). It is known that step sites are much more active during catalysis, so it is no surprise that chemistry is done at a lower temperature on a surface with introduced defects. A similar shift in the CO top site frequency is observed up to 523 K as observed on Pt(111) which is attributed to anharmonic coupling to the frustrated translational mode.[27,28] The difference between Pt(557) and Pt(111) is that once the Pt(557) surface is heated to 548 K, the top site CO frequency no longer shifts below 2077 cm^{-1}, but the amplitude of the peak decreases over time. The SFG spectrum

evolves differently for Pt(557) at the dissociation temperature as compared to Pt(111) and there does not appear to be any evidence for the production of platinum carbonyls as observed on Pt(111). Since it is most likely that step and kink sites are needed for CO dissociation, it requires the Pt(111) surface to be heated to 673 K in the presence of 40 Torr of CO to roughen the surface. Because the stepped Pt(557) surface already has introduced step sites, the surface does not need to be heated to a temperature to induce surface roughening and the production of binary carbonyls. This explains why the Pt(557) surface does not need to be heated to 673 K to dissociate CO as needed for Pt(111). The red shift is believed to be due to anharmonic coupling and not due to the decrease in coordination of platinum atoms because surface roughening is not occurring on Pt(557).

Pt(100)

Pt(100) exhibits the lowest temperature to dissociate CO. Under 40 Torr of CO, the dissociation temperature is observed to be 500 K. This temperature is considerably lower than dissociation observed on Pt(111). When a Pt(100) surface is properly cleaned, the outermost surface layer of metal atoms will reconstruct to form what is known as a pseudo-hexagonal Pt(100) (5×20) surface structure.[21,22,23] This hexagonal surface structure will remain until CO or other contaminants such as NO are introduced to the surface at which time the surface reconstruction will lift to reveal the truncated square Pt(100) (1×1) surface.[24,25] Because Pt(100) easily reconstructs, the surface atoms are most likely very mobile as compared to Pt(111), the lowest energy surface of Pt. Because of this, the surface atoms can roughen and produce platinum binary carbonyls at a much lower temperature.

Conclusions

Using sum frequency generation surface vibrational spectroscopy, the structure sensitivity of CO dissociation was investigated. The surface of platinum single crystals can either be roughened or annealed depending on the crystal temperature. It was found that CO dissociates at 673 K, 550 K, and 500 K for Pt(111), Pt(557) and Pt(100), respectively. The frequency of the top-site CO peak shifted to lower frequencies as the sample was heated above 300 K. Below the dissociation temperature, the frequency shift is attributed to anharmonic coupling to the frustrated translational mode. At the temperature where CO dissociation occurs, the frequency shifts to near 2055 cm^{-1}, which is similar to the frequency observed for platinum carbonyl species. From UHV studies, it is known through the literature that CO will only dissociate on step or kink sites on platinum. Under 40 Torr of CO, Pt(111) and Pt(100) must be heated to a temperature at which the surface is roughened to produce step and kink sites by the production of platinum carbonyls, which may be the precursors to CO dissociation. Pt(557) is essentially a (111) surface with defects already introduced as steps. Because of this, the Pt(557) surface does not need to be heated to 673 K, the dissociation temperature on Pt(111), to produce defects. CO is able to dissociate on the steps of Pt(557) at a lower temperature than needed to roughen the surface through the production of platinum carbonyls. Pt(100) has the lowest dissociation temperature probably because the outermost surface platinum atoms are more mobile since the Pt(100) surface can easily reconstruct. Because of this mobility, the (100) surface can roughen at a lower temperature than the other two surfaces.

References

[1] Hagen, D.I., Nieuwenhuys, B.E., Rovida, G., and G.A. Somorjai, *Surf. Sci.* 1976, **57**, 632.

[2] Doyen, G., and G. Ertl, *Surf. Sci*., 1974, **43**, 197.

[3] Morgan, A.E., and G.A. Somorjai, *J. Chem. Phys*. 1969, **51(8)**, 3309.

[4] Akimoto, K., Sakisaka, Y., Nishijima, M., and M. Onchi, *Surf. Sci.,* 1979, **88**, 109.

[5] Baro, A.M., and H. Ibach, *J. Chem. Phys.,* 1979**, 71** , 4812.

[6] Sheppard, N., and T.T. Nguyen, *Adv. Infrared Raman Spectrosc.* 1978, **5**, 66.

[7] Broden, G., Rhodin, T.N., Brucker, C., Benbow, R., and Z. Hurych, *Surf. Sci*. 1976, **59**, 593.

[8] Iwasawa, Y., Mason, R., Textor, M., and G.A. Somorjai, *Chem. Phys. Lett.* 1976, **44**, 468.

[9] Clements, P.J., and F.R. Sale, *Metallurgical Transactions B (Process Metallurgy),* 1976, **7B**, 171.

[10] Manceron, L., Tremblay, B., and M.E. Alikhani, *J. Phys. Chem.* 2000, **104**, 3750.

[11] Jensen, J., Rider, K.B., Salmeron, M., and G.A. Somorjai, *Phys. Rev. Lett.* 1998, **80**, 1228.

[12] Hayden, B.E., and A.M. Bradshaw, *Surf. Sci.* 1983, **125**, 787.

[13] Klunker, C., Balden, M., Lehwald, S., and W. Daum, *Surf. Sci.* 1996, **360**, 104.

[14] Lin, T.H., and G.A. Somorjai, *Surf. Sci.* 1981, **107**, 573.

[15] Ohno, Y., Sanchez, J.R., Lesar, A., Yamanaka, T., and T. Matsushima, *Surf. Sci.* 1997, **382**, 221.

[16] Somorjai, G.A., Joyner, R.W., and B. Lang, *Proc. R. Soc. Lond. A.* 1972, **331**, 335.

[17] Li, X.Q.D., Radojicic, T., and R. Vanselow. *Surf. Sci. Lett.* 1990, **225** L29.

[18] Park, Y.O., Masel, R.I., and K. Stolt, *Surf. Sci.* 1983, **131**, L385.

[19] Davis, S.M., Zaera, F., and G.A. Somorjai, *J. Catal.* 1982, **77**, 439.

[20] Hayden, B.E., Kretzshmar, K., Bradshaw, A.M., and R.G. Greenler, *Surf. Sci.* 1985, **149**, 394.

[21] Heilmann, P., Heinz, K., and K. Muller, *Surf. Sci.* 1979, **83**, 487.

[22] Morgan, A.E., and G.A. Somorjai, *Surf. Sci.* 1968, **12**, 405.

[23] Broden, G., Pirug, G., and H.P. Bonzel, *Surf. Sci.* 1978, **72**, 45.

[24] Behm, R.J., Thiel, P.A., Norton, P.R., and G. Ertl, *J. Chem. Phys.* 1983, **78**, 7437.

[25] Gardner, P., Martin, R., Tushaus, M., and A.M. Bradshaw, *J. Electron Spec. Relat. Phenom.* 1990, **54/55**, 619.

[26] Kung, K.Y., Chen, P., Wei, F., Shen, Y.R. and G.A. Somorjai, *Surf. Sci.* 2000, **463**, L627.

[27] Persson, B.N.J., and R. Ryberg, *Phys. Rev. B.* 1985, **32**, 3586.

[28] Harle, H., Mendel, K., Metka, U., Volpp, H.R., Willms, L., and J. Wolfrum, *Chem. Phys. Lett.* 1997, **279**, 275.

[29] Brandt, R.K., Sorbello, R.S., and R.G. Greenler, *Surf. Sci.* 1992, **271**, 605.

[30] Crossley, A., and D.A. King, *Surf. Sci.* 1977, **68**, 528.

[31] Crossley, A., and D.A. King, *Surf. Sci.* 1980, **95**, 131.

Chapter 7: Structure Sensitivity of CO Oxidation Ignition

Introduction

In this work we discuss our recent findings of the mechanisms of CO oxidation. This is a total oxidation or combustion process that has been studied by experiments at low as well as at high pressures,[1,2,3,4,5,6,7,8] and has been modeled by computer simulations.[9,10] Platinum surfaces, which are excellent catalysts for this reaction (in addition to that of palladium) were the focus of most of these investigations.

Using SFG to study catalysis, we carried out CO oxidation over platinum single crystal surfaces, both flat ((111) and (100)) and stepped ((557)), to explore the structure sensitivity of the catalytic combustion process. High CO (40 Torr) and O_2 (100 Torr) pressures were used at temperatures in the 300 – 700 K range. These reaction conditions are similar to those utilized for CO combustion in the automobile catalytic converter or other catalytic combustion reactors. The reaction has two regimes, separated by the ignition point that depends both on the CO partial pressure[3,5,7] and the platinum surface structure. Sum frequency generation was employed to monitor the reaction intermediates on the platinum surface during the reaction. Gas chromatography was used to monitor the gas composition as a function of time and temperature, thereby determining the reaction rates.

When CO oxidation experiments are performed, we find by SFG that the surface is covered with molecular CO occupying top platinum sites below ignition reaction conditions. At a particular temperature, the onset of ignition occurs, and the temperature can rise by several hundred degrees. This temperature coincides closely with the CO dissociation temperature, and so the ignition temperature is also structure sensitive. The ignition temperature also rises with CO pressure, an added complexity in the reaction mechanism. SFG spectra above the ignition temperature indicate that CO is absent from the surface. This can be interpreted assuming that the reaction is mass transport limited because of the rapid surface reaction rates and the platinum surfaces are oxygen covered, which reacts with impinging CO on impact.[3]

Experimental

The platinum single crystals were mounted and prepared as described in Chapter 3. After the crystal was cleaned as determined by Auger electron spectroscopy, the crystals were exposed to 4L of CO. Vacuum SFG spectra were acquired to assure that the surface was prepared properly. The chamber was then isolated from the vacuum pumps and high-pressures of CO and O_2 were introduced into the chamber. Experiments either consisted of heating stepwise the crystal in the high-pressure gasses acquiring spectra at each temperature and measuring the oxidation rate, or the SFG intensity at a single frequency was monitored as a function of temperature to determine the ignition temperature.

Results

Under high-pressure reaction conditions, there are two activity regimes associated with CO oxidation, and an ignition temperature at which point the reaction becomes highly exothermic and self-sustaining separates these two regimes.[3,4] Below the ignition temperature, the reaction rate is slow and above the ignition temperature, the reaction rate is high. From previous studies, it has been found that the ignition temperature depends on the relative concentrations of CO and O_2.[3] In this work, we report the results of CO oxidation under a condition of 40 Torr CO and 100 Torr of O_2 for all three surfaces. The SFG spectra above and below the ignition temperature are considerably different as are the rates.

For all three surfaces, the SFG spectra are essentially the same when compared to each other for both above and below the ignition temperature. Below the ignition temperature, the top site CO peak slowly shifts as a function of temperature until the ignition temperature is reached. At the ignition temperature, the crystal temperature increases rapidly, and the top site CO peak decreases rapidly. Once above the ignition temperature, no spectral feature is observed under these pressure conditions. The specifics for CO oxidation on Pt(557) will now be discussed.

To begin the CO oxidation reaction on Pt(557), the crystal was cleaned as described above and 4L of CO was exposed of the surface. Once SFG spectra were obtained under UHV conditions, the sample was introduced to 40 Torr of CO, 100 Torr of O_2, and 630 Torr of He. SFG spectra were then acquired at 300K and then as a function of temperature up to 623 K (Figure 7.1). At 300 K, the top site CO peak was

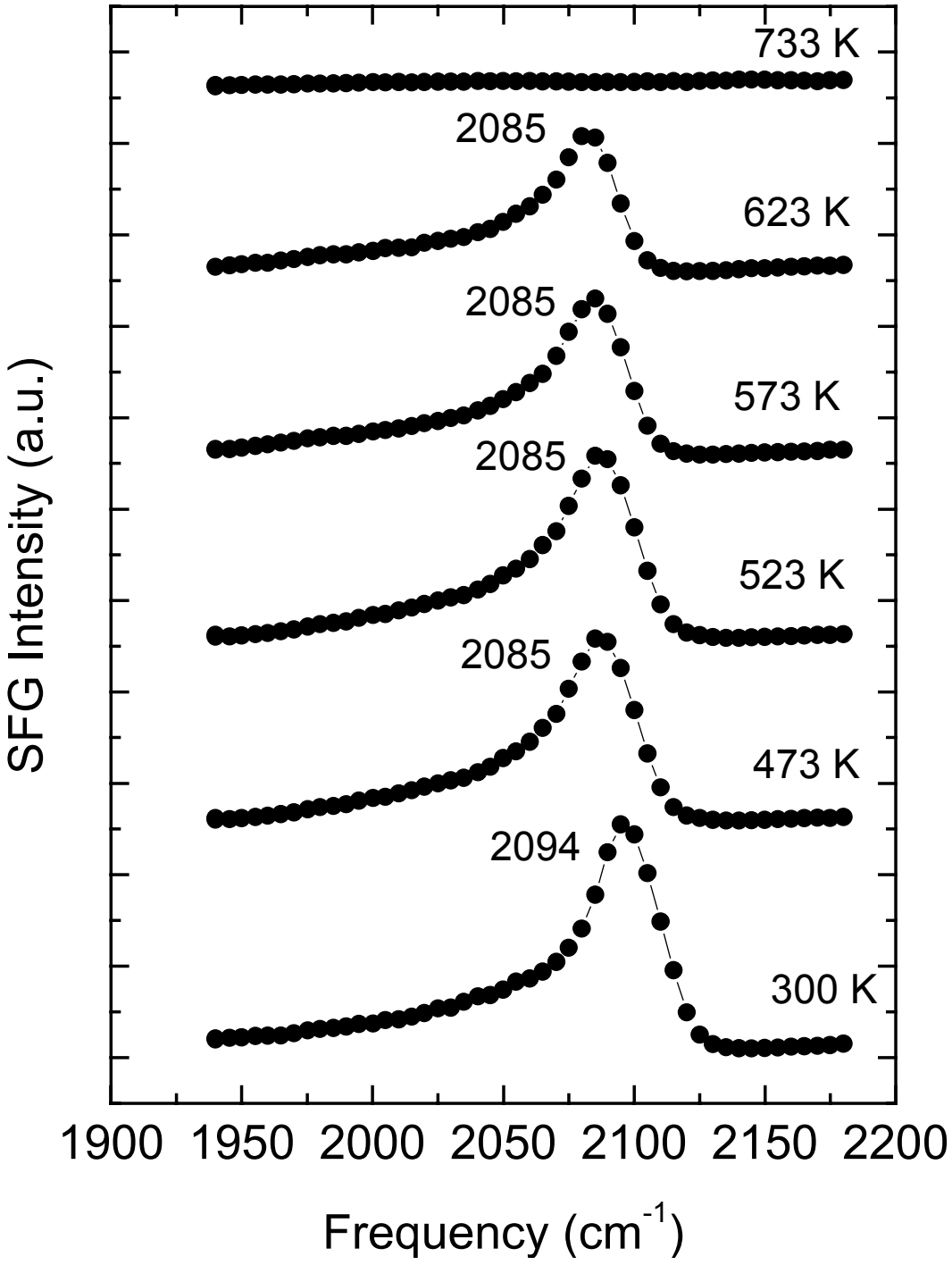

Figure 7.1 SFG spectra of Pt(557) under 40 Torr of CO and 100 Torr of O2 and 630 Torr of He at temperatures below and above ignition.

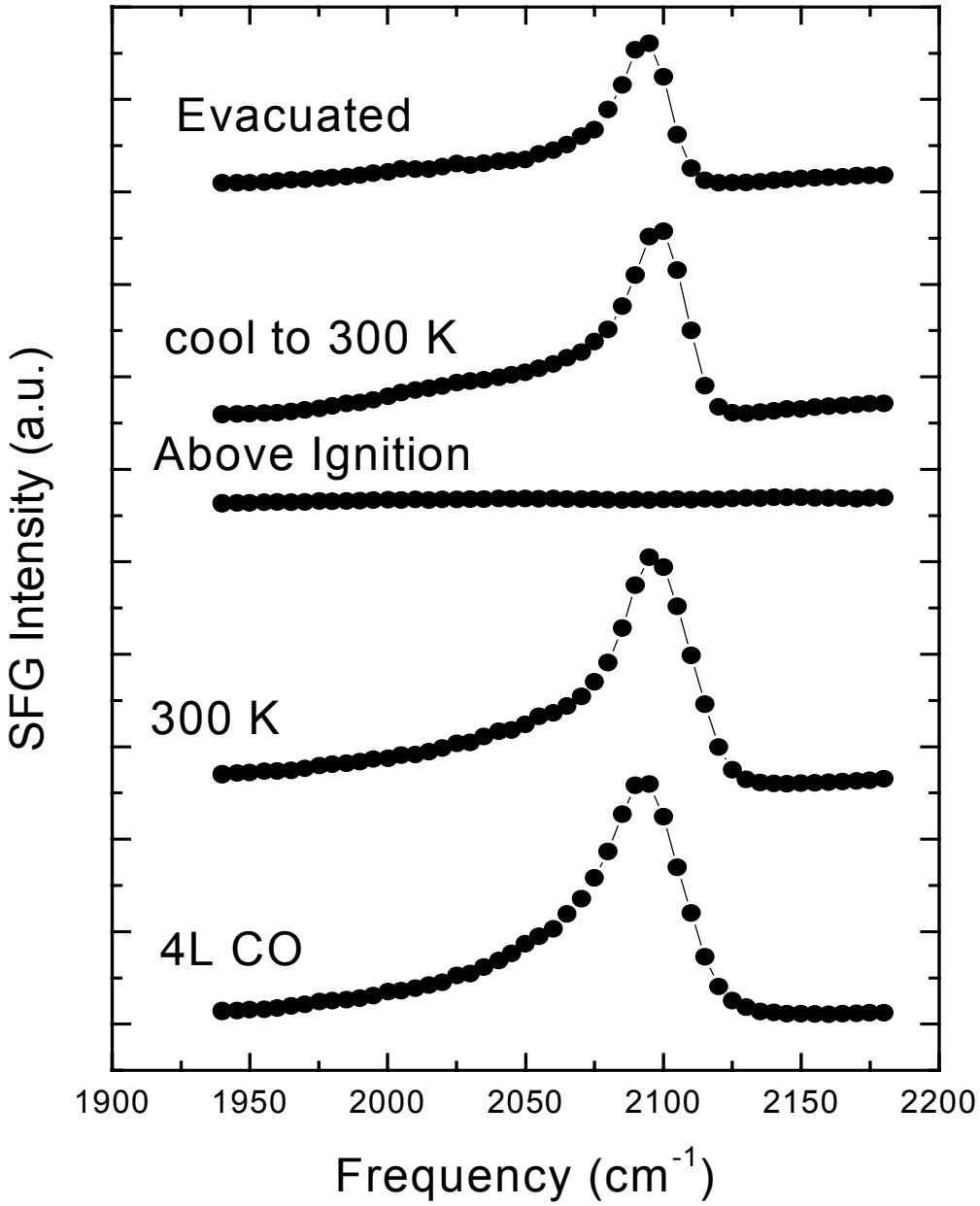

Figure 7.2 SFG Spectra of CO on Pt(557) before and after ignition in the presence of 40 Torr of CO, 100 Torr of O_2 and 630 Torr of He.

at 2094 cm^{-1}. As the temperature was raised to 623 K the CO peak shifted to 2085 cm^{-1}. Around 640 K, the ignition temperature was reached, and the reaction became self-sustained and crystal temperature rose to 733 K. The ignition temperature was observed to be slightly dependent on the heating rate as the temperature approached the ignition point. An error of ±20 K was determined for the measured value of the ignition temperature. At the ignition point, the CO top site peak was no longer detectable, and the spectrum remained essentially free of any spectral features.

The sample was then cooled back down to room temperature to quench the reaction. The SFG spectra at 300 K before and after ignition are compared with the spectrum above the ignition temperature in Figure 7.2. The spectrum at 300 K after the reaction is essentially the same, indicating no irreversible process has occurred as a consequence of the CO oxidation reaction as compared to the CO decomposition experiment. Figure 7.3 monitors the SFG signal of the CO top site frequency at 2085 cm^{-1} and temperature as a function of time. At 623 K, the SFG intensity is large compared to the baseline. The temperature is slowly ramped to the ignition point at which time the temperature increases rapidly, and the SFG intensity rapidly decreases to baseline. After 30 minutes, the sample was slowly cooled to quench the reaction and the SFG intensity did not recover until the temperature dropped below the ignition temperature.

As stated previously, the SFG spectra were very similar for all three crystals. However, the ignition temperature was considerably different for the Pt(100) surface as compared to the Pt(111) and Pt(557) surfaces. Table 1 compares the CO decomposition temperature and the CO oxidation ignition temperatures for the three

surfaces. As evident from the table, the Pt(100) surface decomposes CO near the same temperature that CO oxidation ignites under these reaction conditions. The ignition temperature for Pt(111) is considerably higher than on Pt(100), but not quite as high as the CO dissociation temperature for Pt(111). A similar trend for the structure sensitivity of both CO dissociation and ignition is observed in that both ignition and CO dissociation occur at a higher temperature for the (111) surface as compared to Pt(100). It is important to note that the CO ignition temperature for Pt(111) and Pt(557) are very similar to each other within experimental error indicating that CO oxidation occurs mainly on the (111) terraces. This agrees with other studies, which indicated that the (111) terrace sites are more important for CO oxidation than step sites.[2,11,12]

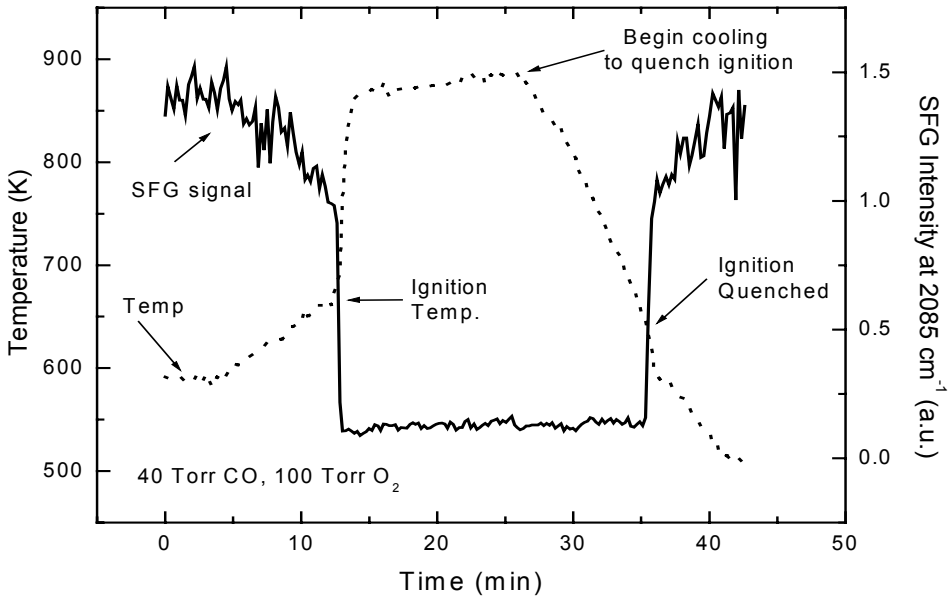

Figure 7.3 SFG top site CO frequency and sample temperature as a function of time during CO oxidation. 40 Torr of CO and 100 Torr of O2.

Discussion

During the CO oxidation experiments under 40 Torr of CO and 100 Torr of O_2, the reaction exhibits two different regimes, which are separated by an ignition temperature. Below the ignition temperature, the rate of CO_2 formation is slow (< 20 molec/site/sec), and CO covers the surface. As the surface is heated, the ignition temperature is reached and the reaction becomes highly exothermic causing an uncontrolled increase in the crystal temperature. The CO_2 formation rate then becomes high (> 1000 molec/site/sec) and the surface becomes oxygen covered. The transition between these two reactivity regimes is very fast.

Table 7-1 Comparison of CO dissociation temperature and CO oxidation ignition temperature for Pt(111), Pt(557) and Pt(100).

	Pt(100)	**Pt(557)**	**Pt(111)**
CO Dissociation Temp. (40 Torr CO)	500 ±10 K	550 ±10 K	673 ± 10 K
Oxidation Ignition Temp. **(40 Torr CO, 100 Torr O_2)**	500 ± 20 K	640 ± 20 K	620 ± 20 K

Below the ignition temperature, the reaction probably proceeds through a Langmuir-Hinshelwood mechanism[7,3,4]

$$CO_{(a)} + O_{(a)} \rightarrow CO_{2(g)}$$

This reaction is inhibited since it depends on atomically adsorbed oxygen. Molecular oxygen requires two sites to dissociate on Pt and if the surface is CO covered, the O_2 dissociation is inhibited.[4]

Above the ignition point, the surface is covered by atomic oxygen, and the rate becomes mass transport limited most likely by the approach of CO to the surface or the departure of CO_2. These results are well known throughout the literature. What remains to be unclear is the mechanism that causes this sudden transition from a CO covered surface to an atomic oxygen covered surface. One explanation describes the ignition as the point at which oxygen adsorption is no longer inhibited once the CO coverage decreases below a critical inhibition coverage. The CO coverage can decrease either by desorption or reaction. Bowker and coworkers using molecular beams, however, showed that even before ignition, a surface under CO oxidation conditions is already covered with oxygen to about one-fourth of the saturation value of oxygen.[4] They also found that ignition would only occur when the CO coverage decreases to below 0.4 ML.

Alone, the critical CO coverage explanation for ignition does not explain our observations. As a Pt(557) single crystal surface is heated in the presence of 40 Torr of CO and 100 Torr of O_2, the CO top site frequency shifts by only 10 cm^{-1} when the sample is heated to 473 K. Between 473 K and 628 K, the peak remains at 2085 cm^{-1}, and the fitted amplitudes of the spectra up to the ignition temperature are essentially the same. If the CO coverage was decreasing as a function of temperature, we would expect to observe a dipole coupling affect in which the top site CO peak frequency

would red shift beyond 2085 cm^{-1}. Also, the fitted amplitudes of the peaks would decrease if the coverage decreased. However, the amplitudes observed do not decrease between 473 K and the ignition temperature.

Under the conditions discussed here, the top site CO peak remains essentially unchanged between 473 K and the ignition point indicating the CO coverage does not change until after ignition. From the CO dissociation studies presented above, a possible explanation for the ignition could be the onset of CO dissociation or the formation of platinum binary carbonyls. When the CO dissociation temperatures are compared to the CO oxidation ignition temperatures for the three crystal surfaces, we find that both the ignition and dissociation temperatures are structure sensitive. The ignition and dissociation temperatures for Pt(100) are essentially the same. The ignition temperature for Pt(111) and Pt(557) are considerably higher than the ignition temperature on Pt(100) indicating a similar trend for the structure sensitivity of ignition as compared to CO dissociation. The similar ignition temperatures on Pt(111) and Pt(557) can be explained if the (111) terrace sites, which are common to both crystal faces, are more important than step sites for CO oxidation.[2,11,12]

Because structure sensitivity is observed for both CO oxidation ignition and CO dissociation, it is likely that CO dissociation is an important mechanism during ignition. In order for the ignition of CO oxidation to occur, CO first dissociates to deposit carbidic carbon on the surface, or platinum binary carbonyls are formed. Either the carbidic carbon or the platinum binary carbonyls may then be oxidized by atomic oxygen to initiate the ignition.

Conclusions

Using sum frequency generation surface vibrational spectroscopy, the structure sensitivity of CO oxidation ignition was investigated. The surface of platinum single crystals can either be roughened or annealed depending on the crystal temperature. From data presented in Chapter 6, It CO dissociates at 673 K, 550 K, and 500 K for Pt(111), Pt(557) and Pt(100), respectively at 40 Torr of CO pressure. From UHV studies, it is known that CO will only dissociate on step or kink sites on platinum. On Pt(111) and Pt(100), the surface must be heated to a temperature at which platinum binary carbonyls are formed which then may facilitate the roughening of the surface to produce step and kink sites. Pt(557) is essentially a (111) surface with defects already introduced as steps. Because of this, the Pt(557) surface does not need to be heated to 673 K, the dissociation temperature on Pt(111), to produce defects. CO is able to dissociate on the steps of Pt(557) at a lower temperature than needed to roughen the surface. Pt(100) has the lowest CO dissociation temperature probably because the outermost surface platinum atoms are more mobile since the Pt(100) surface can easily reconstruct, therefore the surface can roughen at a lower temperature.

The CO oxidation ignition temperatures were also structure sensitive. The Pt(111), Pt(557), and Pt(100) have ignition temperatures of 620 K, 640 K, and 500 K respectively. These ignition temperatures follow the same trend in structure sensitivity as the CO dissociation temperatures on the three crystal faces. The one exception is the CO oxidation ignition temperature on Pt(557). This ignition temperature is similar to

ignition found on Pt(111). Because the rate of CO_2 formation is mass transport limited above the ignition temperature, the terrace sites are more important for CO_2 formation than the step edges. Pt(557) has a similar ignition temperature as compared to Pt(111) because they share the same (111) hexagonal terrace structure. Because of the structure sensitivity of both CO dissociation and the CO oxidation ignition, it is possible that CO dissociation or platinum binary carbonyl formation may be needed to initiate the ignition mechanism. The carbon or carbonyls are oxidized in addition to the oxidation of molecular CO. The two exothermic reactions produce the temperature rise that facilitates CO desorption to allow the metal surface to become oxygen covered.

References

[1] Hong, S.; Richardson, H. H. *J. Phys. Chem.* 1993, **97**, 1258.

[2] Ohno, Y.; Sanchez, J.R.; Lesar, A.; Yamanaka, T.; Matsushima, T. *Surf. Sci.* 1997, **382**, 221.

[3] Rinnemo, M.; Kulginov, D.; Johansson, S.; Wong, K.L.; Zhdanov, V.P.; Kasemo, B. *Surf. Sci.* 1997, **376**, 297.

[4] Bowker, M.; Jones, I.Z.; Bennett, R.A.; Esch, F.; Baraldi, A.; Lizzit, S.; Comelli, G. *Catal. Lett.* 1998, **51**, 187.

[5] Su, X.; Cremer, P.S.; Shen, Y.R.; Somorjai, G.A. *J. Am. Chem. Soc.* 1997, **119**, 3994.

[6] Wartnaby, C.E.; Stuck, A.; Yeo, Y.Y.; King, D.A. *J. Chem. Phys.* 1995, **102**, 1855.

[7] Berlowitz, P.J.; Peden, H.F.; Goodman, D.W. *J. Chem. Phys.* 1988, **92**, 5213.

[8] Imbihl, R.; Cox, M.P.; Ertl, G. *J. Chem. Phys.* 1986, **84**, 3519.

[9] Hafner, J.; Eichler, A. *Surf. Sci.* 1999, **433**, 58.

[10] Imbihl, R.; Cox, M.P.; Ertl, G. *J. Chem. Phys.* 1985, **83**, 1578.

[11] Szabo, A.; Henderson, M.A.; Yates, J.T. Jr. *J. Chem. Phys.* 1992, **96**, 6191.

[12] Akiyama, H.; Moise, C.; Yamanaka, T.; Jacobi, K.; Matsushima, T. *Chem. Phys. Lett.* 1997, **272**, 219.

Chapter 8: CO Oxidation on Pt(557)

Introduction

The oxidation of carbon monoxide on catalyst surfaces is one of the simplest and most studied heterogeneous catalytic reactions. Under certain pressures of CO and O_2, the reaction proceeds under two different kinetic regimes separated by an ignition temperature. Below the ignition point, the CO oxidation reaction mechanism follows Langmuir-Hinshelwood kinetics and the surface is primarily CO covered.[1,2,3,4,5,6,7,8]

$$CO(a) + O(a) \rightarrow CO_2(g)$$

From many studies, it has been determined that the reaction is positive 1st order in O_2 and negative 1st order in CO when the reaction proceeds through a Langmuir-Hinshelwood reaction below ignition.

At the ignition point, the reaction becomes highly exothermic and the rate of CO oxidation increases considerably as compared to the rate observed at temperatures below the ignition temperature. Above the ignition point, the surface becomes primarily oxygen covered and the reaction is believed to be mass transport limited of either CO approaching the surface or CO_2 leaving.

$$CO(g) + O(a) \rightarrow CO_2(g)$$

Even though this reaction has been studied extensively, our understanding of CO oxidation is still incomplete, especially at and above ignition. What remains to be

unclear is the mechanism that causes this sudden transition from a CO covered surface to an atomic oxygen covered surface. One explanation describes the ignition as the point at which oxygen adsorption is no longer inhibited once the CO coverage decreases below a critical inhibition coverage. In this view, the CO coverage can decrease either by desorption or reaction. Bowker and coworkers using molecular beams, however, showed that even before ignition, a surface under CO oxidation conditions is already covered with oxygen to about one-fourth of the saturation value of oxygen.[4] They also found that ignition would only occur when the CO coverage decreases to below 0.4 ML.

In addition to this explanation for the onset of ignition, it is also believed that CO dissociation may contribute to the decrease in CO coverage at the ignition point. Previously in the Somorjai group, it was found that both CO dissociation and the ignition temperature of CO oxidation are surface structure sensitive on platinum single crystal surfaces.[9] The three surfaces studied were the (111), (557) and (100) faces of platinum. CO was observed to dissociate at 673 K, 548 K, and 500 K, respectively, when the surfaces were exposed to 40 Torr of CO. These results clearly showed that CO dissociation is surface structure sensitive. The ignition temperature for CO oxidation (40 Torr CO, 100 Torr O_2) was also observed to be surface structure sensitive and showed the same trend of decreasing temperature for Pt(111) and Pt(100) as observed for CO dissociation. Because of the similar trend, it was concluded that CO dissociation is important for the onset of ignition. Once carbon is deposited, it is immediately oxidized and through the release of excess energy as thermal energy, the single crystal heats up causing desorption or reaction of adsorbed

CO allowing the surface to become predominantly covered with atomic oxygen. The reaction then moves into the mass transport regime.

In this work, we report on further CO oxidation experiments which have been performed using sum frequency generation to elucidate reaction mechanisms at and above ignition on Pt(557). Experiments were performed under three different pressure regimes: excess O_2 (40 Torr CO, 100 Torr O_2), excess CO (100 Torr CO, 40 Torr O_2), and equal pressures of CO and O_2 (70 Torr CO, 70 Torr O_2). Under each pressure regime, the reaction was performed both on clean prepared platinum and carbon-covered platinum. The carbon-covered platinum was prepared by first introducing CO at the pressure of interest and heating to 573 K to dissociate CO and deposit carbon on the surface before the introduction of O_2. Once O_2 was introduced at 573 K after the deposition of carbon, the SFG background increased considerably and any remaining peak attributed to CO immediately disappeared. From Auger electron spectroscopy, it was determined that the large SFG background results only from the presence of both carbon and oxygen on the surface. Carbon or atomic oxygen alone will not generate the SFG background observed. As the relative concentration of atomic oxygen increases, the intensity of the SFG background increases. This is a good indicator on whether carbon is being deposited on the surface during reaction or being gasified away as CO_2. From similarities in the properties of this surface carbon oxide to activated carbon studies, it was determined that this surface carbon oxide species responsible for the large SFG background is due to a carboxyl anhydride species.

Several interesting results were found from this study. The first being that the carboxyl anhydride species is a better oxidizer than platinum alone as the reaction rates on carbon covered platinum surfaces below ignition were observed to be larger than the rates on clean prepared platinum surface. In addition, when the reaction was studied under equal pressures of CO and O_2, the ignition temperature was lowered 50 degrees when carbon was first deposited on the surface.

Another interesting result was that the rate or CO_2 production above ignition for the excess O_2 and equal pressure of O_2 and CO conditions didn't follow the half order dependence in CO and O_2 above ignition as determined in a previous study.[5] This indicates that there is an additional surface reaction channel above ignition not previously described.

Further evidence that CO dissociation is an important step for ignition was found when CO oxidation was performed on a clean prepared platinum surface under equal pressures of CO and O_2. As the sample was heated in this gas mixture, the SFG background began to increase below ignition indicating CO was being dissociated and the carbon deposited was oxidized. This is the first evidence that CO dissociation can occur under oxidation conditions.

Experimental

A Pt(557) single crystal was mounted in an ultrahigh vacuum (UHV) chamber that is also used as a high-pressure reaction cell. The single crystal was cleaned by two cycles of argon ion bombardment followed by annealing in 5×10^{-7} Torr of

oxygen at 1123 K for 2 minutes. The oxygen was then pumped out and the crystal was annealed at a pressure below 2×10^{-9} Torr at 1133 K for 1 minute. Once the crystal was shown to be clean by Auger spectroscopy, the sample was exposed to high-pressures of CO (Scott Specialty 99.99%) and O_2. The CO was further purified by flowing it through a liquid nitrogen trap before introducing it to the sample. When catalytic experiments were performed, the chamber acted as a batch reactor. A recirculation loop was attached to the chamber so the gas would be mixed and a GC was used to sample the composition of the gas mixture during the reaction. For SFG experiments, the chamber was equipped with CaF_2 window at the end of an inverted flange to allow the IR light to pass to the sample with minimum gas phase absorption. The pathlength from the window to the crystal is approximately 4 cm. To normalize for any gas phase absorbance of the IR beam, an IR cell was attached to the sample loop to allow for the acquisition of gas phase IR transmission spectra of gas mixtures.

It is known from Chapter 6 that carbon can be deposited on Pt(557) by heating to 548 K in high-pressure CO. In this work, CO oxidation was performed on both clean and carbon cover surfaces which were prepared by heating the crystal in the desired pressure of CO before introducing O_2.

Results

SFG Background from a Carbon and Oxygen Surface Species.

In addition to the SFG signal enhancement when the infrared beam is at the same frequency, there can also be SFG enhancement when the visible beam is near an

electronic resonance. If this is the case, the SFG background increases and is considerably higher than the normal SFG non-resonant background. In this study, under certain conditions, the SFG background was found to increase. To determine the cause of this background, control experiments were performed.

The sample was heated in pure CO or pure O_2 to high temperatures to determine whether either one of these species were responsible for the observed background. When the Pt(557) crystal was heated in high pressures of CO, it was found that CO dissociates and deposits carbidic carbon as determined by Auger spectroscopy. The addition of this carbon species did not contribute to the SFG background as seen in previous studies. When a clean prepared platinum surface is heated in a high pressure of O_2, the SFG background remains at the same level of the non-resonant background for clean platinum. Auger spectroscopy reveals a clean platinum surface, and no evidence of atomic oxygen on the surface is observed in the Auger spectrum. This result is expected since platinum does not readily become oxidized, as do other transition metals.

Because it was known that the SFG background increased in the presence of both CO and O_2, an experiment was performed in which the sample was heated first in 40 Torr of CO. Similar to experiments discussed in chapter 6 and Figures 6.5-6.8, CO was dissociated and carbon was deposited onto the surface. Once the carbon was deposited, the system was evacuated. Auger spectroscopy revealed a carbon covered platinum surface as shown in Figure 6.8. The carbon covered surface was then titrated with 5×10^{-7} Torr of O_2 as a function of temperature starting at 300 K. After heating at the various temperatures, the crystal was cooled and three SFG spectra were acquired

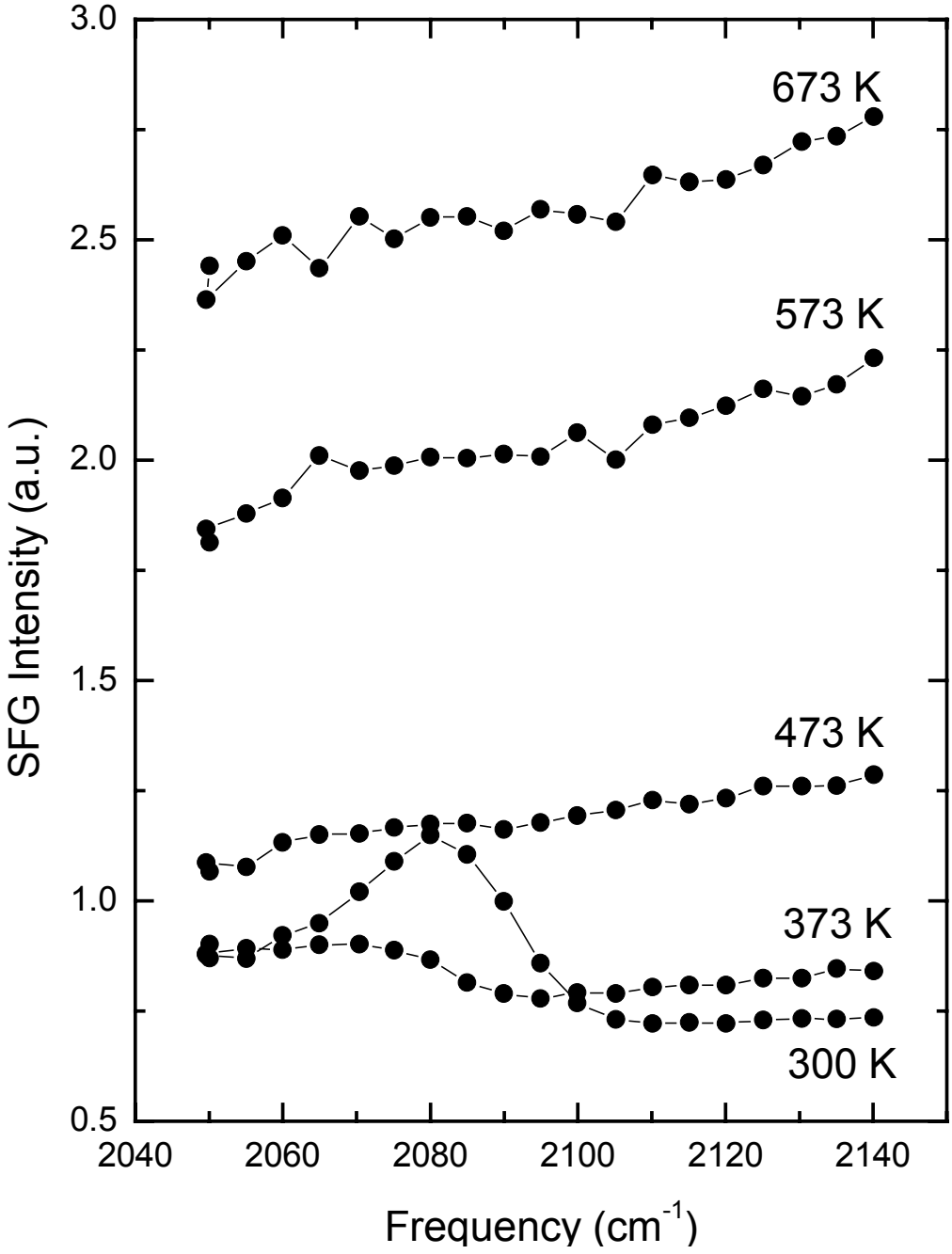

Figure 8.1 SFG spectra of SFG background as a function of O_2 titration temperature. This is an absolute intensity plot and not a stack plot as other spectra are presented.

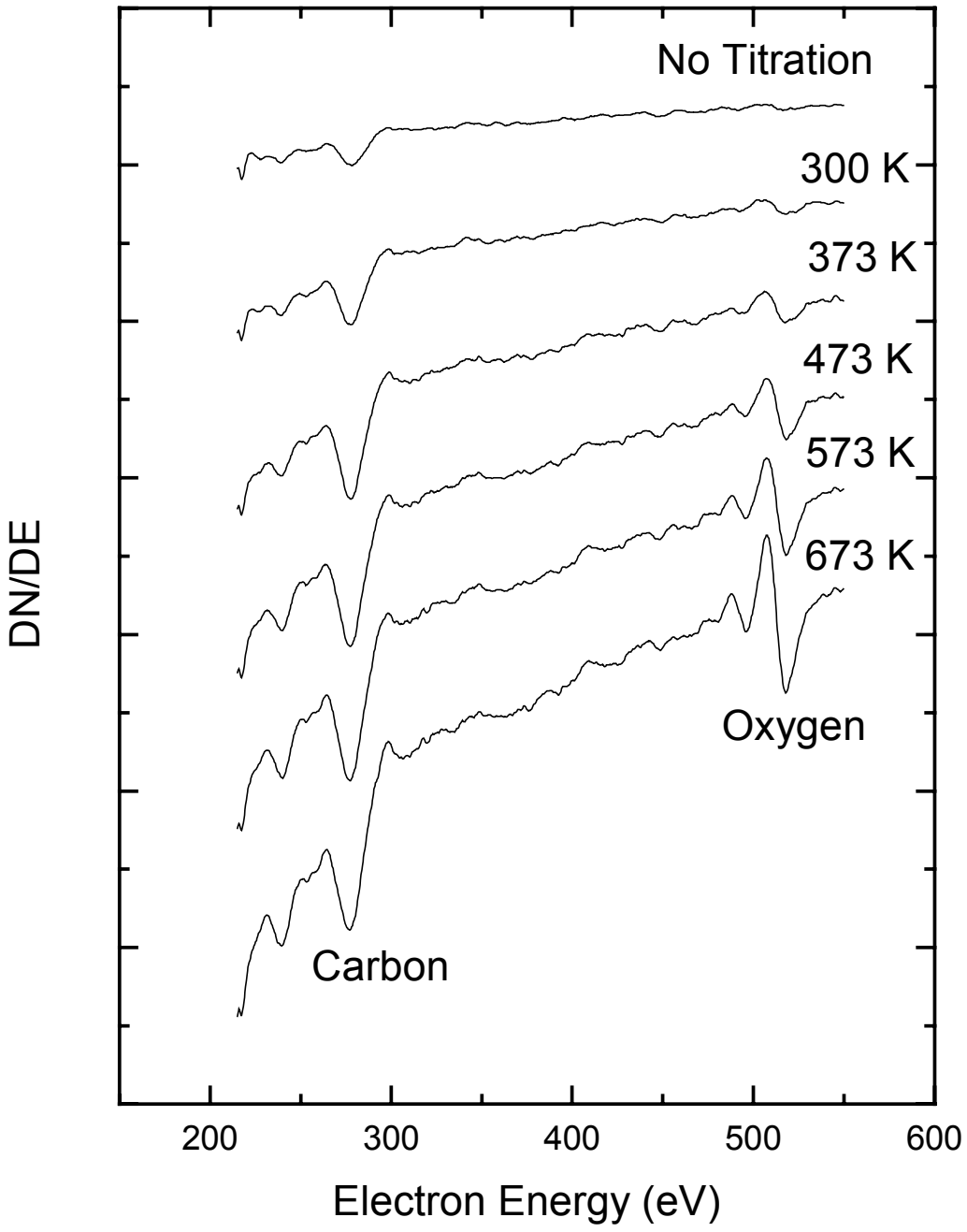

Figure 8.2 Auger spectra of Pt(557) as a function of O_2 titration temperature.

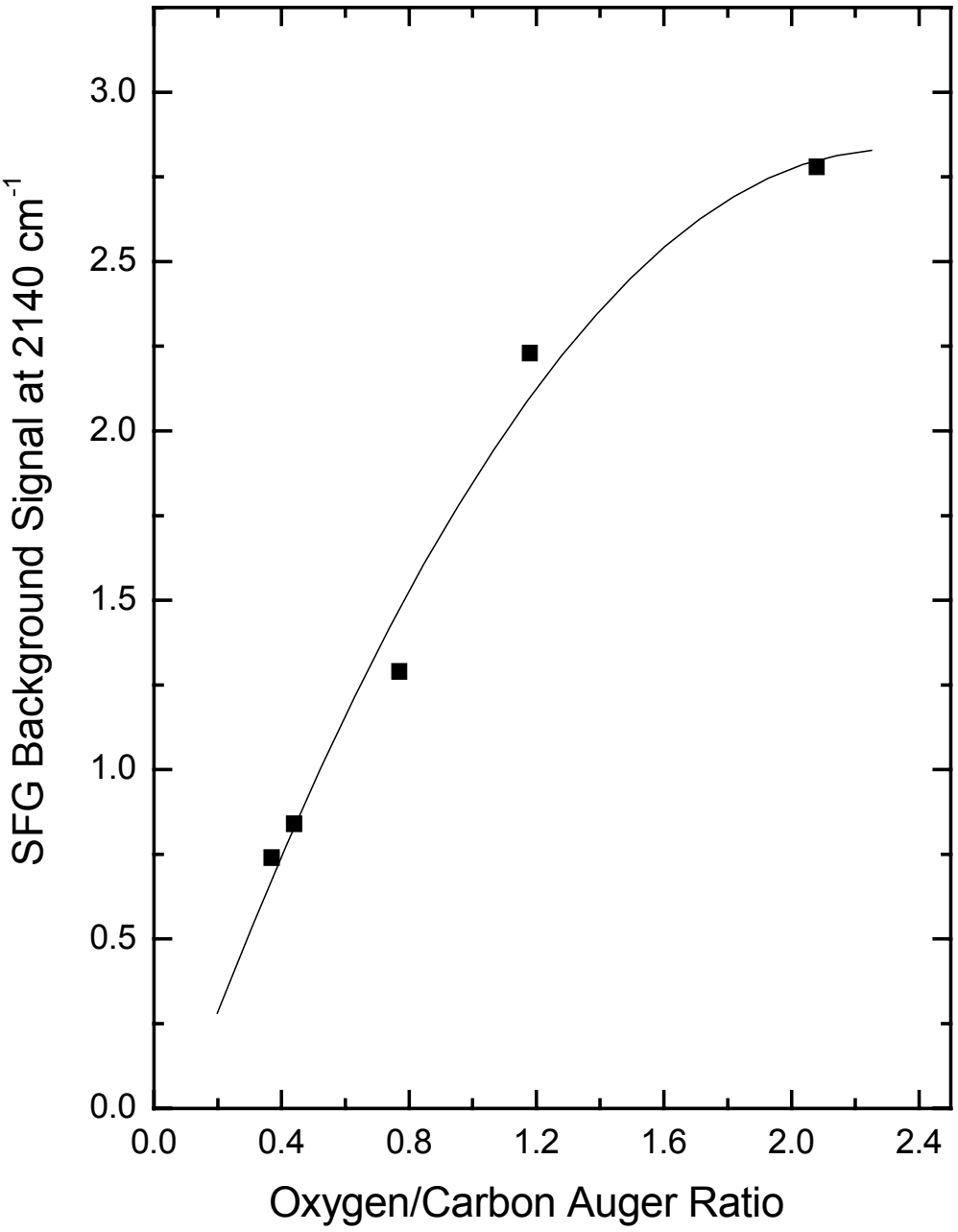

Figure 8.3 SFG background at 2140 cm^{-1} plotted against the corresponding oxygen to carbon Auger peak ratio.

and averaged. After the third SFG scan, the O_2 feed was closed and Auger spectra were acquired. Figure 8.1 shows the SFG spectra of Pt(557) under vacuum after titrating in O_2. The SFG background increases as a function of titration temperature. Auger spectroscopy then revealed both carbon and oxygen on the surface as shown in Figure 8.2. Without carbon on the surface, the size of the oxygen peak is considerably smaller than what is observed with carbon. Also, whenever the SFG background increased, it was found that carbon and oxygen were present on the surface and the SFG background is dependent on the relative concentration of carbon and oxygen on the surface. The SFG background intensity at 2140 cm^{-1} is plotted against the oxygen to carbon Auger ratio in Figure 8.3. Clearly, as the O/C ratio increases, the SFG peak increases.

Various carbon oxides are known to exist on activated carbon throughout the literature. These species have been characterized using diffuse reflectance infrared Fourier transform spectroscopy (DRIFTS) and TPD experiments.[10,11,12] Depending on how the surface is prepared, different oxide species of carbon can form. A temperature programmed desorption experiment was performed on the carbon and oxygen species found on Pt(557). CO and CO_2 were monitored by mass spectrometry as a function of temperature to determine at which temperature this unknown species decomposes. Both CO and CO_2 evolved at the 1100 K with similar pressures indicating a single type of species was decomposing around 1100 K.

CO oxidation with excess O_2

After the Pt(557) single crystal surface was cleaned as described earlier, it was introduced to 40 Torr of CO, 100 Torr of oxygen and 630 Torr of He at 300 K. SFG spectra are shown in Figure 8.4 at different temperatures during the experiment. Each

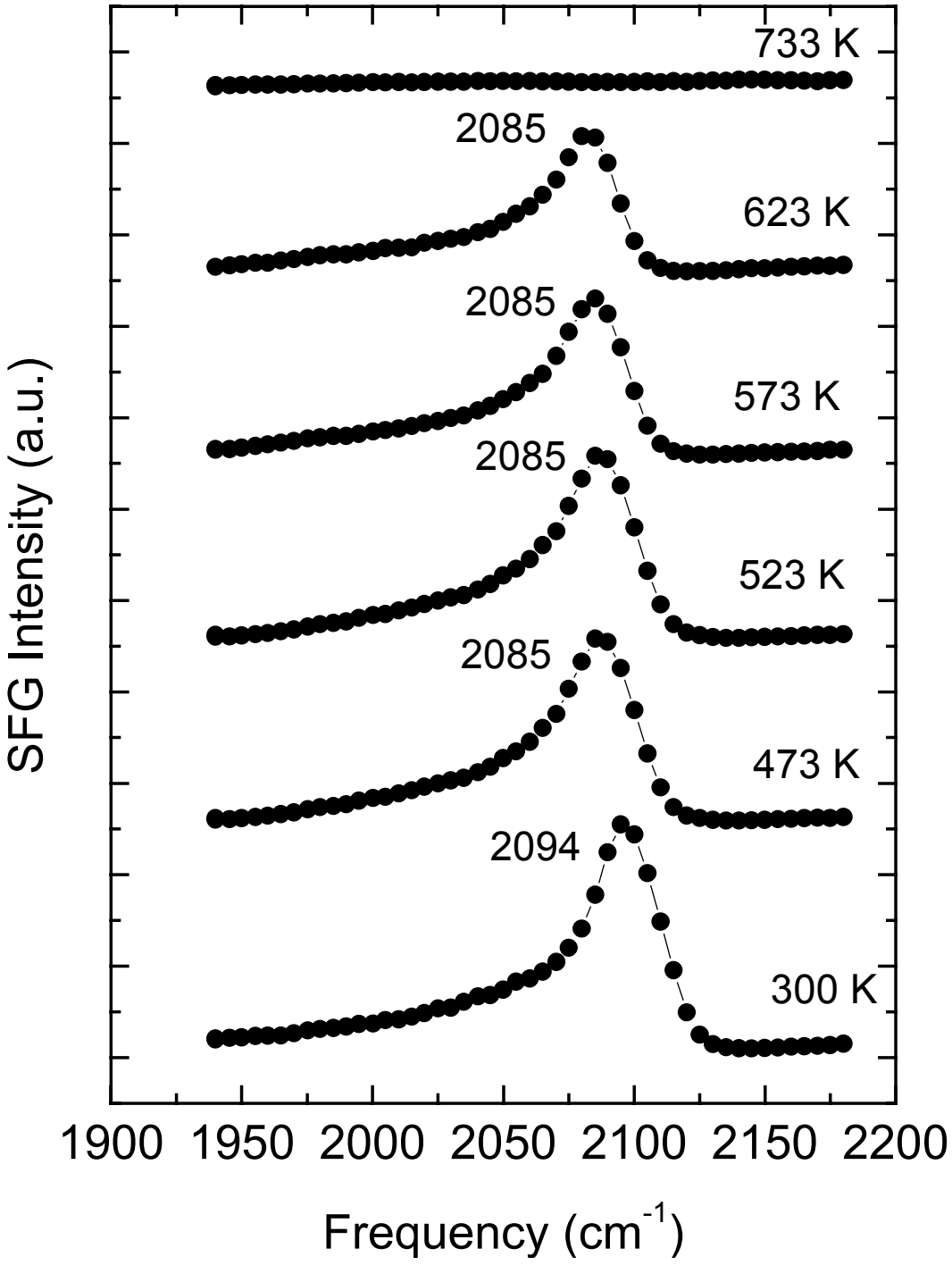

Figure 8.4 SFG spectra of Pt(557) under 40 Torr of CO and 100 Torr of O_2 as a function of temperature. The peak is absent once ignition is reached.

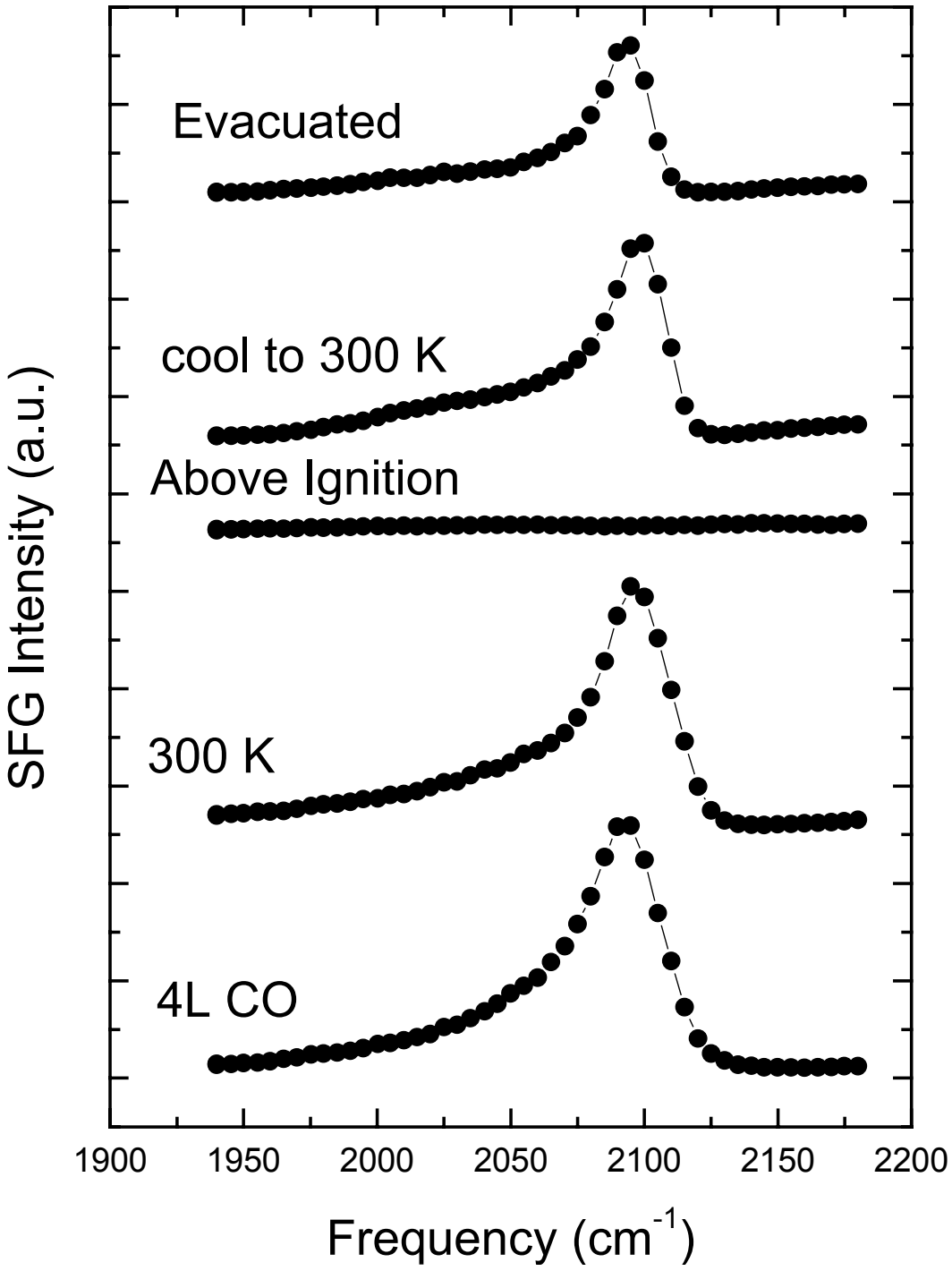

Figure 8.5 SFG spectra of Pt(557) before and after CO oxidation under 40 Torr of CO and 100 Torr of O_2. The process is completely reversible.

spectrum is the average of 3 consecutive scans. At 300 K, a single resonance is observed centered at 2094 cm^{-1}. The sample was then heated to 473 K and the resonant CO peak red-shifted to 2085 cm^{-1}. The CO peak remained at the same frequency and intensity as the temperature was increased to 623 K. The turnover rate for the production of CO_2 was calculated to be 20 molecules/site/sec. Once the sample was heated to the ignition temperature, 640 K, the reaction became highly exothermic and the temperature raised to 723 K. The turnover rate was calculated to be 1400 molecules/site/sec. At 723 K, the SFG spectrum was completely flat. If the sample was cooled below the ignition point, the reaction was quenched and the CO resonant

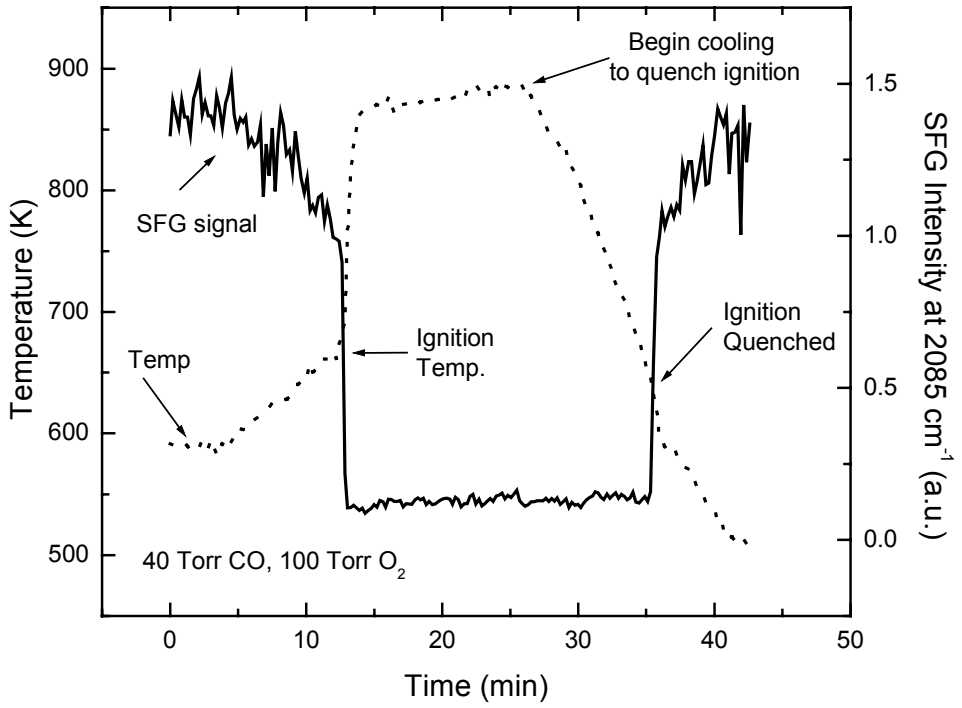

Figure 8.6 Ignition curves for both temperature and SFG signal at 2085 cm^{-1} of Pt(557) under 40 Torr of CO and 100 Torr of O_2.

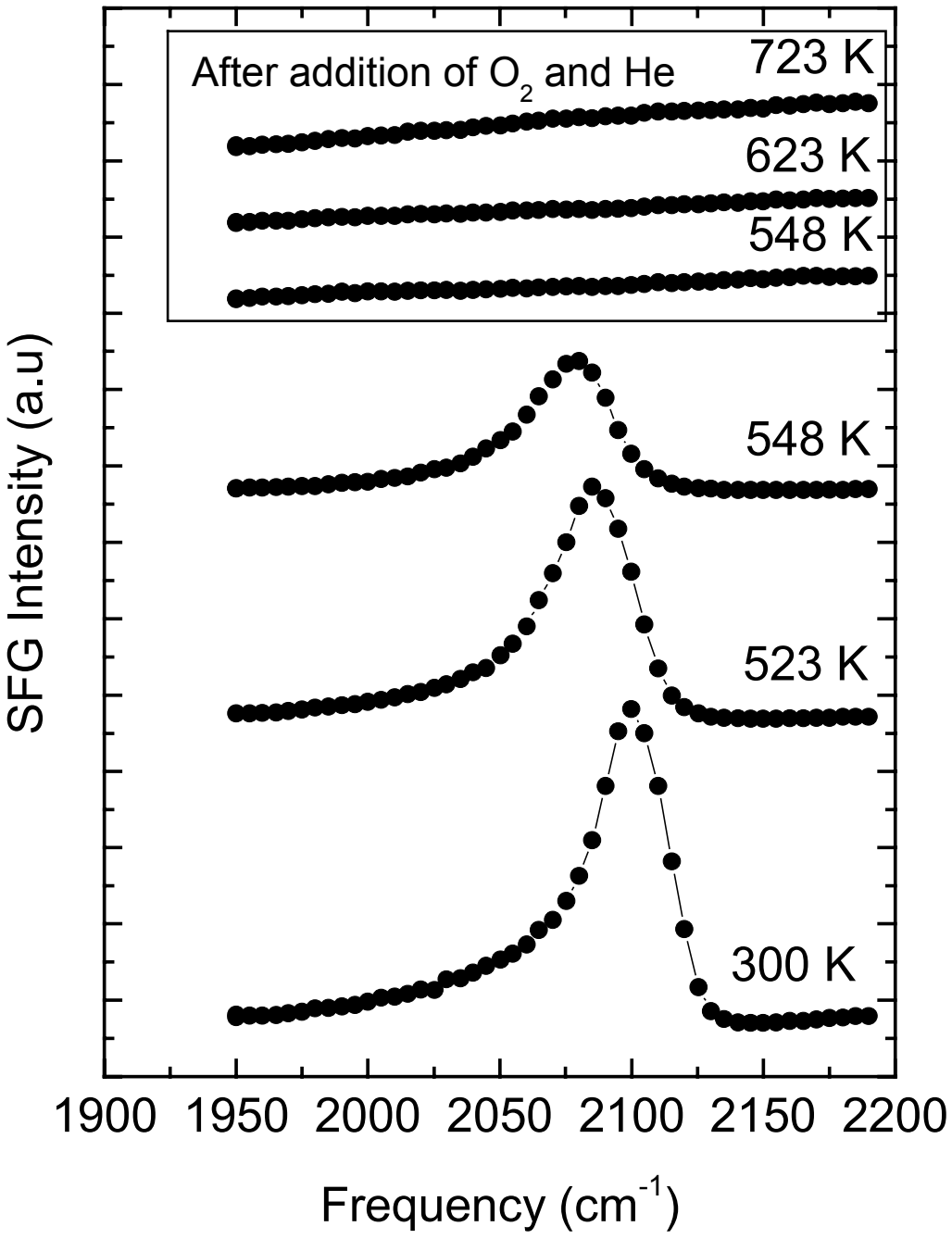

Figure 8.7 SFG spectra of Pt(557) during CO Oxidation. CO was first dissociated by heating to 548 K in 40 Torr of CO.

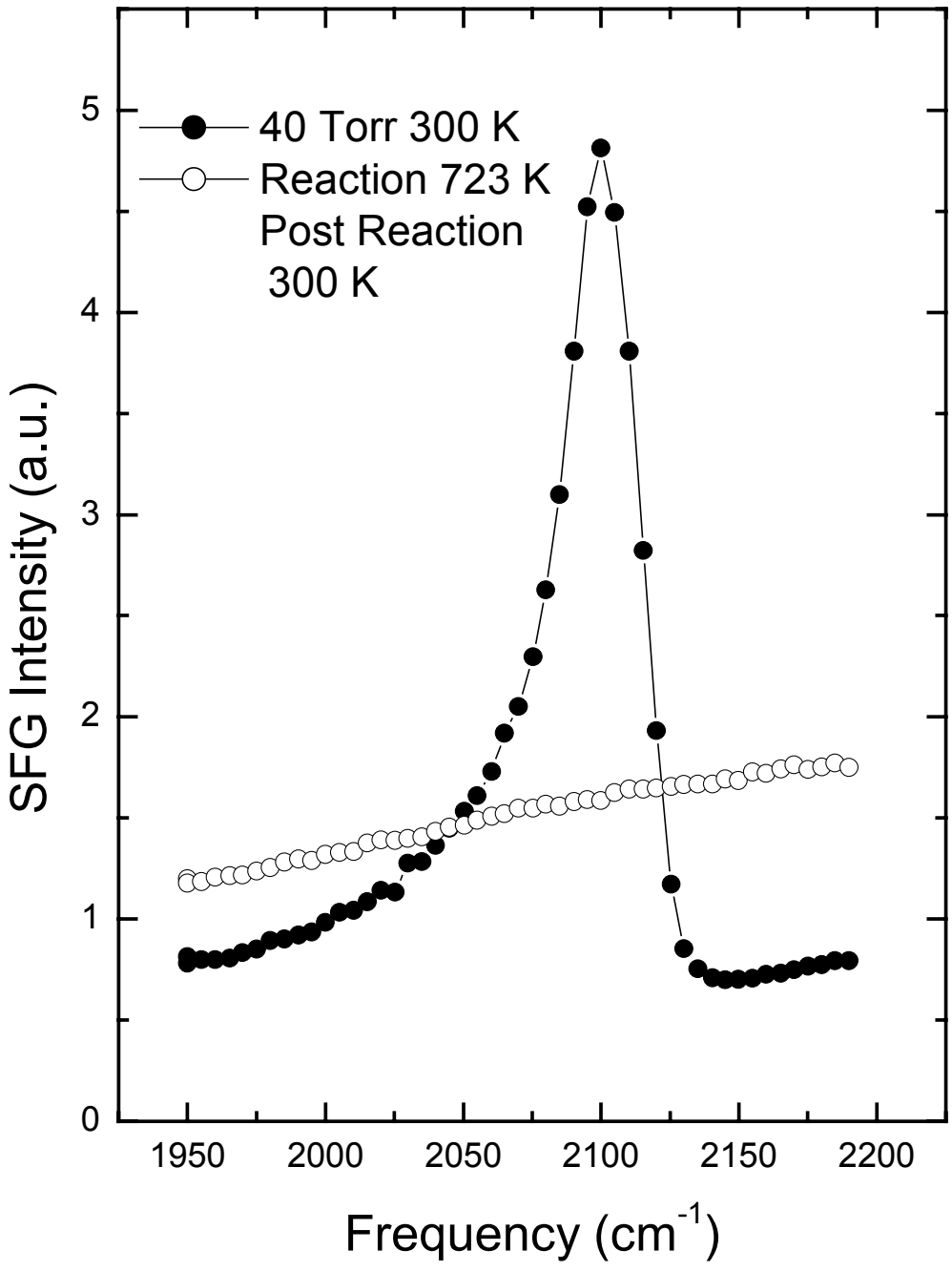

Figure 8.8 SFG spectra before and after CO oxidation on a carbon covered Pt(557) surface. The spectra are not reversible.

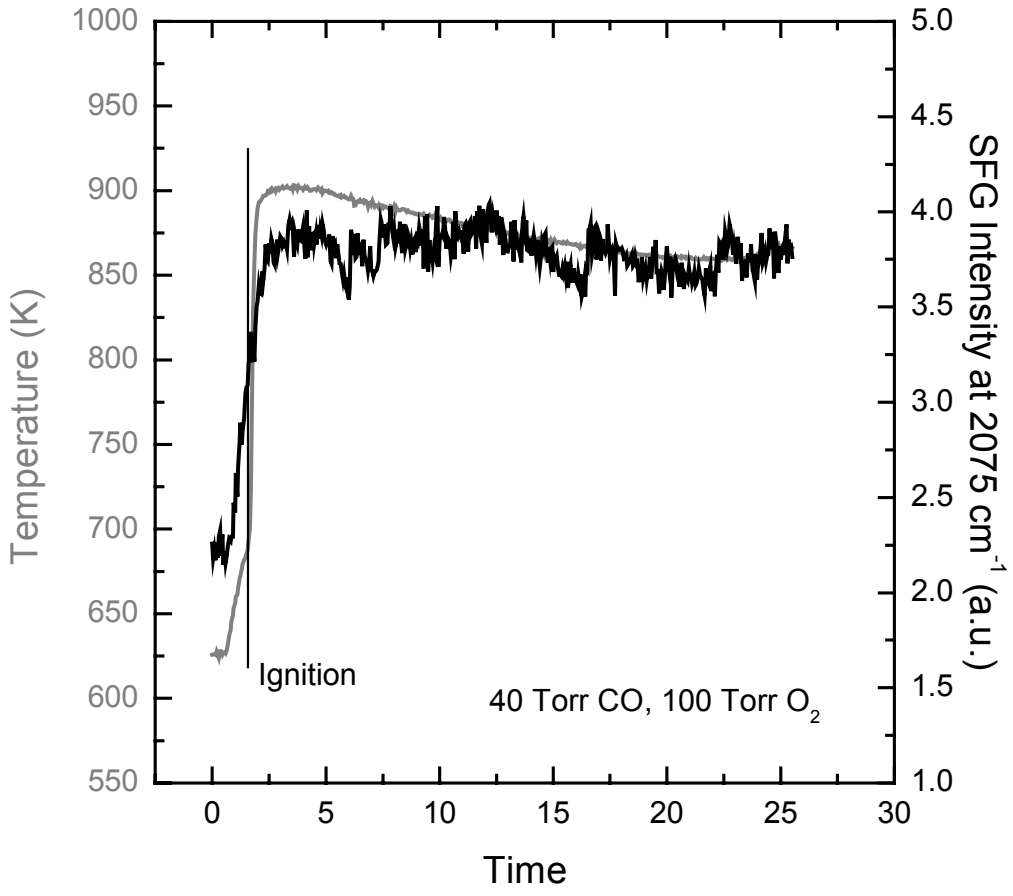

Figure 8.9 Ignition trace for both temperature and SFG signal at 2075 cm^{-1} for a carbon covered Pt(557) surface. The SFG background increases as ignition occurs.

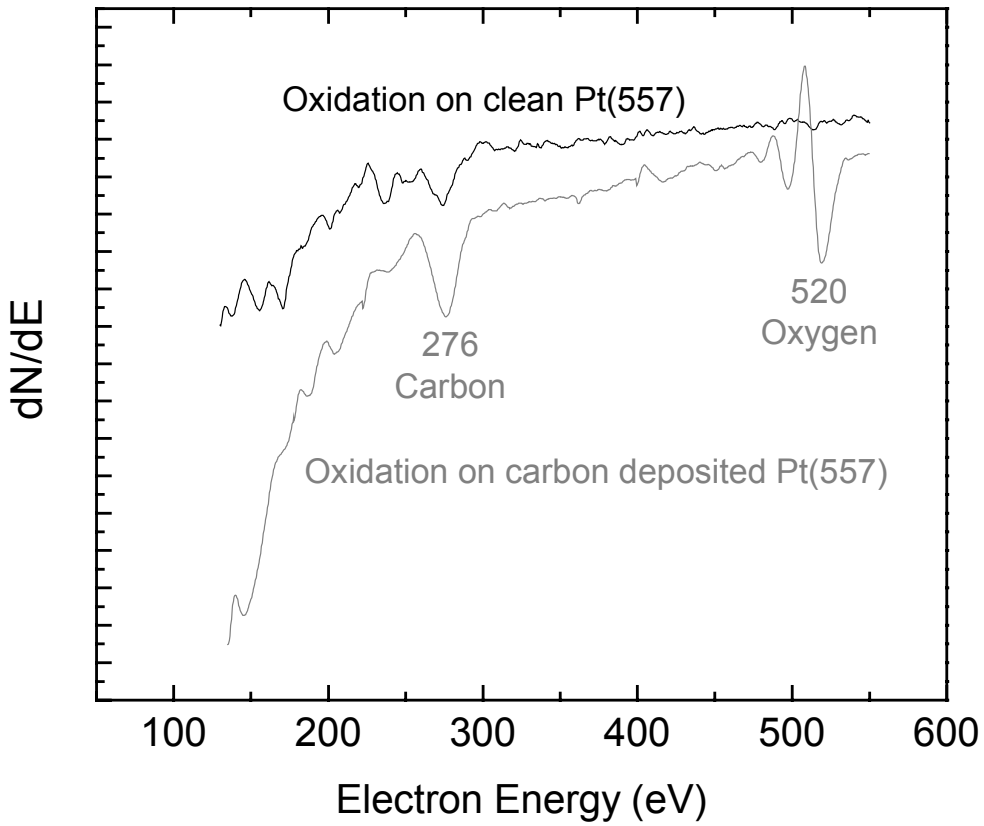

Figure 8.10 Auger spectra of clean and carbon covered Pt(557) after CO oxidation experiments.

peak recovered to the same frequency and intensity that was observed before ignition as shown in Figure 8.5. An ignition curve is shown in Figure 8.6 in which the temperature and SFG intensity of the CO top site peak is plotted against time. Once ignition is reached, the SFG CO peak intensity is observed to decrease immediately and the intensity immediately recovers as the temperature is cooled below ignition.

To determine how carbon affects the reaction under excess O_2, a carbon covered platinum surface was prepared as described earlier and the reaction was performed. Figure 8.7 shows the SFG spectra as the sample is heated from 548 K to the ignition temperature. As soon as the 100 Torr of O_2 was added at 548 K, any residual CO peak disappeared and the SFG background increased significantly. Once the ignition temperature was reached, the background increased as a function of temperature and did not decrease as the sample was cooled back down to room temperature. The turnover rates below and above ignition were 20 and 1280 molecules/site/second, respectively. Figure 8.8 shows the absolute intensity of the CO peak before reaction and the SFG background at ignition. Figure 8.9 shows the ignition curve for the sample temperature and SFG signal at 2075 cm^{-1}.

Auger spectra acquired after CO oxidation on both clean and carbon covered platinum surfaces are shown in Figure 8.10. The Auger spectrum of the clean surface after CO oxidation revealed a small carbon peak, in addition to the platinum peaks, which is attributed to electron beam dissociation of CO. It is important to note that oxygen is not observed in this Auger spectrum. The Auger spectrum of the carbon covered platinum surface reveals both a large carbon peak and a large oxygen peak. This indicates that the SFG background originates from this carbon-oxygen species.

CO Oxidation with Excess CO

After the Pt(557) crystal was determined to be clean with Auger spectroscopy, 100 Torr of CO, 40 Torr of O_2, and 630 Torr of He were introduced to the chamber. At 300 K, a single SFG peak at 2100 cm^{-1} was observed. The crystal was then heated gradually up to 1048 K incrementally. As the crystal was heated, the SFG peak slowly

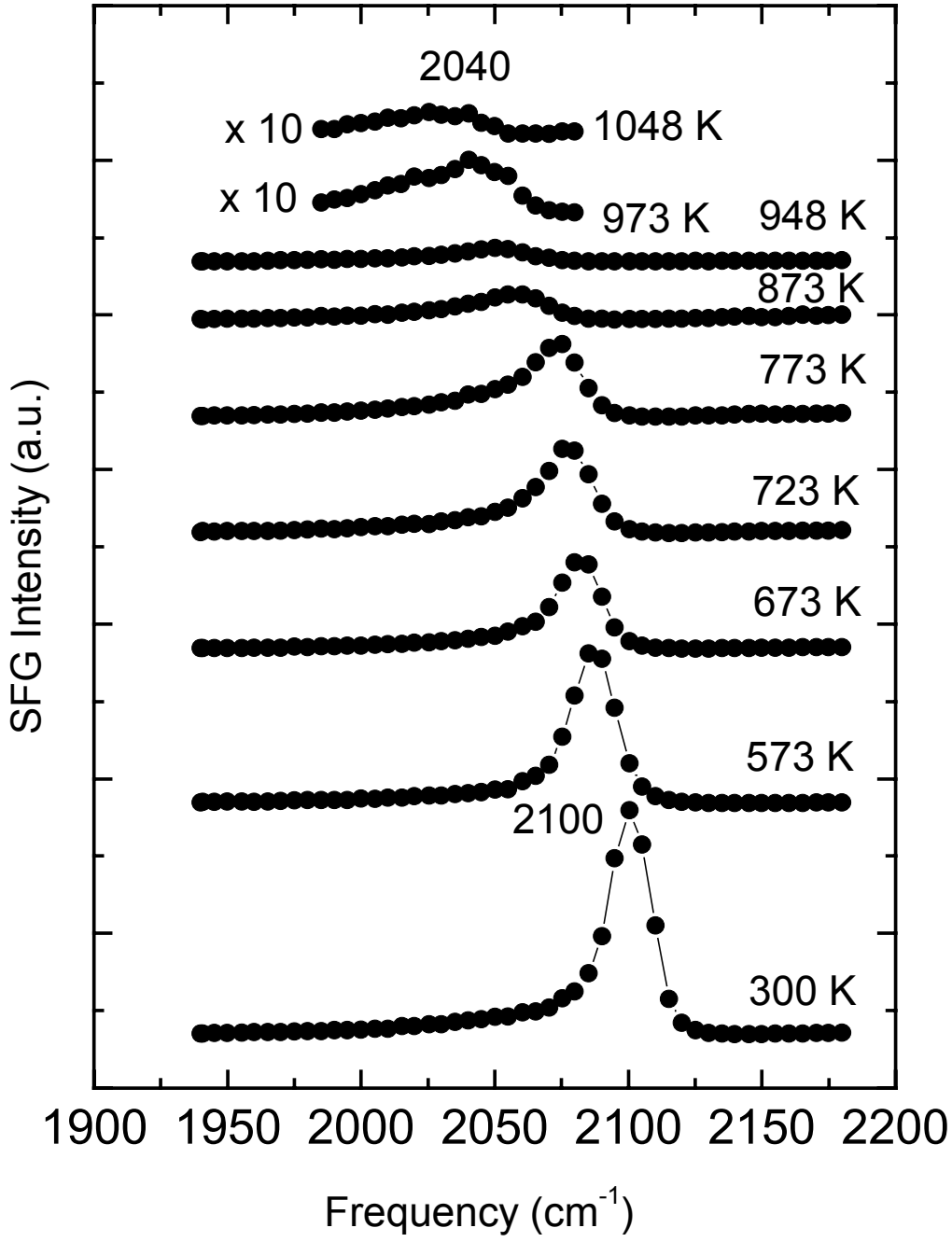

Figure 8.11 SFG spectra of Pt(557) under 100 Torr of CO and 40 Torr of O_2. No distinct ignition is observed under these conditions

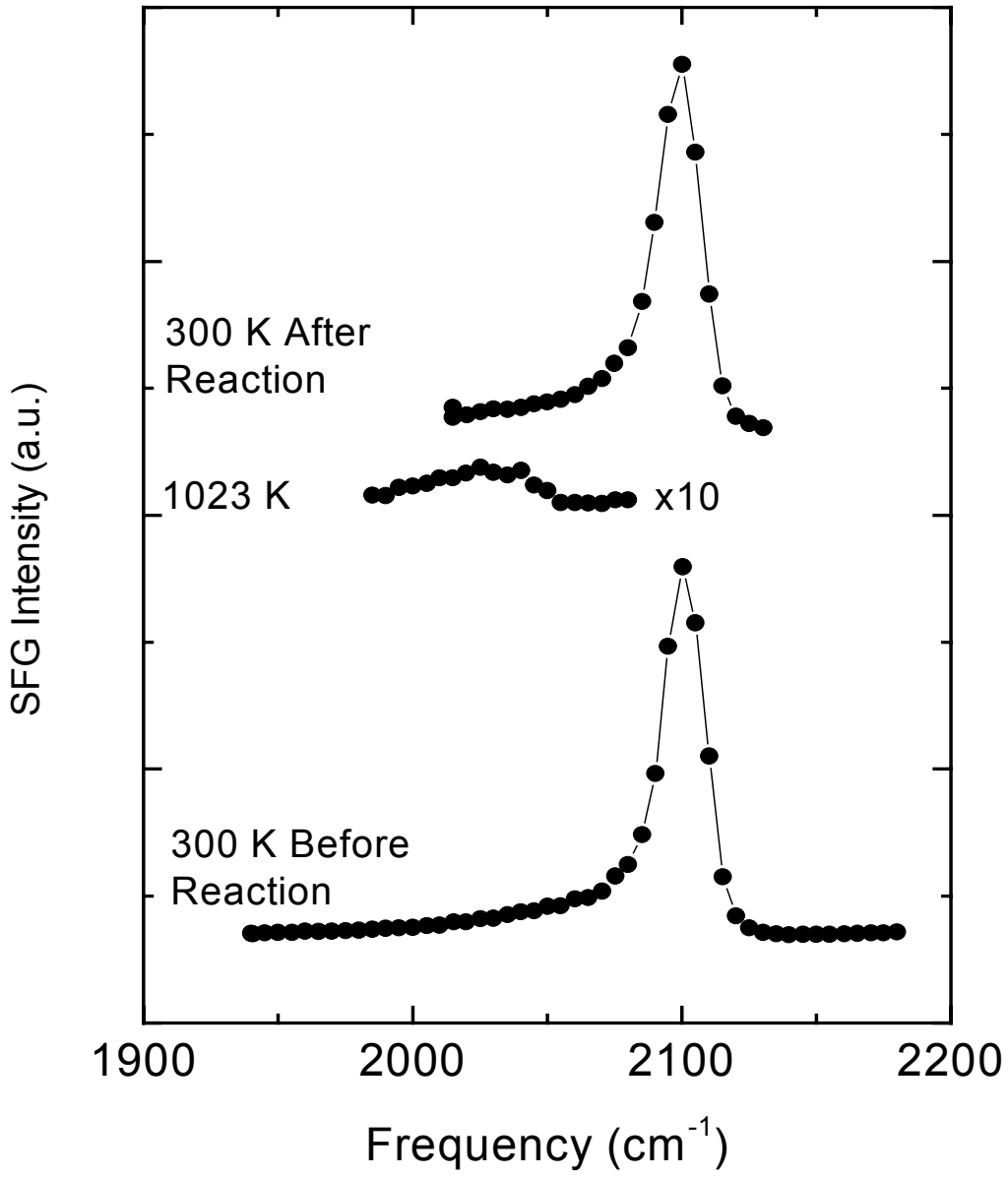

Figure 8.12 SFG spectra of Pt(557) under 100 Torr of CO and 40 Torr of O_2 before and after reaction. The spectra are reversible.

shifted to 2040 cm^{-1} at 1048 K as shown in Figure 8.11. Detectable CO_2 production

began at 673 K, although the turnover rate did not become high (990 molecules/site/sec) until 723 K. The crystal was allowed to cool and the SFG spectrum after the reaction was identical as seen before the reaction (Figure 8.12).

CO oxidation under excess CO was also performed on a carbon covered platinum surface. The carbon covered surface was prepared by heating the Pt(557) single crystal in 100 Torr of CO at 573 K. After heating for 20 minutes, 40 Torr of O_2 and 630 Torr of He were introduced into the chamber. Immediately, any residual CO peak vanished and the SFG background increased substantially. The SFG background was then monitored as a function of temperature as shown in Figure 8.13. A high turnover rate for CO_2 production began at 673 K, 50 degrees lower than observed on the clean surface. As the sample temperature was increased to 723 K, the SFG background increased substantially. A small SFG peak at 2070 cm^{-1} was also observed in addition to the large background at 723 K. Continuing to increase the temperature above 723 K, the SFG background began to decrease, and the small peak decreased in frequency as well. By 1023 K, the SFG spectrum was flat without any features or large background. The spectrum at 300 K after the crystal was heated to 1023 K is very similar to the spectrum at 300 K before dissociating CO (Figure 8.14), which indicates the surface is free of atomic carbon.

Figure 8.15 compares the turnover rates versus temperature for the clean and carbon covered platinum surface under excess CO. The turnover rate on the carbon-covered surface is much higher at lower temperatures than on the clean surface. Around 873 K, the turnover rates become essentially the same. It appears that the gasification of carbon also contributes to the production of CO_2 but doesn't completely

explain the increased activity on the carbon-covered surface. The rates converge for the two different surfaces when the SFG background decreases for the carbon covered surface indicating any residual carbon on the surface is being oxidized away revealing a clean CO covered surface at 300 K.

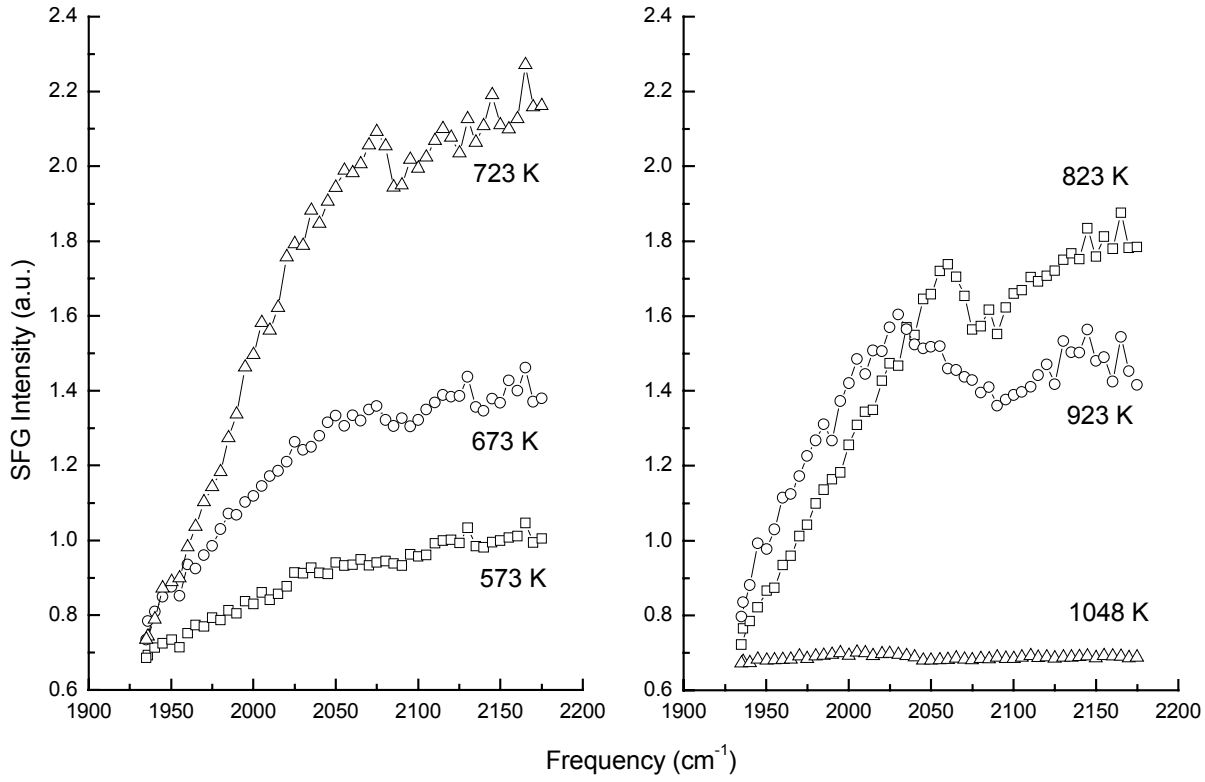

Figure 8.13 SFG spectra of a carbon covered Pt(557) surface under 100 Torr of CO and 40 Torr of O_2. As the surface is heated, the SFG intensity goes through a maximum before decreasing revealing a featureless spectrum at 1048 K.

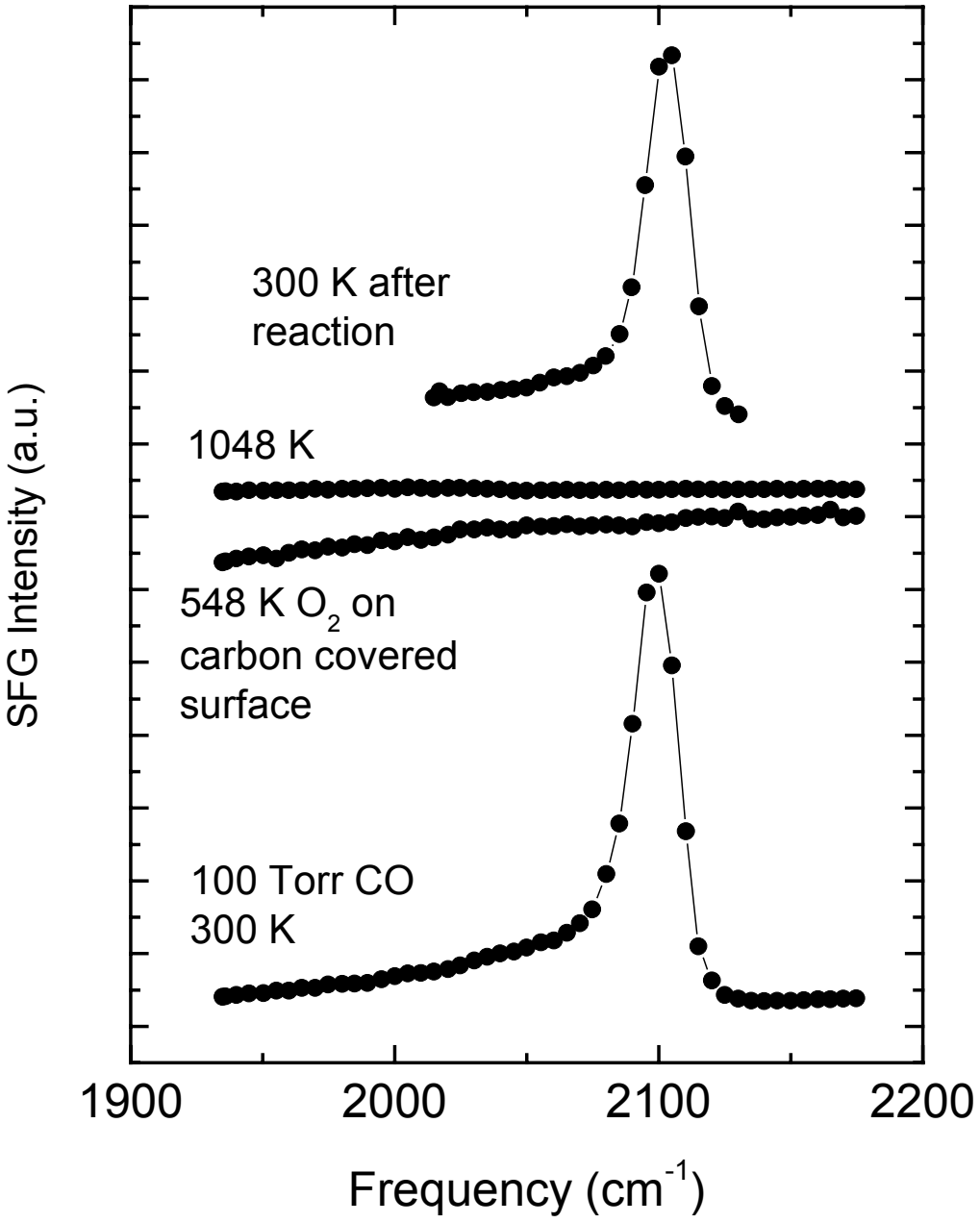

Figure 8.14 SFG spectra of Pt(557) before and after CO oxidation under 100 Torr of CO and 40 Torr of O_2. The spectra before and after were the same indicating a hysteresis.

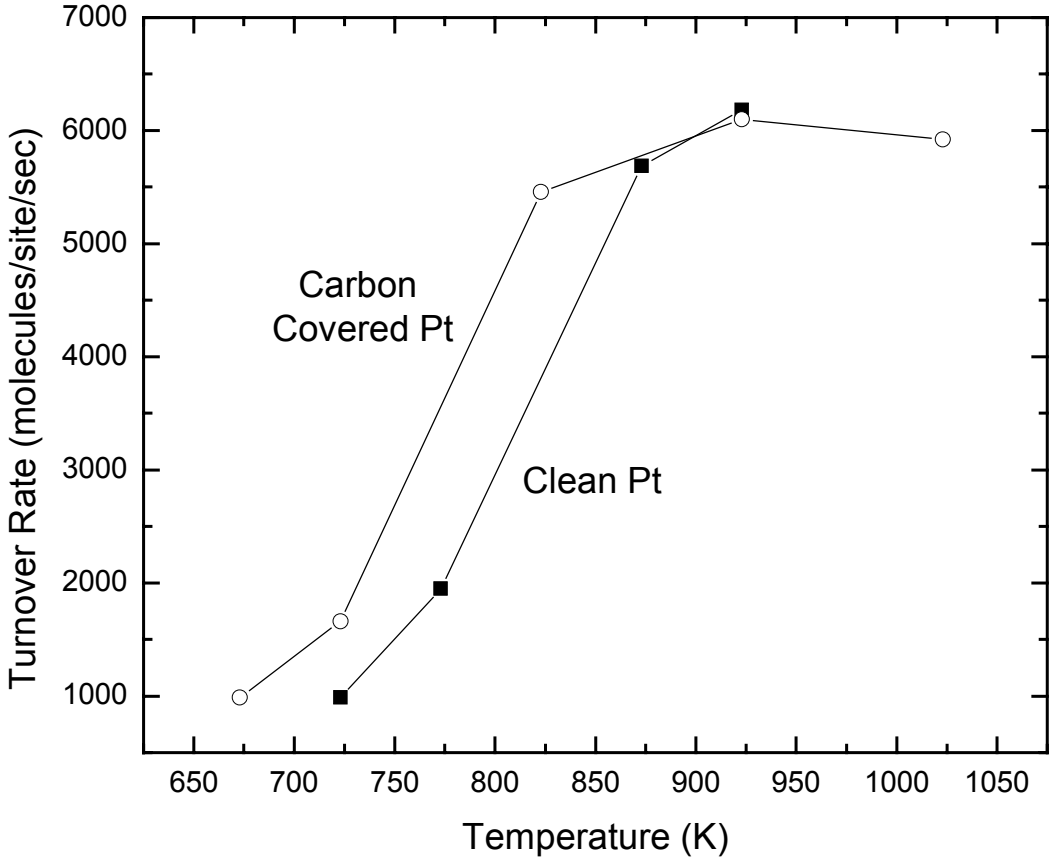

Figure 8.15 Comparison of the turnover rates for both clean and carbon covered Pt(557) as a function of temperature.

Equal Pressure of CO and O_2

The Pt(557) crystal was cleaned as described previously and introduced to 70 Torr of CO, 70 Torr of O_2, and 630 Torr of He at 300 K. The sample was then gradually heated to just below the ignition temperature (Figure 8.16). Interestingly, the

SFG background begins to increase around 623 K unlike the other two regimes in which the SFG background does not increase under reaction conditions for a clean crystal. As the sample is heated higher, the background increases. As stated previously, the background is due to both atomic oxygen and atomic carbon co-adsorbed on the surface. Because carbon was not deposited before the reaction began, this is evidence that CO is actually dissociating under these oxidizing conditions. The reaction rate at 673 K, which is below the ignition temperature for these conditions, is 900 molecules/site/sec. The ignition temperature was approximately 700 K, and the temperature increased to 790 K. The turnover rate at 790 K was approximately 4300 molecules/site/sec. After the reaction, the sample was cooled back down to 300 K and the SFG spectra at 300 K before and after heating are shown in Figure 8.17. The peak position for both spectra is at 2100 cm^{-1}, although it appears that CO is now adsorbed on a modified platinum surface after ignition. The modified surface has a carbon oxide species co-adsorbed with CO, which explains the increased background.

The same pressures of CO and O_2 were also used on a carbon covered Pt(557) crystal. After the crystal was cleaned, 70 Torr of CO was introduced into the chamber and the sample was heated to 300 K. After 20 minutes, 70 Torr of O_2 was added along with 630 Torr of He. Immediately, any residual CO peak disappeared and the SFG background increased (Figure 8.18). At 623 K, below the ignition point, the turnover rate was 800 molecules/site/sec. This rate is substantially higher than observed on the clean Pt surface under the same conditions at 623 K. The sample was gradually heated

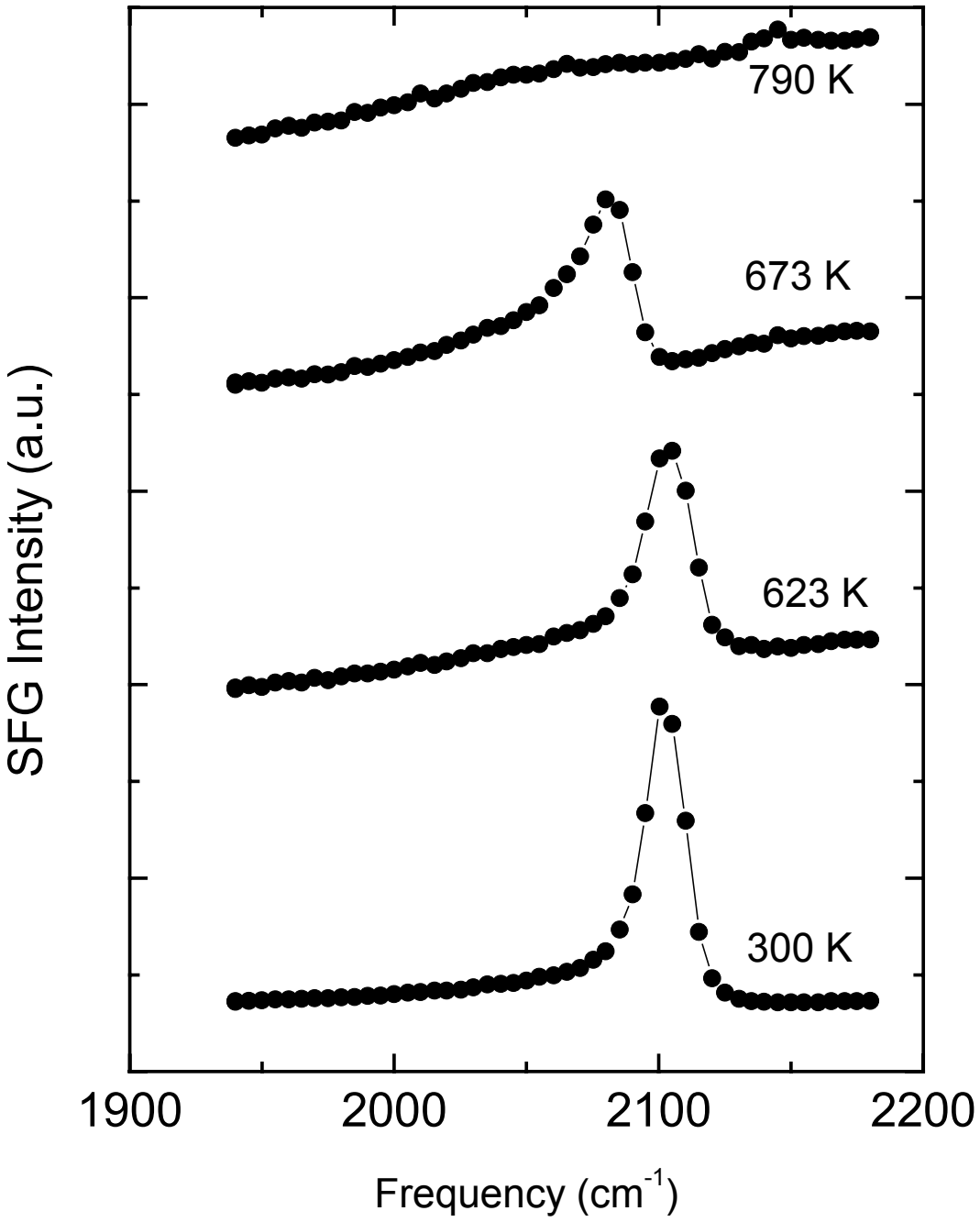

Figure 8.16 SFG spectra of Pt(557) under CO oxidation conditions. 70 Torr CO and 70 Torr of O_2.

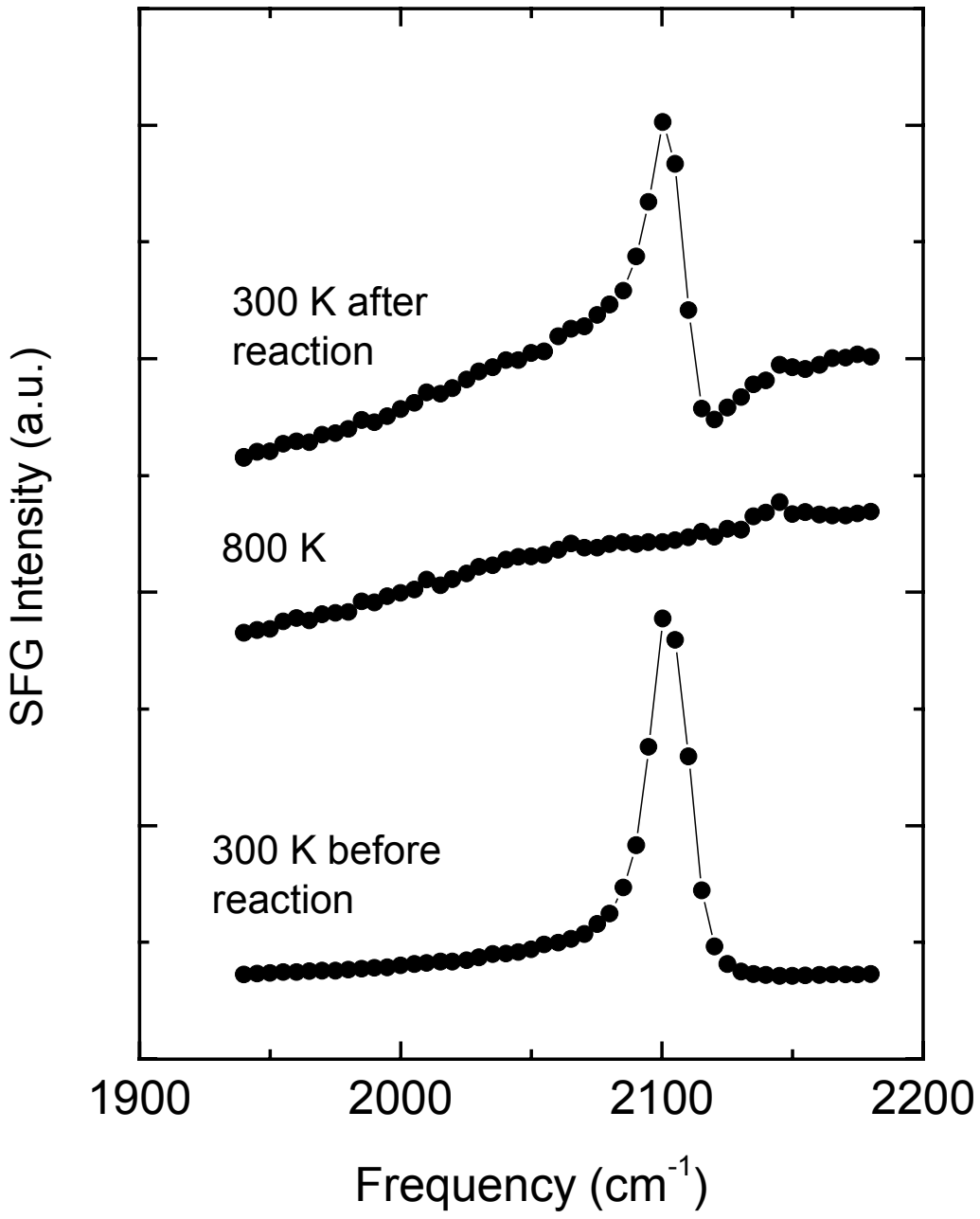

Figure 8.17 SFG spectra of Pt(557) under 70 Torr of CO and 70 Torr of O_2 before and after reaction.

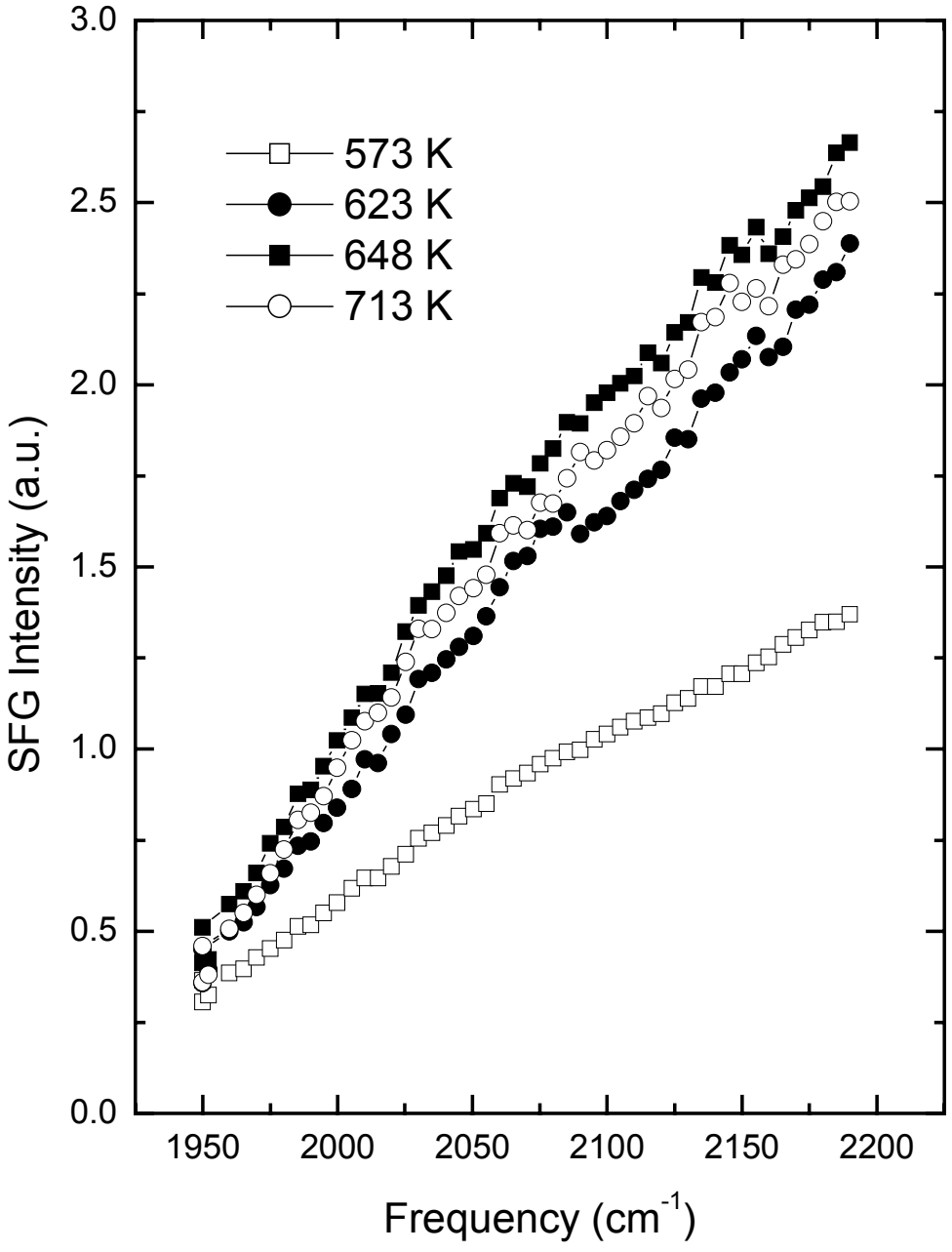

Figure 8.18 SFG spectra of a carbon covered Pt(557) crystal under 70 Torr of CO and 70 Torr of O_2.

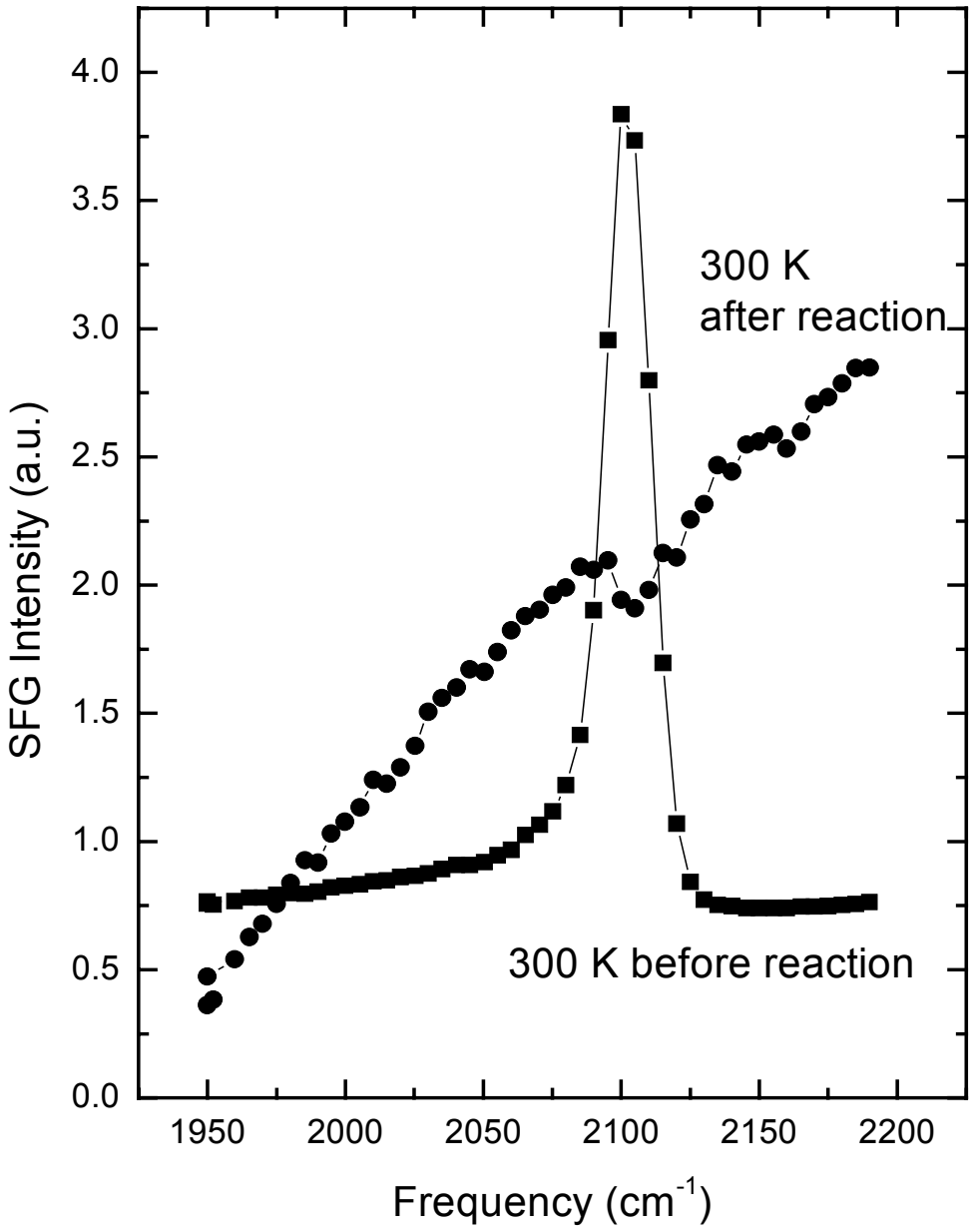

Figure 8.19 SFG spectra of a carbon covered Pt(557) crystal before the deposition of carbon and after reaction under 70 Torr of CO and 70 Torr O_2.

to 648 K, the ignition point under these conditions. This ignition at 648 K is 50 degrees lower than the temperature observed for the clean crystal. The SFG background increased as a function of temperature above ignition, but did not increase appreciably after ignition indicating that the relative concentrations of carbon and oxygen on the surface were not changing. At 790 K, above ignition, the rate was 4400 molecules/site/sec. The sample was then cooled to 300 K and the spectra before and after the reaction are shown in Figure 8.19. Because the SFG background is still considerable, the carbon was not oxidized away as in the previous case with excess CO.

Discussion

Carbon and Oxygen Surface Species

It is believed that when CO is dissociated, carbidic carbon islands are formed on the surface. When the carbon covered platinum surface is then heated in the presence of O_2, the carbon islands become terminated with oxygen, which then gives rise to the SFG background and also allows oxygen to be observed in the Auger spectrum. Obviously, the size of the carbon islands will determine the amount of oxygen observed in the Auger spectrum. The intensity of the SFG background is also dependent on the concentration carbon and oxygen on the surface. As the carbon to oxygen ratio decreases, the SFG background increases.

Activated carbon is a common support used in catalysis and there have been many studies on activated carbon surfaces.[10,11,12] Under oxidizing conditions, the activated carbon is oxygen terminated, and work has been done to identify the types of

carbon oxide species using many techniques. One such technique that has proved to be very useful for this system is temperature programmed desorption (TPD). Otake and coworkers oxidized their active carbon either by heating in air or by exposing the carbon to concentrated nitric acid. When the carbon was heated in air, they found that the surface began to oxidize significantly at 573 K, and upon further heating, the amount of oxidation became much more considerable. These temperatures are similar to those used in this study in which the large SFG background is observed to grow.

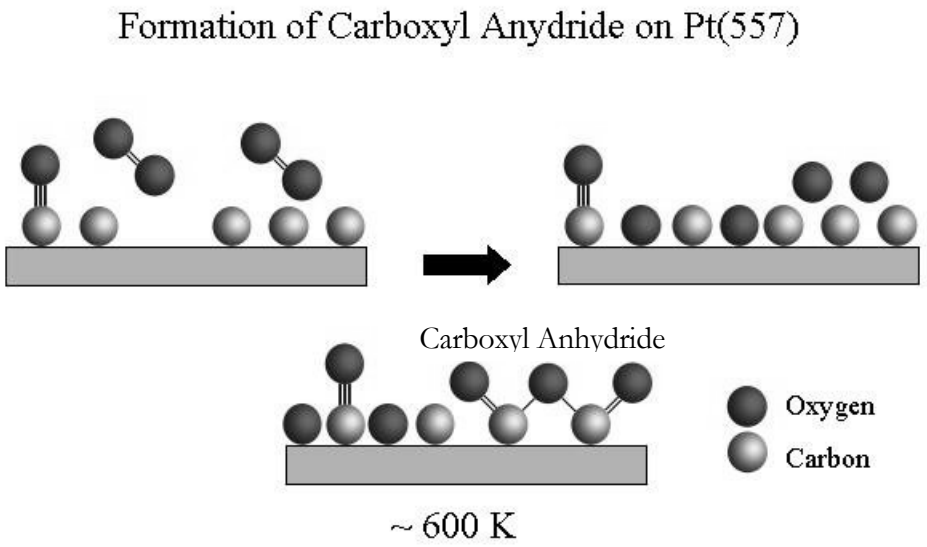

Figure 8.20 Formation of carboxyl anhydride from a carbon covered Pt(557) surface. The formation begins around 548 K and increases with temperature.

Once the carbon was oxidized, Otake and coworkers performed TPD experiments on the oxidized carbon. The amounts and temperatures that CO and CO_2 are evolved gives indication on the type of oxide species present on the surface. They observed two significant CO peaks at 900 and 1175 K. One CO_2 peak at 900 K was also observed. Otake and coworkers assigned the species that gives rise to these desorption peaks to carboxyl anhydride (-(CO)O(CO)-). When this species decomposes, both CO and CO_2 will be evolved simultaneously. 900 K is very similar to the temperature of CO and CO_2 evolution in our experiments and also for the gasification of the carbon oxide species under oxidation conditions observed during catalytic experiments. Due to the similarity in the data, it is likely that an important carbon oxide species on the Pt surface is also carboxyl anhydride. It is also possible due to the probable conjugation of this species on activated carbon islands, it could be responsible for the observed electronic resonance that gives rise to the large SFG background.

From this information, the mechanism of formation for carboxyl anhydride on the surface is shown in Figure 8.20. After carbon has been deposited through the dissociation of CO, carbon islands are formed. When these carbon islands are exposed to O_2 near 600 K, the carboxyl anhydride species form from the reaction of surface oxygen and carbon.

Reaction Mechanisms for CO Oxidation on Clean and Carbon Covered Pt(557) Surfaces

For all the conditions studied in this work, the rate of CO_2 production at 623 K for clean prepared Pt(557) were essentially the same as expected from the negative

order in CO and positive order in O_2 dependence, which is well known from the literature. These results are listed in Table 8.1. As stated from the literature, the mechanism above ignition is believed to mass transport limited. There have not been many studies, which have specifically measured the kinetics above ignition and so the dependence on CO and O_2 on the reaction is not as well known for the mass transport limited regime. A previous study in the Somorjai group revealed that there was a 1/2 reaction order for both CO and O_2 above ignition. If this were the case, then the rate of CO_2 production should be the same for any pressures of CO and O_2 at the same temperature. In this study, distinct ignition temperatures were only observed for CO oxidation under excess CO or equal pressures of CO and O_2. At 723 K, the rate of CO_2 production was measured to be near 1400 and 4000 molecules/site/sec for the excess O_2 and equal pressures of CO and O_2 conditions, respectively (Table 8.1). Obviously, these are considerably different, and there must be another reaction channel in addition to a mass transport mechanism above ignition to explain the large difference in rates. This additional channel must be a surface reaction not previously observed and further studies must be performed to understand the nature of this mechanism.

Table 8-1 Turnover reaction rates above and below ignition on clean prepared Pt(557).

	100 Torr O_2 40 Torr CO	70 Torr O_2 70 Torr CO	40 Torr O_2 100 Torr CO
Below Ignition (623 K)	20 mol/site/sec	28 mol/site/sec	22 mol/site/sec
Above Ignition (723 K)	1400	4000	NA

CO oxidation reactions were performed on both clean and carbon covered Pt(557) and turnover rates were measured above and below the ignition temperature for both types of surfaces. The reaction on a clean Pt surface under excess O_2 is well known. From previous studies it has been explained that below ignition, the reaction follows Langmuir-Hinshelwood kinetics and CO_2 is produced by the reaction of adsorbed CO and adsorbed atomic oxygen. Above ignition, in addition to mass transport reactions, an addition surface mechanism must exist above ignition as discussed above. The known mechanisms above and below are shown in Figure 8.21.

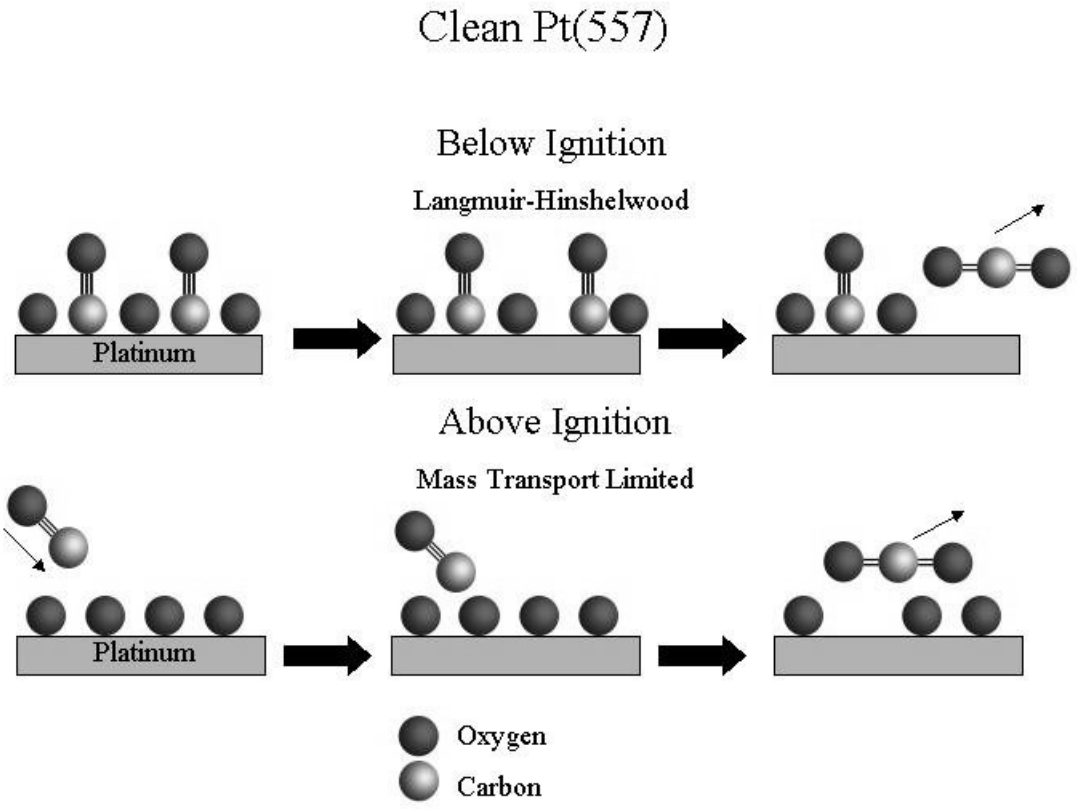

Figure 8.21 Mechanism for the production of CO_2 under excess O_2 over clean prepared Pt(557).

When CO oxidation is performed on a carbon covered Pt(557) surface under excess oxygen, the reaction kinetics are essentially the same as observed on the clean Pt(557) surface. This means that the carbon oxygen species also acts as a support for oxygen similar to clean Pt. The mass transport mechanism for CO_2 production on a carbon-covered surface is shown in Figure 8.22.

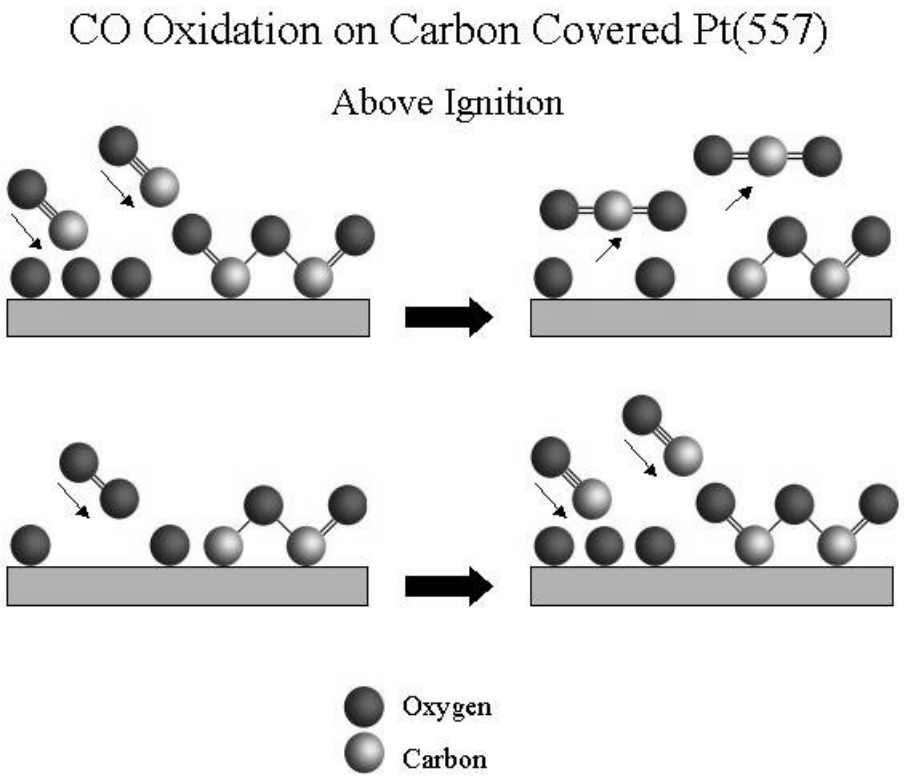

Figure 8.22 Proposed mechanism for the production of CO_2 above ignition on a carbon prepared Pt(557) surface.

When the reaction was performed on a carbon covered Pt(557) surface under excess CO, the rate of CO_2 production below ignition is significantly higher than that on a clean prepared platinum surface. The surface oxide species, believed to be

carboxyl anhydride, appears to be better at oxidizing CO than a clean prepared Pt surface as the rate is considerably higher on the carbon-covered surface than on clean Pt under these conditions. As stated, the amount of the carbon oxygen species is proportional to the intensity of the SFG background. The background increased up to 723 K and the proposed mechanism that accounts for the higher rate of CO_2 production below ignition is shown in Figure 8.23. Essentially, the rate of CO_2 production through the reaction of CO and oxygen from carboxyl anhydride is faster than the rate of production of CO_2 from the reaction of adsorbed CO and O on platinum.

Once above 723 K, the SFG background begins to decrease as a function of temperature indicating the carboxyl anhydride species is gasifying at these temperatures. By 900 K, the background is essentially gone and the rate is the same as that observed on a clean prepared Pt(557) surface indicating the surface carbon was completely gasified. At these temperatures, the reaction is probably mass transport limited due to the absence of adsorbed CO in the SFG spectra. The mechanism for the gasification of carbon is shown in Figure 8.24. It is believed that the carboxyl anhydride species decomposes to produce CO_2.

When CO oxidation is performed on both clean and carbon-covered Pt(557) surfaces under equal pressures of CO and O_2, the kinetics follow the mechanisms proposed for the excess O_2 case. The only difference is that it appears that CO dissociates under these conditions on the clean prepared surface. Also, the ignition temperature under these conditions is lower for the carbon-covered surface than on the clean prepared surface. From this data and the data presented in Chapters 6 and 7, the

dissociation of CO through the Boudouard reaction is very likely to be important for the onset of ignition.

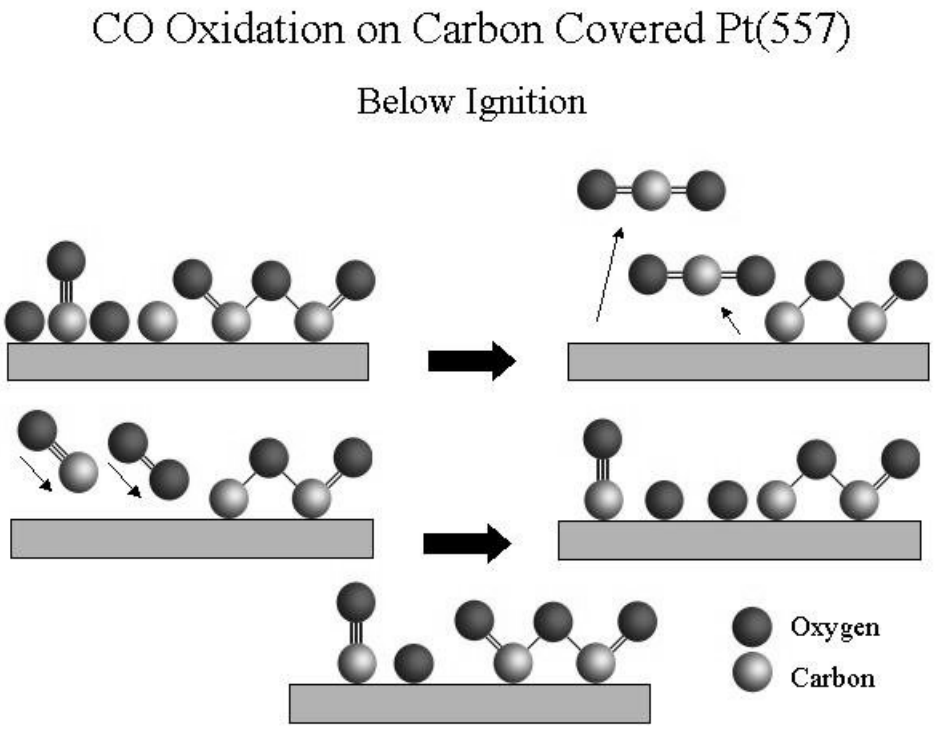

Figure 8.23 Proposed mechanism for the production of CO_2 below ignition on a carbon prepared Pt(557) surface. Adsorbed CO, or C and O can react with oxygen from carboxyl anhydride to produce CO.

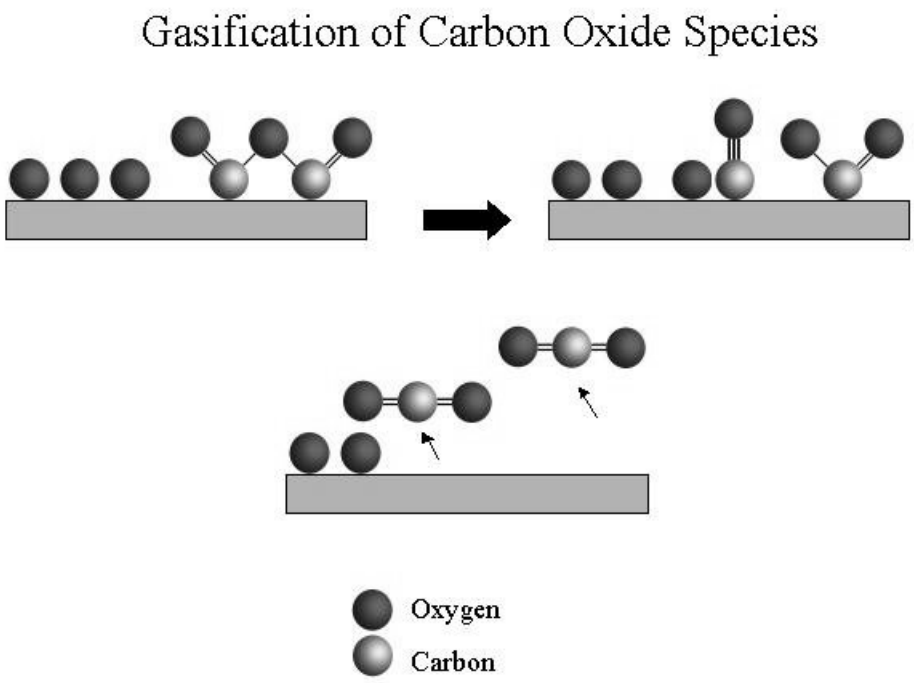

Figure 8.24 Gasification of carbon to produce CO_2 above 723 K.

Conclusions

The production of CO_2 over Pt(557) was monitored as a function of temperature and surface carbon with SFG, TPD, Auger electron spectroscopy, and gas chromatography. It was found below the ignition temperature the reaction follows Langmuir-Hinshelwood kinetics. Above ignition, CO_2 production proceeds through at least two reaction channels. One reaction channel is mass transport limited while the

other must be another surface reaction, which has not been previously studied. These reaction mechanisms below and above ignition were the same whether the reaction was performed on a clean prepared or carbon covered Pt(557) surface. The difference was that the rate of reaction below ignition was considerably higher on the carbon prepared surface when the reaction was performed in excess CO or equal pressures of CO and O_2. For the excess O_2 condition, ignition was very close to the start of CO_2 production and so pre-ignition kinetics could not be studied as in depth as the other two cases.

In addition to the higher turnover rates on the carbon-covered surface, the SFG background was significantly larger than observed on the clean surface. It was determined that the background was due to the presence of a carbon oxide species on the surface which has an electronic resonance in the visible region near 532 nm, the frequency of the visible beam used in these SFG experiments. Because of the higher rate and the existence of the carbon oxide species, this surface is better at oxidizing CO than clean Pt. The carbon oxide species is proposed to be carboxyl anhydride as observed in studies on activated carbons. This species decomposes near 900 K with similar concentrations of both CO and CO_2. Additionally, it gasifies near this temperature under oxidation conditions.

It was proposed from the data presented in chapters 6 and 7 that CO dissociation through the Boudouard reaction may be important for the onset of ignition. Further evidence that this might be the case was found when the reaction was performed under equal pressures of CO and O_2. When performed on a clean prepared surface, the SFG background was observed to increase slightly, indicating CO was decomposing. In addition, the ignition temperature was found to be 50 degrees lower

for the carbon covered surface than the clean prepared platinum surface. This is strong evidence that CO dissociation is an important step for the ignition mechanism.

References

[1] Hong, S., and H.H. Richardson, *J. Phys. Chem.* 1993, **97**, 1258.

[2] Ohno, Y., Sanchez, J.R., Lesar, A., Yamanaka, T., and T. Matsushima, *Surf. Sci.* 1997, **382**, 221.

[3] Rinnemo, M., Kulginov, D., Johansson, S., Wong, K.L., Zhdanov, V.P., and B., Kasemo, *Surf. Sci.* 1997, **376**, 297.

[4] Bowker, M., Jones, I.Z., Bennett, R.A., Esch, F., Baraldi, A., Lizzit, S., and G. Comelli, *Catal. Lett.* 1998, **51**, 187.

[5] Su, X., Cremer, P.S., Shen, Y.R., and G.A. Somorjai, *J. Am. Chem. Soc.* 1997, **119**, 3994.

[6] Wartnaby, C.E., Stuck, A., Yeo, Y.Y., and D.A. King, *J. Chem. Phys.* 1995, **102**, 1855.

[7] Berlowitz, P.J., Peden, H.F., and D.W. Goodman, *J. Chem. Phys.* 1988, **92**, 5213.

[8] Imbihl, R., Cox, M.P., and G. Ertl, *J. Chem. Phys.* 1986, **84**, 3519.

[9] McCrea, K. R., Parker, J. and G.A. Somorjai,. Accepted for publication in honor of Wyn Roberts, Kluwer, April 2001.

[10] Otake, Y., and R.G. Jenkins, *Carbon*, 1993, **31**, 109.

[11] Dandekar, A., Baker, R.T.K., and M.A. Vannice, *Carbon*, 1998, **36**, 1821.

[12] Haydar, S., Moreno-Castilla, C., Ferro-Garcia, M.A., Carrasco-Marin, F., Rivera-Utrilla, J., Perrard, A., and J.P. Joly, *Carbon*, 2000, **38**, 1297.

Chapter 9: Conclusions

In this dissertation, the effect of structure on several catalytic reactions, both structure sensitive and structure insensitive, was studied using sum frequency generation and gas chromatography.

The data presented here show clearly that SFG is a flexible tool that allows molecular-level characterization of surfaces at ambient pressures between 10^{-11} and 10^{3} Torr, a range of more than 14 orders of magnitude. Low-pressure experiments served two purposes; they allowed correlation of results with those of previous experiments carried out with electron spectroscopies and ion scattering techniques, and they provided information about possible reaction intermediates under high pressures. By correlating high-pressure SFG spectra recorded under reaction conditions and kinetics data, it has been possible to determine the important reaction intermediates of several surface catalytic reactions.

The effect of the surface structure of Pt(111) and Pt(100) was investigated for cyclohexene hydrogenation and dehydrogenation, and ethylene hydrogenation by using sum frequency generation. Cyclohexene dehydrogenation is a structure sensitive reaction, and the rate was found to proceed more rapidly on the Pt(100) crystal surface than on the Pt(111) crystal surface. On Pt(100), the major reaction intermediate during cyclohexene dehydrogenation was 1,3-cyclohexadiene, whereas on Pt(111), both 1,3-

and 1,4-cyclohexadiene were present. Both 1,3- and 1,4-cyclohexadiene can dehydrogenate to form benzene, although the reaction proceeds more rapidly through the 1,3-cyclohexadiene intermediate. Because of this, the structure sensitivity of cyclohexene dehydrogenation is explained by noting that there is both a fast and a slow reaction pathway for Pt(111), whereas there is only a fast reaction pathway on Pt(100).

Ethylene hydrogenation is a structure insensitive reaction. Both ethylidyne and di-σ bonded ethylene are present both Pt(111) and Pt(100) under reaction conditions, although the ratio of the concentrations of the two species are different. The rate of the reaction was found to be 11±1 and 12±1 molecules/site/sec for Pt(111) and Pt(100) respectively. Since the reaction rate is essentially the same on the two surfaces, while the concentration of ethylidyne and di-σ bonded ethylene are different, these species must not be the active species which turnover under catalytic ethylene hydrogenation. The most likely species which turnover are weakly bound π-bonded ethylene and ethyl species as revealed by SFG.

Using sum frequency generation surface vibrational spectroscopy, platinum single crystal surfaces were investigated at high-pressures and high-temperatures under pure CO or CO and O_2 environments. The crystals under investigation were the (111), (100), and (557) faces of platinum. In 40 Torr of CO, the molecule dissociates on the (111), (557) and (100) surfaces of platinum single crystals at 673 K, 548 K, and 500 K, respectively, indicating CO dissociation is structure sensitive. The Pt(111) surface must be heated to a temperature where the surface is roughened creating step and kink sites, which are known to dissociate CO. The stepped Pt(557) surface does not need to

be heated as high as Pt(111) to dissociate CO since there are step sites already available on the surface. The outer most surface atoms of Pt(100) are mobile compared to the low energy (111) surface and so the surface can roughen at a much lower temperature than observed on Pt(111). Under 40 Torr of CO and 100 Torr of O_2, CO oxidation ignition temperatures of 620 K, 640 K and 500 K were observed for Pt(111), Pt(557) and Pt(100), respectively, indicating ignition is also structure sensitive. The ignition temperature for Pt(111) and Pt(557) are similar because the higher concentration of surface atoms on the (111) terraces, common to both surfaces, are more dominate during oxidation than step sites. Since both CO dissociation and CO oxidation ignition are structure sensitive and follow the same trend of decreasing temperatures for the two processes, it is likely that CO dissociation is important for the onset of ignition.

Carbon monoxide oxidation was studied in detail on the Pt(557) single crystal surface under different pressure and temperature regimes. The reaction was studied on both clean prepared and carbon covered Pt(557) surfaces. It was found under all conditions that the reaction followed Langmuir-Hinshelwood kinetics below ignition and above ignition the reaction was mass transport limited. Under excess CO and equal CO and O_2 pressures, it was found that the carbon-covered surface was more reactive than a clean prepared surface. In addition, the SFG background increased as a function of temperature up to 723 K. The background resulted from the production of a carbon oxide species when carbon that was first deposited was exposed to O_2 above 548 K. The carbon oxide species is believed to be carboxyl anhydride and is a better oxidizer than pure platinum, which explains the higher turnover rate on the carbon-covered surface below ignition. As the temperature was increased above 723 K, the background

decreased and the turnover rates converged for the clean and carbon covered surfaces indicating the carbon on the surface had been gasified. In addition, further evidence that CO dissociation is important for the onset of ignition was found when CO oxidation was performed under equal pressures of CO and O_2. On a clean surface, the SFG background slightly increased, indicating carbon was being deposited and then oxidized on the surface. Also, the ignition temperature for the carbon-covered surface was 50 degrees lower than on the clean prepared surface. This is supporting evidence that CO dissociation is an important step for ignition.